Sea Ice Variability in a Warmer Past: Last Interglacial Paleoceanography of the (Sub)Arctic Oceans

Kristine Steinsland

Thesis for the degree of Philosophiae Doctor (PhD)
University of Bergen, Norway
2024

UNIVERSITY OF BERGEN

Sea Ice Variability in a Warmer Past: Last Interglacial Paleoceanography of the (Sub)Arctic Oceans

Kristine Steinsland

Thesis for the degree of Philosophiae Doctor (PhD)
at the University of Bergen

Date of defense: 13.05.2024

Year: 2024

Title: Sea Ice Variability in a Warmer Past: Last Interglacial Paleoceanography of the (Sub)Arctic Oceans

Name: Kristine Steinsland

Print: Skipnes Kommunikasjon / University of Bergen

Scientific environment

This PhD research was carried out at the Norwegian Research Centre (NORCE), department of Climate and Environment, where I was a part of the Molecular Ecology and Paleogenomics (MEP), and the Ocean Observations research groups. My research was funded as part of the European Research Council Consolidator Grant, **AGENSI**- "**A** **Gen**etic View into Past **S**ea **I**ce Variability in the Arctic" led by Dr. Stijn De Schepper. During my PhD, I was a member of the Bjerknes Centre for Climate Research (BCCR) in the Polar Climate research group and I was enrolled in the in the Research School on Changing Climates in the Coupled Earth System (CHESS). I spent two research stays at the Alfred Wegener Institute for Polar and Marine Research (AWI) at the department of marine geology, hosted by Dr. Kirsten Fahl and Prof. Rüdiger Stein where I processed and analyzed all the biomarker data included in this PhD thesis. I participated in three research cruises to the Fram Strait; two led by Dr. Jochen Knies at the previously known Centre for Gas Hydrates, University of Tromsø, and one led by Dr. Stijn De Schepper with AGENSI, NORCE. On these cruises, I collected the "giant piston" sediment core that provided the basis for paper II, and I collected and sampled surface sediments for ancient DNA, biomarkers and palynology to be incorporated into a surface sediment database by AGENSI.

Acknowledgements

I thank all the great people who have supported me along my PhD journey- my brilliant colleagues, friends, family, and all the inspiring people I have been so lucky to cross paths with- there would not be a thesis without you.

Firstly, I greatly thank my supervisor, Stijn for teaching me about the strange and beautiful microscopic world of dinoflagellate cysts. Thank you for always making it easy to drop by for big and small questions and for always reading my work on the shortest notice. I thank my co-supervisor, Ulysses for discussions on the complex topics of the ocean. If not for your input my thesis would look quite different. I thank my co-supervisor, Rüdiger for your invaluable help in navigating the world of biomarkers, and I thank my co-supervisor Kirsten, for whom I could not have done this without- for your help in the lab, your contagious joy, and encouraging words. I am grateful to both of you for giving me the opportunity to spend several great research stays in Bremerhaven.

I thank Walter for your fantastic patience in the lab. I thank Dag Inge for the great late-night company in the sediment lab, and together with Stig, I thank you both for the fierce donkey competition and fiercer laughs on our several expeditions to the Fram Strait. My times spent in labs, especially at sea, and out on deck, have been the absolute best, much because of you.

To my extraordinary friends in Bergen and elsewhere, I thank you a million times. Thank you to Danielle for being part of every up and downhill from day one. I feel so lucky to have had the opportunity to share some of the best adventures of my life with you exactly. Thank you to the world's best office mates Mats, Manuel, Wanyee, Adria, Ana (and Danielle). I thank the rest of the Monday Procrastinators- Jonathan, Anne Kari, Lander and Nadine, and I thank my tiny and much-missed Realfagsbygget gang- Alexios and Paul. An immense thanks to my friends, both on and off of Høyden, over the past years, especially Vår, Karita, Sonja, Laura, Xabier, Jakob, Karl, Deron, and not least, David and Anaïs for the extra motivation towards the end. Thank you to the Havenhostel crews of 2021 and 2022, to the Dampfloks, the Freunde von Fiets, and thank you to Vincent- for being my best friend and supporter over the past years.

Takk til min kjære familie- Morfar, Mormor, Farmor, Farfar, til lille Millie, og ikke minst til Martin, Morten og Bente – jeg hadde ikke klart det uten dere.

Kristine Steinsland
Bergen, March 2024

"Our planet has changed colour.. Today, from space, the top of the world in the northern summer looks blue instead of white. We have created an ocean where there was once an ice sheet. It is Man's first major achievement in reshaping the face of his planet, and it is of course an unintended achievement, with dubious and possibly catastrophic consequences to follow".

In; A Farewell to Ice- A Report from the Arctic
(*Wadhams*, 2017)

Abstract

The extensive to permanent state of the Arctic Ocean's sea ice cover is changing rapidly, inevitably turning the surface of the Arctic Ocean from white to blue. Understanding this profound transformation and its implications for the climate, oceans and ecosystems in, and beyond, the Arctic and Subarctic regions requires an understanding of natural sea ice variability throughout geologic time. Past intervals of warming in Earth's history provide insights into the climatic and environmental responses that may be triggered in a globally warming world. The Last Interglacial (LIG; 128–116 thousand years ago), Marine Isotope Stage (MIS) 5e, had many characteristics similar to model projections of our future climate. It had a warmer climate than present, but is also thought to have had a less stable climate. One key factor that has the potential to influence ocean and climate variability is sea ice, but its presence and extent throughout the LIG is poorly constrained. Thus, what role sea ice may have played in interglacial climate variability remains an unresolved question. Large discrepancies exist regarding the state of Arctic sea ice cover through the LIG, and the glacial-interglacial transitions characterised by large climatic and environmental shifts. Sea ice variability is intricately linked with the flow of surface ocean currents and dynamic ice sheets through time. Understanding how these different parameters of the Earth's ice-ocean-climate system interact is crucial to ultimately understand better the mechanisms that lead to sea ice variability, and additionally understand how the sea ice may influence other components of the ice-ocean-climate system. The importance of elucidating the uncertainties related to sea ice variability, nature and extent, combined with uncertainties related to interglacial climate variability, makes up the overall aim of this thesis; to better understand the role of sea ice in the Earth's ice-ocean-climate system throughout the LIG and its glacial transitions.

To investigate the aim, this PhD thesis resolves millennial to centennial-scale LIG and glacial-interglacial sea ice variability and surface ocean hydrography in the Arctic and Subarctic Oceans. This includes the late glacial MIS 6, Termination II, MIS 5e/LIG, and MIS 5d covering a total time span from ca. 140–90 thousand years ago. From marine sediment cores, we analyze the fossil and geochemical remains of the microorganisms that once lived in the sea ice and surface ocean, now providing a natural archive of past

sea ice and hydrographic variability. Specifically, sea ice reconstructions are based on the sedimentary abundance of the sea ice algae biomarker IP_{25} combined with open-water phytoplankton biomarkers, and dinoflagellate cyst assemblage analysis. These data are compared to new and previously published proxy-records that together provide new insights into the sea ice and paleoceanographic history of the (sub)Arctic Oceans. This PhD thesis includes two proxy reconstructions from the Labrador Sea and the Fram Strait regions. Both regions reveal an evolution of sea ice from maximum glacial extents, through marginal ice zone conditions, to minimum interglacial sea ice extents (Paper I and II). In paper I, our reconstruction from the subpolar Labrador Sea reveals a detailed insight into the connection between sea ice, and the dynamic surface circulation of the subpolar gyre (SPG). In paper II, our Fram Strait proxy-reconstruction reveals insights on sea ice variability and productivity in the context of ice sheet dynamics, polynya formation, and Atlantic water influence. In paper III, our data shed light on the potential use of coupled benthic and planktic foraminiferal stable oxygen isotopes to infer sea ice, stratification and deep convection in the subpolar Labrador Sea.

The findings presented in this thesis contribute new insights into LIG sea ice variability, and into the evolution of sea ice across glacial to interglacial climates within the broader context of the paleoceanographic history of the Arctic and Subarctic. Furthermore, this thesis offers input information for enhancing the accuracy of climate model predictions of future climate, and it offers data for evaluating novel proxies for sea ice reconstructions. Ultimately, the findings are important for a better understanding of interglacial climates and natural sea ice variability, crucial for fully grasping the consequences associated with a future sea ice-free Arctic summer.

Sammendrag

Det omfattende og permanente havisdekket som i dag karakteriserer det Arktiske havet er i rask endring med en havoverflate som uunngåelig er i endring fra hvit til blå. Forståelse for en slik omfattende endring og dets konsekvenser for hav, klima, og økosystemer i, og utenfor, de Arktisk og Subarktiske hav krever en forståelse for havisens naturlige variasjoner gjennom geologiske tid. Tidligere intervaller in jordens historie som var varme gir innsikt inn i hvordan klima og miljø responderer på et globalt varmere klima. Den Siste Interglasiale Perioden (LIG), Marine Isotop trinn (MIS) 5e, hadde mange karakteristikker som liknet på modellerte projeksjoner av vårt framtidige klima. Den hadde et varmere klima enn dagens, men også et mer ustabilt klima. En nøkkelfaktor som har potensial for å påvirke klima- og havvariasjoner er havis, men dets tilstedeværelse og utbredelse gjennom LIG er lite kjent. Hvilken rolle havis kan ha spilt i interglasial klimavariabilitet er dermed et uløst spørsmål. I tillegg, eksisterer det store uenigheter om tilstanden til Arktisk havis gjennom LIG, og den glasiale til interglasiale overgangen som er karakterisert av betydelig klima og miljøendringer. Havisen er intrikat knyttet til både variasjoner i havstrømmer og dynamiske isdekker gjennom tid. En forståelse for hvordan disse forskjellige parameterne i jordens is-hav-klima system henger sammen er viktig for å bedre forstå mekanismene som fører til havisvariasjoner, og i tillegg, forstå hvordan havisen kan påvirke de ulike komponentene i is-hav-klima systemet. Viktigheten av å forstå usikkerhetene knyttet til havisens variabilitet, og utbredelse, kombinert med usikkerhetene knyttet til interglasial klimavariasjoner utgjør det overordnede målet for denne avhandlingen; å bedre forstå hvilken rolle havis kan ha spilt i jorden is-hav-klima system gjennom den siste interglasiale perioden, og dets glasiale overganger.

For å undersøke det overordnete målet løser denne doktorgradsavhandlingen årtusen til århundre skala LIG, og glasial til interglasial havisvariasjon og hydrografi i de Arktiske til Subarktiske havene. Dette inkluderer den siste delen av den glasiale perioden MIS 6 og dens avsmelting (Terminasjon II), MIS 5e/LIG og MIS 5d, noe som dekker en total tidsperiode fra ca. 140–90 tusen år siden. Fra marine sedimentkjerner analyserer vi fossile og geokjemiske rester av mikroorganismer som en gang levde i havisen og i overflatehavet. Disse danner nå et naturlig arkiv av tidligere havis- og hydrografisk

variasjon. Spesifikt, er havisrekonstruksjonene basert på sedimentær mengder av isalge biomarkøren IP_{25}, kombinert med fytoplanktonbiomarkører for åpent hav, og analyse av dinoflagellatcyster. Disse dataene sammenlignes med nye og tidligere publiserte proxirekonstruksjoner som avdekker et bredere bilde av den paleoseanografiske historien til (sub)Arktis. Denne doktorgradsavhandlingen inneholder to proxirekonstruksjoner fra Labradorhavet og Framstredet. Begge områdene avslører en utvikling av havis fra maksimale glasiale utbredelse, gjennom randis, til minimale interglasial havisutbredelse (Artikkel I og II). I artikkel I fra det subpolare Labradorhavet gir våre data et detaljert innblikk i interaksjonene mellom havis og dynamikken til overflatestrømmene som danner den subpolare gyren (SPG). I artikkel II gir våre proxirekonstruksjoner fra Framstredet innsikter om havisvariabilitet og produktivitet i sammenheng med isdekkedynamikk, dannelse av polynyaer og innstrømmende Atlanterhavsvann. I artikkel III gir våre data innsikt i mulig bruk av stabile oksygenisotoper fra kombinerte planktiske og bentiske foraminiferer for å avdekke havis, stratifisering og dypvannsdannelse i Labradorhavet.

Resultatene presentert i denne avhandlingen gir ny kunnskap om utviklingen av havis gjennom den siste interglasiale perioden, og gir innsikt i evolusjonen av havis gjennom glasial til interglasiale klimaoverganger i en bredere kontekst av den paleoseanografiske historien til de Arktiske og Subarktiske regionene. Dessuten gir denne avhandlingen verdifull informasjon som kan brukes til å forbedre klimamodeller for mer nøyaktige projeksjoner av fremtidig klima, og tilbyr data for å evaluere nye proxier for havisrekonstruksjoner. Til sist, er disse dataene viktige for å bedre forstå interglasiale klima og naturlige havisvariasjoner, avgjørende for å bedre forstå konsekvensene assosiert med en fremtidig havisfri Arktisk sommer.

List of publications

I. Kristine Steinsland, Danielle Magann Grant, Ulysses Silas Ninnemann, Kirsten Fahl, Rüdiger Stein, Stijn De Schepper. *Sea ice variability in the North Atlantic subpolar gyre throughout the Last Interglacial.* Quaternary Science Reviews, **303**, 108198, 2023.

II. Kristine Steinsland, Danielle Magann Grant, Kirsten Fahl, Rüdiger Stein, Tine Rasmussen, Bjørg Risebrobakken, Ulysses Silas Ninnemann, Jochen Knies, Julie Heggdal Velle, Stijn De Schepper. *Sea ice variability throughout the Penultimate Deglaciation and Last Interglacial in the eastern Fram Strait.* Manuscript in review for Palaeogeography, Palaeoclimatology, Palaeoecology.

III. Kristine Steinsland, Ulysses Silas Ninnemann, Rüdiger Stein, Kirsten Fahl, Danielle Magann Grant, Stijn De schepper. *Proxy signals for sea ice, hydrography and deep convection in the subpolar gyre- a critical review of the Last Interglacial.* Manuscript in preparation for submission.

Contributions not included in this thesis

IV. Danielle Magann Grant, Kristine Steinsland, Tristan Cordier, Ulysses Silas Ninnemann, Umer Zeeshan Ijaz, Håkon Dahle, Stijn De Schepper, Jessica Louise Ray. *Sedimentary Ancient DNA sequences reveal marine ecosystem shifts and indicator taxa for Glacial-Interglacial sea ice conditions.* Manuscript accepted for publication in Quaternary Science Reviews.

Contents

Chapter 1

Introduction

1.1 Motivation

By 2019, the global climate had warmed approximately 1.1 °C above preindustrial levels due to anthropogenic carbon emissions to the atmosphere, according to the International Panel on Climate Change's Sixth Assessment Report (*IPCC*, 2021). Thus, human activities may be pushing components of the Earth system towards critical thresholds which, when crossed, can lead to non-linear, fast, and irreversible changes with large-scale impacts on human and ecological systems (*Lenton et al.*, 2008). Global climate warming is impacting everyday life as sea levels rise, while natural disasters and extreme weather are becoming more intense and frequent. To avoid the most severe economic, social, and environmental consequences, the Paris Agreement was signed by 195 countries in 2015, agreeing to keep the increase in global mean temperature relative to preindustrial values below 2°C by the end of the 21st century, with efforts to limit the temperature increase to 1.5°C. However, alarmingly, global temperatures are on track to increase to 2.7 °C by the end of the century (*UNEP*, 2021).

In the polar regions, the temperature rises twice as fast as the global average (*Notz and Stroeve*, 2016; *Notz and Stroeve*, 2018) and the concurrent loss of Arctic sea ice is now recognized as one of the most prominent signatures of anthropogenic warming (*Meredith et al.*, 2019). The sea ice loss is transforming the Arctic Ocean into a new state with implications for Arctic communities and ecosystems (*Meier et al.*, 2014; *Ingvaldsen et al.*, 2021), stratification (*Polyakov et al.*, 2017; *Polyakov et al.*, 2020), and ocean- and atmospheric circulation patterns that impact climate in the mid latitudes, far beyond the Arctic (*Francis and Vavrus*, 2012; *Cohen et al.*, 2014; *Deser et al.*, 2016; *Screen*, 2017; *Screen et al.*, 2018). The urgency to study sea ice in the Arctic and Subarctic

regions comes from the predictions that summers (September) in the Arctic may be sea ice-free well within this century, possibly even by ∼2050 (*Collins et al.*, 2013b), yet the implications of such a decline are largely unknown. Additionally, IPCC models significantly underestimate the observed rate of Arctic sea ice decline (*Stroeve et al.*, 2007), indicating that we do not fully understand the underlying mechanisms of sea ice variability.

In the context of sea ice decline, past intervals of warming provide excellent case studies for comparison and provide insights into potential future scenarios, equipping us with invaluable knowledge about climate change processes, and potential challenges. The Last Interglacial (LIG), Marine Isotope Stage (MIS) 5e, occurred around 128–116 thousand years ago, representing the most recent geological period during which conditions were similar to the present interglacial, but without human-induced warming. While interglacial periods were long considered to be accompanied by a relatively stable climate, associated with a stable Atlantic Meridional Overturning Circulation (AMOC), interglacial stability has been questioned recently by contemporary measurements (*Smeed et al.*, 2014), future projections (*Stocker et al.*, 2013), and throughout the past four interglacial periods (*Galaasen et al.*, 2014, 2020).

Sea ice plays a key role in the climate system with the potential to influence oceanic and climate patterns. However, to what extent sea ice may have modulated oceanic conditions throughout the LIG remains unresolved because sea ice extent and variability during the LIG is neither well documented nor understood. Thus, sea ice remains a potential "wild card" in climate variability. The importance of understanding interglacial climates, coupled with the importance of understanding sea ice variability, led to the overall aim of this thesis: to understand the role of sea ice in the larger ocean-climate system throughout the LIG, and the glacial transitions leading into and out of it. By documenting sea ice variability throughout the past we can better understand the complex dynamics of the ice-ocean-atmosphere system. Ultimately, this needs to be resolved to understand the implications of the contemporary and future sea ice decline, evaluate challenges, and develop mitigation pathways now and for the future.

1.2 Arctic and Subarctic sea ice

The Arctic Ocean's vast seasonal to extensive sea ice cover is the most prominent feature of the Arctic Ocean- yet. Covering roughly 9% of the world's oceans for at least parts of the year (*nsidc accessed oct*, 2023), it makes up one of the largest known biomes on Earth (*Dieckmann and Hellmer*, 2010). Despite its enormous spatial extent, sea ice only grows

a few meters thick, making it vulnerable to small oceanic or atmospheric perturbations, and climate changes throughout time. The resulting changes in sea ice cover, on both short and long-term geologic scales, have substantial impacts for the oceans, climate, and the ecosystems which it supports.

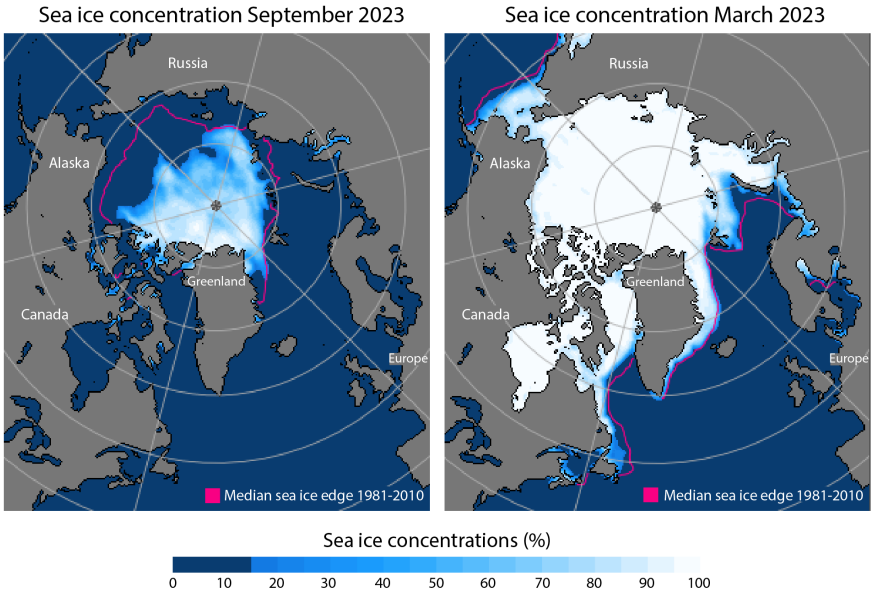

Figure 1.1: Modern Arctic Ocean sea ice extent for A) September 2023 and B) March 2023. Pink lines indicate the median sea ice extent from 1981–2010. The figures are from the National Snow and Ice Data Center; sea ice index, accessed October, 2023 (*nsidc accessed oct*, 2023).

In the Arctic and Subarctic oceans, sea ice has a large (natural) seasonal variability due to the pronounced difference in summer and winter insolation which leads to summer sea ice melt and winter sea ice growth (Figure 1.1). Through brine formation in winter and the release of freshwater during summers, the sea ice importantly influence the thermohaline properties of the upper water column (*Thomas*, 2017). When seawater freezes it produces ice crystals and small droplets of accumulated sea salt (brines) which drain out into the ocean. This process increases the salinity and the density of the seawater, which ultimately sinks when the seawater is dense enough. Thus, brine rejection associated with sea ice formation affects local, vertical water masses movements, deep-water formation and thereby the AMOC (*Dieckmann and Hellmer*, 2010). Brines can also be enriched in CO_2 which sink into the deep ocean during sea ice formation. This is an important mechanism contributing to the ocean CO_2 sink today (*Rysgaard et al.*, 2011), and throughout geologic time (*Bouttes et al.*, 2010).

Additionally important, sea ice forms a freshwater source that, upon melting, reduces

the surface ocean salinity and density, contributing to enhanced surface stratification. This surface freshwater may reduce deep water formation, weakening deep circulation, in turn implying less northward heat transport by the AMOC. Under the influence of the polar surface currents and wind stress, sea ice is in nearly constant motion across the Arctic Ocean (*Leppäranta*, 2011). In western Fram Strait, sea ice exits the Arctic Ocean and is steered towards the Subarctic North Atlantic by the East Greenland Current (EGC) (*Aagaard and Coachman*, 1968; *Haine et al.*, 2015; *Smedsrud et al.*, 2017; *Rudels et al.*, 1999). Thus, sea ice drifts away from its formation area and melts elsewhere, redistributing freshwater in the Arctic and Subarctic Oceans, and influences thermohaline properties far away from its original formation area. In summary, the seasonal cycle of Arctic sea ice and the longer-term sea ice variability is an important component of the thermohaline circulation, and the AMOC.

Sea ice has intrinsic value for the ecosystem and biodiversity it supports. The transition to sea ice-free summer conditions may cause substantial shifts to phytoplankton community structure, driving transitions in regional marine ecology (*Meredith et al.*, 2019). Sea ice, in its different forms, has a profound effect on the biota as it controls light and the distribution of phototrophic organisms, and also determines the timing of nutrient release to surface water when sea ice melts (e.g. *Meier et al.*, 2011). Under perennial sea ice there is generally little primary production. In contrast, very high biogenic productivity occurs along the seasonal sea ice margins under the sea ice (*Arrigo et al.*, 2012) and in polynyas (e.g. *Tremblay and Smith*, 2007).

When sea ice forms, it incorporates biogeochemical material (e.g., macro-nutrients, iron, organic matter, sediments), which is stored, transformed, and later released in seawater when the ice melts. In addition, organic matter accumulates in the sea ice as a result of auto- and heterotrophic production (e.g. *Vancoppenolle et al.*, 2013). Starting in late autumn, sea ice algae (mainly diatoms) are incorporated into sea ice, where they hibernate in small channels formed during sea ice formation (*Gradinger and Ikävalko*, 1998). In spring, when sufficient light and nutrients become available the algae start to grow. Thus, sea ice algae adapted and bound to this specific environment contribute to organic carbon and biomass release (*Gosselin et al.*, 1997; *Gradinger*, 2009) and form the basic level of the Arctic food chain by photosynthesis (*Arrigo et al.*, 2009). Some of the algae synthesize specific biomarkers, which may be preserved in the sediments on the seafloor and are used to reconstruct past sea ice cover (*Belt et al.*, 2007; *Brown et al.*, 2014) (see also chapter 3.1).

Not least, sea ice is an important amplifying feedback which causes it to be one of the most rapidly changing areas of the Arctic environment (*Meredith et al.*, 2019). Sea ice impacts the Earth's global energy budget through albedo feedback mechanisms at the

ocean's surface (*Flanner et al.*, 2011; *Thackeray and Hall*, 2019). The white surface of sea ice and its snow cover leads to high albedo, meaning that it reflects a large amount of the incoming radiation (50–70%) that hits the sea ice surface back into space, compared to the darker surface of an open ocean which reflects only 6% and thus has a low albedo (*nsidc accessed oct*, 2023). This high albedo of sea ice prevents heat from being absorbed into the ocean and helps to keep the Arctic region cool. On the other hand, as sea ice melts, it exposes a much darker ocean surface, which absorbs more radiation, amplifying the warming. Sea ice cover also acts as a lid to the surface ocean, separating the relatively cold atmosphere at high latitudes from warmer ocean waters beneath. This prevents surface ocean-atmosphere coupling such as heat and gas exchange, evaporation, and surface ocean mixing due to reduced wind forcing (*Dieckmann and Hellmer*, 2010). A loss of sea ice leads to both increased heat absorption due to a weakened albedo effect, and to increased exposure of warmer ocean waters to the high latitude atmosphere in the Arctic. Both processes result in an amplified and larger warming in the Arctic compared to the global average (*Screen and Simmonds*, 2010), a phenomenon that is referred to as polar amplification.

Due to polar amplification, over the past three to four decades, Arctic sea ice has significantly decreased in extent, thickness, and age (Figure 1.2), coincident with global warming and atmospheric CO_2 increase (*Stroeve et al.*, 2007; *Stroeve et al.*, 2012; *Cavalieri and Parkinson*, 2012). The decline means that currently about half as much of the Arctic Ocean is covered by sea ice in September compared to when satellite measurements began 40+ years ago (*Notz and Stroeve*, 2018). As the Arctic ice cover thins, it becomes more vulnerable to anomalous atmospheric and/or oceanic forcing that can lead to rapid ice loss events, and a fast transition toward a seasonally ice-free Arctic Ocean (*Holland et al.*, 2006; *Vavrus et al.*, 2012).

With the sea ice loss, in the coming decades we may expect to enter a new regime, in which the interior Arctic Ocean is entirely ice free in summer and sea ice is thinner and more mobile in winter (e.g. *Haine and Martin*, 2017). Throughout the Anthropocene a seasonally sea ice-free Arctic Ocean is unprecedented, and thus we do not know the full implications of ice free summers. Additionally, some of the most dramatic Arctic changes evident in the observational data have been poorly captured by climate models which have generally underestimated the amount of lost sea ice in recent decades (*Stroeve et al.*, 2007, 2012; *Jahn et al.*, 2016; *Rosenblum and Eisenman*, 2017; *Diebold and Rudebusch*, 2023). The discrepancies between models and observations imply that the climate models do not yet adequately describe the underlying processes and feedback mechanisms in the Arctic. Nevertheless, the current knowledge of the Arctic sea ice dynamics and decline is based on only about 40 years of satellite observations, an interval insufficient to document the full range of its natural variability and to fully assess feedbacks on the

global ocean, climate, and ecosystems. Measurements of sea ice variability on longer geologic timescales are therefore crucial to assess the processes and feedbacks of the Arctic.

Today, large-scale sea ice retreat is evident in the Fram Strait and the Barents Sea regions. Implications of this retreat is indeed evident in changed phytoplankton distributions, increased heat absorption and increased exposure of warmer ocean waters to the high-latitude atmosphere in the Arctic (e.g. *Ingvaldsen et al.*, 2021). The sea ice decline additionally leads to an increased freshwater flux to the Subarctic regions where decreases in ocean water density influence the circulation in important deep water formation sites in the North Atlantic Labrador Sea (*Yang et al.*, 2016). In the context of the ongoing decline, investigating how sea ice responded to changes in climate and ocean in these areas and how sea ice may have impacted ocean and climate variability throughout the past is crucial in order to understand the current, and future implications, of the changing sea ice cover.

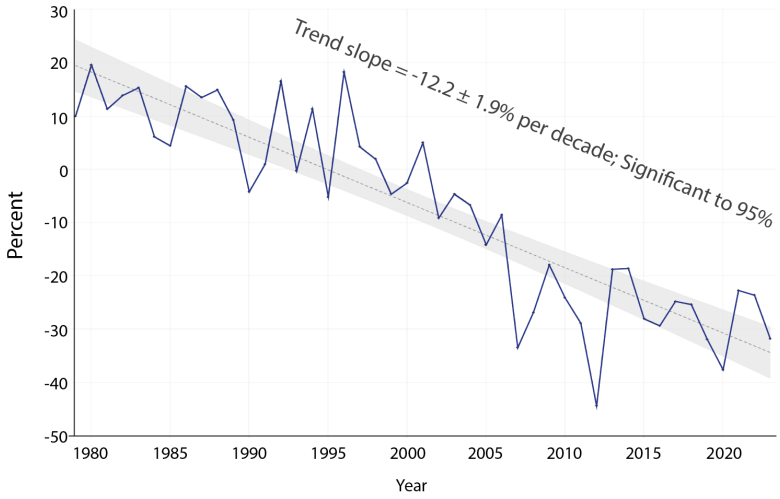

Figure 1.2: Northern Hemisphere sea ice extent anomalies during September for the period from 1979 to 2023, showing and average decline of ca. 12% per decade. Monthly sea ice extent anomalies are plotted as percent difference between the extent for September of each year and the mean extent for September based on data from January 1981 to December 2010. The dashed grey line indicates the trend line based on a simple linear regression. The figures are from the National Snow and Ice Data Center; sea ice index, accessed October, 2023 (*nsidc accessed oct*, 2023).

1.3 Arctic and Subarctic oceanography

The extent and variability of sea ice in the Arctic and Subarctic regions is driven by a range of processes included in oceanic and atmospheric circulation patterns. The northward transport of warm surface water via the upper branch of the AMOC largely influences the high-latitude climates. In fact, the climate of northwest Europe is up to 6°C warmer than the analogous location in the Pacific Ocean due to the northward transported heat released to the atmosphere (e.g. *Palter*, 2015). The warm and saline surface Atlantic water progressively cools and increases in density as it encounters polar water (and air), sinking to form deep water in the Nordic and Labrador Seas. Subsequently, these waters move south as North Atlantic Deep Water (NADW) to ultimately upwell, primarily in the Southern Ocean. These movements create a net poleward transport of heat that together with the atmosphere, establishes the global and regional climates and offsets the radiation inequities imposed by the differential heating of Earth (*Trenberth and Caron*, 2001; *Ganachaud and Wunsch*, 2003).

The Gulf Stream is the main conduit of tropical heat to the high northern latitudes. It transports the warm and salty water of tropical/subtropical origin into the mid-latitudes of the northern hemisphere, as the upper limb of the AMOC (e.g. *Käse and Krauß*, 1996). After the separation from the continental slope, the Gulf Stream is referred to as the North Atlantic Current (NAC) and it crosses into the eastern Atlantic Ocean (e.g. *Rhein et al.*, 2011). From here, the Atlantic waters diverge into two major flows; the Norwegian Atlantic Current (NwAC) going northward into the Nordic Seas and further toward the Fram Strait, and the Irminger Current (IC) flowing westward across the North Atlantic to the Labrador Sea.

1.3.1 Fram Strait oceanography

The warm and saline Atlantic waters enter the Arctic Ocean via eastern Fram Strait (Figure 1.3) as the northernmost continuation of the NAC, where it is referred to as the Western Spitsbergen Current (WSC) (*Aagaard*, 1982; *Schauer et al.*, 2004; *Carmack et al.*, 2015). The Fram Strait, between Svalbard and Greenland, is the only deepwater connection between the Arctic Ocean and the North Atlantic (*Jakobsson et al.*, 2012; *von Appen et al.*, 2015; *Haine et al.*, 2015) and is therefore crucial for the exchange of water masses between high and low latitudes. Between 78°N and 80°N the WSC branches into a northeastward flowing Svalbard branch (SB), and a westward flowing Yermak Branch (YB) (*Manley*, 1995). As these surface water continuously cool, densify and subsequently sink, the Atlantic water eventually returns as the Return Atlantic

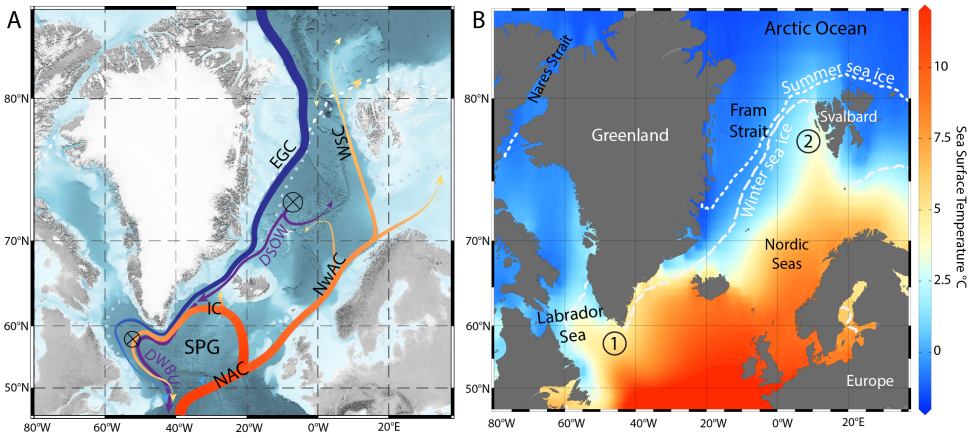

Figure 1.3: Oceanography of the North Atlantic Ocean including the Labrador Sea, the Nordic Seas, and the Fram Strait gateway into the Arctic Ocean. A) Major surface and deep ocean currents indicated on bathymetry; blue and orange currents represent the surface currents; NAC: North Atlantic Current, NwAC: Norwegian Atlantic Current, WSC: Western Spitsbergen Current, IC: Irminger Current, EGC: East Greenland Current, and the cyclonic SPG: Subpolar gyre. Purple currents represent deep flows; the Labrador Sea basin is dominated by the DWBU: Deep Western Boundary Undercurrent, of which DSOW: Denmark Strait Overflow Water makes up a large part. Circled crosses indicate deep convection cells in the Greenland Sea and Labrador Sea, B) Annual sea surface temperature °C from the World Ocean Atlas, 2019. Sea ice minimum (September) and sea ice maximum (March) average extents between 1981 and 2010 are marked with white dashed lines. The circled numbers present the regions studied for this PhD thesis; (1) corresponding to papers I and III, and (2) corresponding to paper II (see chapter 3). Map A is made in QGIS and map 2 is made in Ocean Data View (*Schlitzer*, 2023).

Current (RAC) (*Bourke et al.*, 1988; *Hattermann et al.*, 2016) as intermediate and deep-waters (*Aagaard*, 1981; *Rudels et al.*, 2002; *Schauer et al.*, 2002; *Beszczynska-Möller et al.*, 2012). Deep convection also occurs near the sea ice edge in the Greenland Sea (*Hansen and Østerhus*, 2000). These newly formed and re-circulated deep waters cross the Greenland-Scotland Ridge as Denmark Strait Overflow Water (DSOW) that flows into the North Atlantic.

The Fram Strait sea ice variability is subject to both anthropogenic global warming and internal variability via different atmospheric (*Ding et al.*, 2017) and ocean (*Carmack et al.*, 2015) processes. Relationships between Atlantic Ocean heat transport and Arctic sea ice conditions have been recognized for more than a century (*Helland-Hansen and Nansen*, 1909) and many studies since, have shown a role of Atlantic warming on sea-ice reduction (*Furevik*, 2001; *Vinje*, 2001a; *Polyakov et al.*, 2004; *Spielhagen et al.*, 2011; *Årthun et al.*, 2012). Thus, the poleward ocean heat transport via the WSC has a strong

influence on the recent changes in Arctic sea ice (*Polyakov et al.*, 2017; *Serreze et al.*, 2019). Increased ocean heat transport since 1997 has mainly been driven by increased ocean temperature (*Beszczynska-Möller et al.*, 2012; *Wang et al.*, 2020) leading to an ongoing "Atlantification" - a transition of Arctic waters to a state more closely resembling that of the Atlantic (e.g. *Ingvaldsen et al.*, 2021). This includes increased Atlantic water temperatures with attendant northward retreat of sea ice, reductions in stratification, increased vertical mixing, and altered primary production (e.g. *Reigstad et al.*, 2002).

The importance of Atlantic water influence on the sea ice state is demonstrated in modern observations, especially in the Barents Sea and north of Svalbard where the retreat of the winter sea ice edge has been most pronounced along the main advection paths of the warm Atlantic water (*Årthun et al.*, 2012; *Ivanov et al.*, 2018; *Ingvaldsen et al.*, 2021). While the eastern Fram Strait has been essentially sea ice-free year-round throughout recent history (1981–2010; Figure 1.3) (*Polyakov et al.*, 2017), large changes in sea ice extent are documented in the area northeast of Svalbard. This area, which has traditionally been ice covered most of the year, has in recent decades experienced larger areas with ice-free conditions for longer periods, primarily due to a contemporary increase in temperature of the Atlantic water inflow (*Ivanov et al.*, 2012; *Onarheim et al.*, 2014). Nevertheless, there are still uncertainties related to the drivers of sea ice loss. While Atlantic water related loss is the most obvious fingerprint of Atlanticfication, atmospheric processes by local and regional winds also play a role (e.g. *Ingvaldsen et al.*, 2021). Thus, there is still no comprehensive understanding of the role that upstream and regional oceanic and atmospheric forcing have in shaping the sea ice changes in the region.

In the western Fram Strait, the EGC is a cold current that is responsible for substantial sea ice discharge from the Arctic Ocean (averaging approximately 3,000 km^3 annually between 1950 and 2000) (*Vinje*, 2001b). This current is predominantly constrained to the western sector of the strait, where the EGC flows southward along the eastern continental margin of Greenland (*Aagaard and Coachman*, 1968; *Rudels et al.*, 2002), transporting sea ice and accompanying freshwater south, ultimately reaching the North Atlantic through the subpolar Labrador Sea.

1.3.2 Labrador Sea oceanography and the subpolar gyre

In the North Atlantic, a large portion of the NAC turns westward transporting the warm and salty Atlantic waters via the IC, forming the anticyclonic subpolar gyre (SPG) circulation (Figure 1.3). The IC releases heat to the atmosphere as it flows westward, where winter cooling of these surface waters causes convection and intermediate water formation in the Labrador Sea (*Lazier*, 1973). This overturning, which can extend as

deep as two kilometers, forms Labrador Sea Water (LSW), which then spreads into the greater North Atlantic Ocean and beyond as one of the major connections between the warm upper branch and the cold lower branch of the AMOC (*Pickart et al.*, 2002). The EGC, flowing southward from the Arctic Ocean with cold, fresh surface water mixes with the IC south of Greenland. Today, the relatively thin (< ca. 150 m) layer of cold, low-salinity Polar Water derived from the EGC, overlies the relatively warm Atlantic-source subsurface water masses derived from the IC.

Importantly, the SPG shares links between the North Atlantic, Labrador Sea with the Nordic Seas, Fram Strait and Arctic Ocean through the surface transport and exchange of heat, salinity, and freshwater (*Born and Stocker*, 2014; *Häkkinen and Rhines*, 2004). The cyclonic circulation of the SPG is a key mechanism for North Atlantic climate variability on a wide range of time scales, driven by both buoyancy and wind forcing (*Born and Stocker*, 2014; *Levermann and Born*, 2007; *Montoya et al.*, 2011), of which sea ice can influence both. While today there is little to no sea ice in the Labrador Sea, it has been found that increased freshwater input to the subpolar Labrador Sea associated with recent sea ice melting in the Arctic may have slowed down the Labrador Sea intermediate water formation, reducing the strength of the SPG, and by implication, the AMOC (*Yang et al.*, 2016). Thus, it has been found that only minor (freshwater) perturbations of the system can cause large shifts in the circulation of the SPG, with implications for the AMOC. Nevertheless the coupling between the SPG and the AMOC is complex, and it remains unclear if and how the SPG contributed to recent changes in the overturning circulation (*Lozier*, 2012; *Lozier et al.*, 2019). Despite the complex circulation coupling, the SPG's potential to alter mass, heat, and buoyancy, and alter climate across the North Atlantic, and beyond, makes it crucial to understand the mechanisms by, and timescales on, which the SPG can vary.

1.4 The Last Interglacial

The potential climatic implications of projected global warming can be understood by investigating past periods in Earth's history that were as warm or warmer than today. The LIG, Marine Isotope Stage 5e (MIS 5e), is one such period that is commonly used as a comparison to the ongoing Holocene interglacial. It has many features in common with model projections of future climate. For example, the LIG climate was characterized by Northern Hemisphere continental summer temperatures that are similar to those expected for the coming centuries. Globally, it is believed to have been at least 2 °C warmer than the present (*Masson-Delmotte et al.*, 2013), while polar temperatures in both hemispheres were about 3–5 °C warmer than today (*Jansen et al.*, 2007). This

is comparable to the 3–6 °C of Arctic warming that is expected to accompany 1–2 °C of global warming (*Kattsov et al.*, 2004), due to polar amplification (e.g. *cape last interglacial project members*, 2006). Also, sea level is estimated to have been 6–9 m above present-day levels, with a significantly reduced Greenland Ice Sheet (GIS) accounting for 0.6–3.5 m of this sea level rise (*Dutton et al.*, 2015).

However, the LIG warmth was forced under different orbital configurations than present, and greenhouse gas concentrations which drive much of modern warming, remained at preindustrial levels during MIS 5e (*Lüthi et al.*, 2008). Thus, the LIG is no perfect analogue for a projected future warm climate, but it does represent an excellent case study to investigate climate feedbacks shaping the response to orbital forcing, gives valuable insights into the climate and environmental responses that may be triggered in a future warmer world, and it provides a reference of interglacial climate variability in the absence of anthropogenic forcing.

Indeed, around 128 thousand years ago, astronomical forcing (*Berger*, 1988) lead to insolation maximum and ice volume minimum (*Shackleton*, 1969), leading to the pacing of the LIG. The response of the climate system to the astronomical forcing includes a diversity of feedbacks involving the atmosphere, ocean, sea ice, vegetation and land ice (*Rohling et al.*, 2012), leading to climate variability and instability superimposed on insolation trends. Starting in the early 1980s, studies suggested that AMOC changes could drive climate fluctuations (*Broecker and Peng*, 1982; *Broecker*, 1991, and references therein) on millennial timescales, and even on decadel, or rapid, timescales (*Stocker and Wright*, 1991; *Rahmstorf*, 1994). The variability in the AMOC's strength and structure as the leading candidate for generating climate variability was discussed in the context of glacial periods, while interglacial periods were long considered to be accompanied by a relatively stable and vigorous AMOC. However, more recently, this interglacial stability has been questioned (*Galaasen et al.*, 2014, 2020).

1.4.1 North Atlantic climate variability

LIG climate variability, and instability, has been documented in a range of marine and terrestrial proxy records from the North Atlantic and Europe, involving several cooling events, consistent with low-intensity disruptions of the overturning circulation (C28-C24 in Figure 1.4) (*Tzedakis et al.*, 2018). Interglacial variability is evident in isotopic, faunal and ice rafted debris (IRD) from marine sediment cores, which revealed the presence of a series of surface-cooling events in the North Atlantic (e.g. *Chapman and Shackleton*, 1999; *Irvali et al.*, 2012; *Irvali et al.*, 2016; *Mokeddem et al.*, 2014; *Oppo et al.*, 2006; *Sánchez Goñi et al.*, 2012). Sea surface temperature (SST) fluctuations have

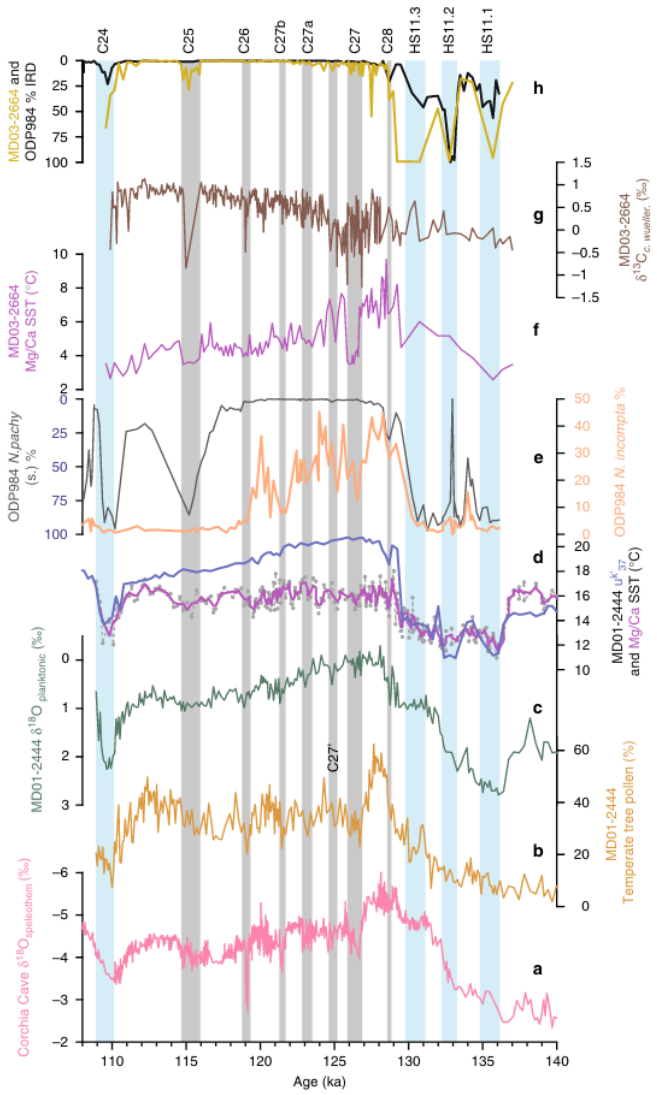

Figure 1.4: Paleoclimate records compiled by *Tzedakis et al.* (2018) demonstrating the widespread climate variability within the Last Interglacial (LIG); a) cave-stacked $\delta^{18}O_{speleothem}$; b) temperate tree pollen; c) $\delta^{18}O_{planktic}$; d) alkenone $U^{k'}_{37}$ and Mg/Ca sea surface temperatures; e) *N. pachyderma* (s) and *N. incompta* percentages f) Mg/Ca reconstructed sea surface temperature; g) δ^{13}C *C. wuellerstorfi*; h) ice rafted debris (IRD). Light blue vertical bars indicate Heinrich Stadial events; grey bars indicate cold events.

been detected in the Nordic Seas (*Fronval and Jansen*, 1996) and North Atlantic (*Irvali et al.*, 2012; *Irvali et al.*, 2016), and lithological variations in the subpolar North Atlantic have indicated multiple incursions of drift ice (*Bond et al.*, 2001). European pollen and

speleothem records (*Moseley et al.*, 2015 ;*Regattieri et al.*, 2016; *Tzedakis et al.*, 2018) demonstrate LIG climate variability, and in numerical simulations, centennial-scale cooling at the surface of the North Atlantic converge towards moderate AMOC weakening (*Tzedakis et al.*, 2018). Additionally, the Greenland NEEM LIG record, reconstructed from a folded ice core, indicates multiple episodes of extensive ice surface melting superimposed on a relatively smooth surface temperature profile with gradual cooling following early peak conditions (*neem community members*, 2013).

One of the largest interglacial excursions was the "C27 cooling event" which likely experienced a major decline in NADW (*Galaasen et al.*, 2014). These authors documented large and abrupt variability in bottom water mass properties (δ^{13}C) during the LIG. This event was compared to the "8.2 event" during the Holocene interglacial where a major decline in NADW in the deep Atlantic (*Kleiven et al.*, 2008), and a weakening of the overturning circulation was caused by a major freshwater outburst associated with ice sheet decay. Major declines in NADW in the deep Atlantic were also demonstrated for the three preceding interglacial periods (*Galaasen et al.*, 2020). Both freshwater and/or atmospheric forcing likely triggered reductions in the AMOC and caused the centennial-scale cooling at the surface of the North Atlantic (*Tzedakis et al.*, 2018). However, also in the latter MIS 5e, transients in the bottom water δ^{13}C suggests that reductions in NADW occurred. During this time conditions favored ice mass expansion rather than rapid retreat, suggesting that decaying ice sheets, and associated freshwater outburst, was likely not the main triggering of these rapid NADW reductions (*Galaasen et al.*, 2014). This illustrates that we still lack an understanding of the mechanisms that may lead to climate variability, instability, and how the surface ocean variability is linked with the deep circulation branch of the AMOC.

1.4.2 Sea ice and North Atlantic climate variability

Alterations in the circulation of the SPG has been extensively deliberated as a plausible mechanism contributing to the widespread variability in the North Atlantic LIG climate (e.g. *Irvali et al.*, 2012, 2016; *Mokeddem et al.*, 2014; *Tzedakis et al.*, 2018). This is attributed to the SPG's links throughout the North Atlantic via surface transport of heat, salinity, and freshwater, coupled with its potential to influence the AMOC as outlined in Chapter 1.3.2. Sea ice holds the potential to influence both wind and buoyancy forcing to which the SPG reacts sensitively. Furthermore, buoyancy forcing affects deep water formation in the subpolar North Atlantic, which in turn affects the strength of the AMOC. Thus, in the subpolar Labrador Sea where deep water formation occurs, the SPG could be especially sensitive to the extent of sea ice and its associated freshwater.

Indeed, previous studies have suggested that sea ice and its associated melt in the Labrador Sea could have modulated the SPG circulation on centennial timescales within the LIG (*Galaasen et al.*, 2014) and during the last glacial inception (*Born et al.*, 2010). However, the absence of direct sea ice proxy evidence from this region impedes the validation of these hypotheses. While sea ice reconstructions within this specific region and time interval are limited, broader compilations (e.g. *Kageyama et al.*, 2021) indicate that south of 79°N, the Atlantic and Nordic Seas were devoid of sea ice during the LIG. Evidence from the preceding MIS 6 and Termination II (T II) indicates that sea ice did exist in the subpolar Labrador Sea (*Irvali et al.*, 2012) and further north along the East Greenland Margin (*Zhuravleva et al.*, 2017a). Nevertheless, these existing data are indirect and do not resolve the potential extent of sea ice within the LIG. Our limited knowledge about sea ice extent and variability in the North Atlantic SPG region, crucially hinders an evaluation of its potential role for modulating ocean circulation and the SPG within the LIG and on glacial-interglacial timescales.

1.4.3 Arctic sea ice and unresolved questions

The Arctic Ocean, and the adjacent Fram Strait are more widely researched in the context of sea ice throughout the past. The Fram Strait is characterised by a complex interplay between atmospheric circulation, ocean currents and ice sheet dynamics, which all leads to profound fluctuations in sea ice conditions through time, providing valuable insights into the Earth's climatic history. During the LIG, and its glacial transitions, the responses of sea ice to various internal and external forces in the Fram Strait resulted in highly dynamic sea ice conditions. While some regions encountered significantly reduced sea ice, resulting in seasonally ice-free conditions (*Stein et al.*, 2017), others exhibited extensive and even perennial sea ice cover (*Kremer et al.*, 2018a; *Kremer et al.*, 2018b). This variability was found to be intricately linked to the fluctuations of warm Atlantic water influence via the WSC and the extent of the Svalbard Barents Sea Ice Sheet (SBIS), where katabatic winds played a role in the opening polynyas to the west and north of the SBIS.

Nonetheless, discrepancies in the climatic evolution of the LIG persist, specifically in relation to the influx and influence of Atlantic waters during this period. While the importance of Atlantic heat flux for sea surface properties in the Fram Strait is well established (chapter 1.3.1), different perspectives exist regarding the strength and extent of Atlantic water influence during the LIG (e.g. *Zhuravleva et al.*, 2017b). Variability in Atlantic water influx, and its influence on the surface ocean and sea ice conditions, have been discussed in connection, freshwater inputs, stratification regimes, wind patterns,

the SPG configuration, and different surface ocean circulation pathways. Nevertheless, understanding the mechanisms regulating the northward directed Atlantic water heat transport remains under discussion, but is crucial to understand in the context of sea ice variability, and the the role of sea ice, and Atlantic waters in climate variability.

Also under debate is the state of the central Arctic Ocean during the LIG and its glacial transitions. There is no consensus on whether the Arctic Ocean was seasonally sea ice free or permanently sea ice covered during the LIG. In the central Arctic Ocean, *Stein et al.* (2017) using biomarkers showed that it was likely covered by extensive to perennial sea ice throughout the LIG, although with a reduced sea ice cover in comparison to the modern Arctic Ocean during the summer season. In contrast, a modeling study by *Guarino et al.* (2020) and a foraminiferal assemblage study by *Vermassen et al.* (2023) suggest that the central Arctic Ocean during the LIG was seasonally sea ice-free during the LIG. Equally debated, is whether the Arctic Ocean during the preceding glacial MIS 6 was covered by a massive thick floating ice shelf extending from the Arctic Ocean to the Fram Strait (*Jakobsson et al.*, 2016; *Geibert et al.*, 2021), whether it was covered with perennial sea ice (*Stein et al.*, 2017), or seasonally sea ice covered with multiple events of ice shelf expansion (*Xiao et al.*, 2020). These discrepancies underscore the imperative need to further investigate sea ice variability in the Arctic region. One key to this understanding is to is to fully understand the environmental conditions and mechanisms that control sea ice in the Fram Strait, where the exchange of water masses, and sensitive sea ice conditions may help elucidate an Arctic-propagating climate signal.

Chapter 2

Objectives

The overall aim of this thesis is to better understand the role of sea ice in the Earth's ice-ocean-climate system throughout the past warmer-than-present LIG climate and the glacial-interglacial transitions characterized by profound climatic and environmental changes. To achieve this aim, I use mainly molecular biomarkers and dinoflagellate cyst fossil assemblages from deep-sea sediment cores. This multiproxy approach provides evidence on the natural variability of sea ice, its extent, and the surface ocean hydrography for the glacial late MIS 6 , through T II, MIS 5e/LIG, and the last glacial inception into MIS 5d, covering a total time span between ca. 140–90 thousand years ago.

Today, and in the past, the Labrador Sea is characterised by the dynamic circulation of the SPG. Sea ice has the potential to influence the SPG, but its variability and extent are poorly documented from the subpolar Labrador Sea through past interglacial intervals. We hypothesize that *sea ice modulated the SPG circulation during the LIG and its glacial transitions* (Paper I). In the eastern Fram Strait sea ice variability, and its decline, is today strongly linked with the inflow of warm Atlantic waters, leading to "Atlantification" of the Arctic regions. We hypothesize that *during the LIG and its glacial to interglacial climate transitions, sea ice together with Atlantic waters and the surrounding ice sheets played an important role in shaping the ocean-climate variability in the eastern Fram Strait* (Paper II). Based on these hypotheses our objectives (Paper I and II) are:

I. To reconstruct sea ice variability in the eastern Fram Strait and the subpolar Labrador Sea on centennial-scale resolution from Late MIS 6, through T II, MIS 5e, and into MIS 5d.

II. To put the sea ice variability and surface hydrography during late MIS 6, T II, MIS 5e and MIS 5d into a broader context of ice sheet evolution and ocean-climate

variability in the (Sub)Arctic Oceans.

Reconstructions of past Arctic and Subarctic sea ice variability crucially rely on proxies. Dinoflagellate cysts and biomarkers are commonly used proxies for sea ice reconstructions. Yet, these sea ice proxies have strengths and weaknesses (*de Vernal et al.*, 2013a). To improve the sea-ice paleo-proxy toolbox, we investigated the potential of using stable oxygen isotopes of foraminifers as sea ice indicators in the subpolar Labrador Sea, discussed in the context of earlier observations by *Lund et al.* (2021) and *Hillaire-Marcel et al.* (2001). Specifically, we hypothesize that *the difference between benthic and planktic foraminiferal stable oxygen isotopes can be used to detect sea ice in the subpolar North Atlantic* (Paper III). Based on this hypothesis our objective (paper III) is:

III. To evaluate the oxygen isotopes of coupled planktic and benthic foraminiferas as a paleo-sea-ice proxy.

Chapter 3

Approach and Methodology

The methodological approach of this PhD thesis relies mainly on the identification and quantification of molecular biomarkers and dinoflagellate cyst fossil assemblages. Both proxies originate from past-living phytoplankton and algae that once thrived in the surface ocean under different environmental conditions. After the death and decomposition of the living organisms, their fossil and geochemical remnants may be preserved in the sedimentary record. Their identification within a sediment sample hence serves as direct indications, "fingerprints", of the past occurrence of the respective source organism at the sampling site. Thus, they serve as natural archives of past climate variability that reflects changes in sea ice cover, surface ocean hydrographic conditions, and productivity on geological timescales. In this thesis, these proxies are supplemented by sedimentology, stable isotopes and inorganic geochemistry for further evaluation of sea ice and surface ocean conditions, and for robust construction of LIG chronologies.

The reconstructions for this thesis are based on two sediment cores from the subpolar Labrador Sea and the Fram Strait (Figure 1.3). Core GS16-204-22-CC-B (22CC-B) was collected by the Ice2Ice research group onboard Research Vessel G.O. Sars in 2016. The CAGE19-3-KH14-GPC02 (KH-14) was collected with the CAGE- Centre for Gas Hydrates, University of Tromsø onboard the Research Vessel Kronprins Haakon in October 2019 (Table 3.1). These cores were specifically selected for the AGENSI project, because the project required uncontaminated and properly stored sediment cores for ancient DNA analyses. Core 22CC-B was split onboard and immediately frozen to be sampled later for ancient DNA, biomarkers and palynology in clean conditions. Core KH-14 was left unopened on the ship, and was later split and sampled for ancient DNA, biomarkers and palynology in the ancient DNA laboratory at NORCE.

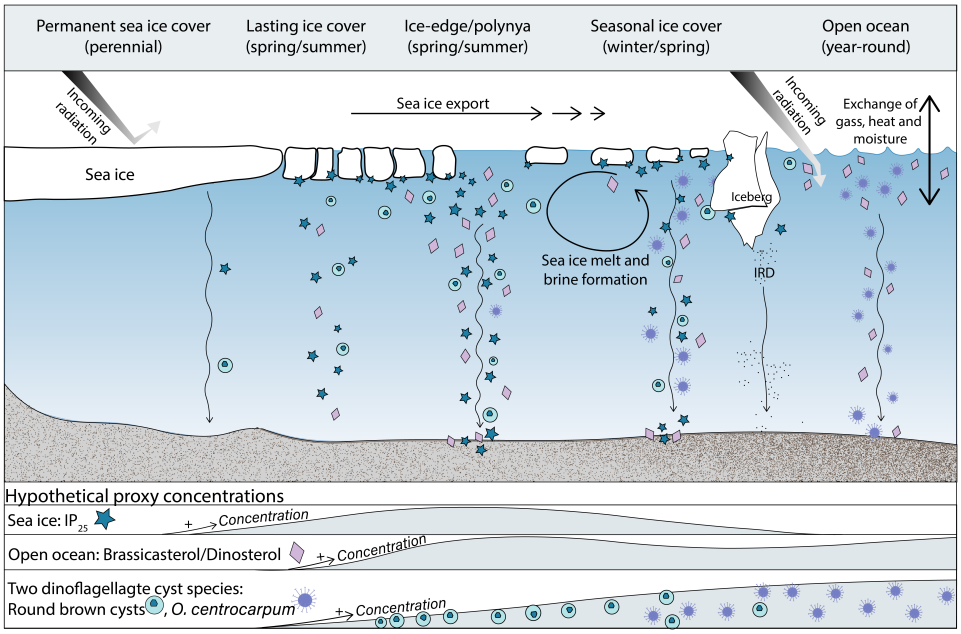

Figure 3.1: Schematic illustration of different influences sea ice exerts in the ice-ocean-atmosphere system (see section 1.2 for details) and on species assemblages in the water column and in the sediment. Illustrated are the idealized concentrations of the sea ice biomarker IP_{25}, and the open ocean biomarkers dinosterol and brassicasterol from perennial sea ice to open water conditions based on the original figure from *Müller et al.* (2011). IP_{25} concentrations are highest in ice-edge/polynya conditions, moderate under lasting sea ice, and seasonal sea ice, but zero under permanent sea ice and in open ocean conditions. The open water biomarkers increase with increasing open water and higher seasonality, peak in ice-edge/polynya conditions, but are zero under permanent sea ice. Additionally, illustrated is the change in the relative abundance of the dinoflagellate cyst species *O. centrocarpum* (typical Atlantic water tracer) and round brown cysts (typical sea ice tracers) from perennial sea ice to open ocean conditions under direct influence of Atlantic water. Further details on how biomarkers and dinocyst taxa relate to sea ice, see sections 3.1 and 3.2.

Table 3.1: Core Identification, coordinates, and the water depth (meters below sea level) for the two cores (Labrador Sea and Fram Strait) investigated in this thesis.

Core ID	Latitude	Longitude	Water depth (m)
GS16-204-22CC-B	58°02.83′N	47°02.36′W	3160
CAGE-19-3-KH-14-GPC02	77°31.38′N	8°08.28′E	2275

3.1 Biomarker approach

3.1.1 IP_{25}

Some microorganisms produce molecular organic compounds that may preserve in the sediments after the organisms that produced the compounds decays. The identification of these specific organic compounds, known as biomarkers, are geochemical fingerprints of the respective source organism. After its discovery by *Belt et al.* (2007), the biomarker IP_{25} (**I**ce **P**roxy with **25** carbon atoms; Figure 3.2) has been established as a reliable proxy for the presence of seasonal spring sea ice in the Arctic and Subarctic (*Brown et al.*, 2014; *Belt*, 2018, 2019; *Stein et al.*, 2012; *Belt and Müller*, 2013; *Xiao et al.*, 2015; *Kolling et al.*, 2020). IP_{25} is a mono-unsaturated highly branched isoprenoid (HBI) alkene biomarker that is exclusively produced by a few diatom species living in Arctic sea ice (*Brown et al.*, 2014; *Limoges et al.*, 2018), namely by the taxa of groups of *Haslea* and *Pleurosigma*, that is *Haslea crucigeroides* (and/or *Haslea spicula*), *Haslea kjellmanii*, and *Pleurosigma struxbergii* var. *rhomboides* (*Brown et al.*, 2014). These microalgae occupy the underside of sea ice, where they receive enough nutrient-rich water and light, penetrating through the ice, which favors their growth (*Dieckmann and Hellmer*, 2010). When the ice melts or the diatoms die, their frustules may not be preserved in the sediment, but their biomarkers (IP_{25}) are preserved. IP_{25} has successfully been used in sea ice reconstructions from Arctic and Subarctic regions covering the last glacial cycle (last 130 thousand years), the Pliocene (ca 4 million years), and even the Miocene (>5 million years) (*Stein and Fahl*, 2013; *Knies et al.*, 2014; *Hoff et al.*, 2016; *Stein et al.*, 2016, 2022), proving itself to be a sensitive and stable proxy for Arctic sea ice.

In modern surface sediments from the Arctic and Subarctic Oceans, increased abun-

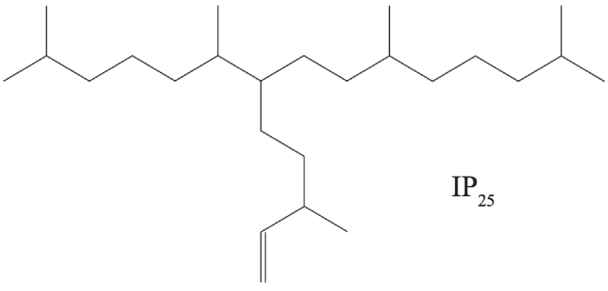

Figure 3.2: The chemical structure of IP_{25} after (*Belt et al.*, 2007). The double bond is located at C_{23-24}

dance of IP_{25} is clearly associated with overlying seasonal sea ice (*Müller et al.*, 2011; *Navarro-Rodriguez et al.*, 2013; *Stoynova et al.*, 2013; *Xiao et al.*, 2015; *Kolling et al.*, 2020). However, reconstructions of sea ice in the paleorecord are not without challenges. For example, permanent sea ice and open water conditions both are characterized by IP_{25} concentrations of zero. These similar outcomes occur because permanent sea ice limits light and nutrient availability which are required for the growth of sea ice phytoplankton and consequently IP_{25} is absent. Likewise, IP_{25} concentrations are zero in open waters because the habitat for the ice algae is missing. Such ambiguity of the signal from permanent sea ice vs. open ocean requires that IP_{25} is analysed in combination with biomarkers reflecting open waters. Two such biomarkers are brassicasterol and dinosterol, which are sterols that are mainly produced by phytoplankton living under ice-free conditions. Their abundance increases close to the sea ice edge (*Stein and Stax*, 1991) or oceanic fronts (*Hirche et al.*, 1991) due to higher abundance of nutrients favoring phytoplankton growth. Dinosterol is almost exclusively produced by (marine) dinoflagellates, although it is not found in all dinoflagellate species (Volkman et al., 1993 and refs therein). Brassicasterol is largely synthesized by marine diatoms, but nevertheless, also by coccolithophores, freshwater diatoms, and perhaps even sea ice diatoms (*Volkman*, 1986; *Fahl and Stein*, 2012; *Belt and Müller*, 2013). Therefor they should also be evaluated with some caution (see below).

3.1.2 The PIP_{25} index

Müller et al. (2011) combined the IP_{25} sea ice proxy with open-water phytoplankton biomarkers, brassicasterol (P_BIP_{25}) and dinosterol (P_DIP_{25}), in the PIP_{25} index to create more reliable estimates of sea ice conditions, and is calculated as:

$$PIP_{25} = IP_{25} \ / \ (IP_{25} + (\text{phytoplankton biomarker} \times C))$$

Here, the balance factor C is included to counterbalance the naturally higher concentrations of the sterols compared to IP_{25}.

$$C = \text{mean } IP_{25} \text{ concentration} \ / \ \text{mean phytoplankton biomarker concentration}$$

With the calculation of the PIP_{25} index sea ice conditions may be quantitatively inferred. Following *Müller et al.* (2011), high PIP_{25} values (0.75–1) refer to a permanent sea ice cover throughout the year, intermediate values (0.5–0.75) reflect seasonal ice cover or a stable ice edge, and low values (0–0.5) indicate less ice or ice-free conditions. Nevertheless, the authors point out that individual biomarker concentrations should always be considered alongside the PIP_{25} indexes when distinguishing different sea ice

environments. For example, when low IP_{25} and phytoplankton biomarker concentrations co-occur, PIP_{25} values may be both high and low, even though the combined low concentrations likely refer to permanent ice conditions. Likewise, co-occurrence of high IP_{25} and phytoplankton biomarker concentrations, likely reflecting marginal ice zone or seasonal ice conditions, can yield the same PIP_{25} values as the above example.

Additional challenges to be aware of involve the unequivocal source identification of all compounds used in the PIP_{25} index-calculation. Brassicasterol and dinosterol are biosynthesized by a relatively broad group of marine phytoplankton (*Boon et al.*, 1979; *Robinson et al.*, 1984; *Volkman et al.*, 1998) and their sedimentary signal might represent variable environmental conditions. Brassicasterol is produced to a small extent by freshwater diatoms (*Yunker et al.*, 1995; *Belt et al.*, 2013), complicating the use of the P_BIP_{25} index in regions of enhanced river runoff (*Fahl and Stein*, 1999). Furthermore, selective biomarker degradation of the structurally differing IP_{25} and phytoplankton compounds may bias the PIP_{25} interpretation (*Stein et al.*, 2012; *Navarro-Rodriguez et al.*, 2013; *Belt and Müller*, 2013). Despite potential limitations, both P_BIP_{25} and P_DIP_{25} show a positive correlation with modern satellite-based sea ice observations (e.g. *Xiao et al.*, 2015; *Kolling et al.*, 2020) and thus we can define paleo sea ice conditions more quantitatively.

3.1.3 "Other" biomarkers

Alongside IP_{25}, there are other HBIs that may be useful in paleoenvironmental reconstructions. For example, HBI II, also known as $IPSO_{25}$ (**I**ce **P**roxy for the **S**outhern **O**cean with **25** carbon atoms) is produced by sea ice/land-fast ice-dwelling diatoms in the Southern Ocean (*Belt et al.*, 2016) and has been proposed as a sea ice proxy there. Although its origin and potential as an environmental proxy in the Northern Hemisphere is unclear, it is often observed together with IP_{25}. Thus, *Belt* (2018) postulated that HBI II may represent an "even better" sea ice proxy than IP_{25} or at least be a useful substitute in cases where IP_{25} is absent. Additionally, HBI trienes (HBI-III), are believed to be synthesized by a small number of marine diatom taxa but its specific ecological controls are not fully understood so far (*Belt et al.*, 2015). Investigation of surface sediment samples from the Barents Sea has revealed that HBI-III is present under open waters, extremely reduced or absent under seasonal and perennial sea ice, and occurs in maximum abundance underneath the marginal ice zone (*Belt et al.*, 2015). Accordingly, HBI-III is hypothesized to represent a potential proxy for retreating sea ice or the marginal ice zone both in the Northern (*Belt et al.*, 2015) and Southern Hemispheres (*Collins et al.*, 2013a).

The sterol biomarkers, such as campesterol and sitosterol, are produced by higher land

plants (*Volkman*, 1986) and can reflect input of terrigenous material to the ocean, similar to IRD. However, marine sea grass has also been shown to potentially produce these sterols (*Rontani et al.*, 2014), but nonetheless, sitosterol and campesterol are often considered for terrigenous input in the Arctic Ocean.

3.2 Biomarker laboratory procedures

In the first step sediment samples were freeze-dried and homogenised. Total organic carbon (TOC) content was measured on 90 mg of this sediment powder using a carbon-sulphur determinator (CS- 125, Leco), after removal of carbonate by adding 500 ml hydrochloric acid to each sample. For biomarker extraction ca. 5 g of the freeze-dried and homogenized sediment was taken and various internal standards were added to each sample for quantification purposes. Thereafter, the biomarkers were extracted using ultrasonication, and centrifugation. The total extracts were then separated into a hydrocarbon fraction and a sterol fraction using open-column chromatography, and analyzed by gas chromatography-mass-spectrometry (GC-MS). For details on laboratory and instrumental measurements see Papers I and II.

Individual compound identification was based on comparisons of their retention times with that of reference compounds and on comparisons of their mass spectra with published data (IP_{25}: (*Belt et al.*, 2007); HBI II: (*Johns et al.*, 1999); HBI III: (*Belt et al.*, 2000); sterols: (*Boon et al.*, 1979; *Volkman*, 1986). Biomarker concentrations were calculated on the basis of their individual GC-MS ion responses compared with those of respective internal standards, using the formula:

$$\text{Compound } [\mu\text{g/g sed}] = ((A_{compound}/A_{IStd}) \text{ x } \mu\text{g IStd}) \text{ / g sediment x Cal.factor}$$

Here, A_{IStd} and $A_{compound}$ refer to the integrated peak Areas of the internal standard and the target compound, respectively; μg IStd refers to the amount of internal standard added to the sediment prior to extraction; Cal.factor is a calibration factor that is generated when the GC-MS instrumental settings change (*Fahl and Stein*, 2012).

IP_{25}, HBI II, and the trienes were quantified using their molecular ions m/z 350 (IP_{25}; Figure 3.3), 348 (HBI II), and 346 (trienes), in relation to the abundance fragment ion m/z 266 for 7-HND. For sterols, the molecular ions were m/z 470 for brassicasterol, m/z 500 for dinosterol, m/z 486 for sitosterol, m/z 472 for campesterol. The quantification was done via the integration of peak areas from the selected ion monitoring (SIM) mode allowing the detection of low concentrations. Concentrations of HBI biomarkers were calculated in relation to the internal standard 7-HND, and concentrations of sterols to

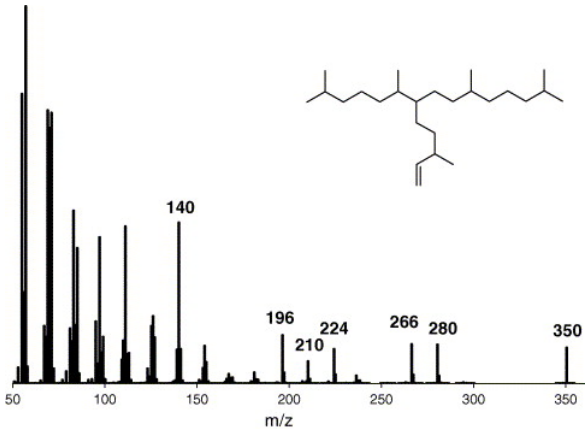

Figure 3.3: The characteristic mass fragmentation pattern corresponding to IP_{25} (*Belt et al.*, 2007).

the internal standards androstanol, which are assumed to be affected equally under the extraction and analytical process as the biomarkers.

All biomarker concentrations are normalised to the TOC, and all chemical sample preparations and biomarker analyses were performed in the organic geochemical laboratory facilities of the Alfred Wegener Institute, Bremerhaven, Germany. More methodological details on biomarker analyses are given in Papers I-II. All data for paper I is available on Pangaea, and will become available for paper II upon publication.

3.3 Dinoflagellate cyst approach

3.3.1 Background and identification

Dinoflagellate cysts have proved to be invaluable for paleoceanographic reconstructions in recent and Quaternary marine sediments, especially in high latitudes where other marine calcareous or siliceous proxies are less abundant (e.g. *de Vernal et al.*, 1997, 2013b, 2020). While originally used as stratigraphic markers in the petroleum industry, the growing body of knowledge about the relationship between the biological dinoflagellate (theca) and their cysts have unraveled their paleoecological and paleoclimatic value for late Quaternary palaeoceanographic studies. Dinoflagellate cysts are produced by dinoflagellates, which are microscopic eukaryotic flagellated algae in the kingdom of Chromalveolata (*Adl et al.*, 2005) and are a major part of the marine primary productivity, together with diatoms and coccolithophorids. As part of their life cycle, some dinoflag-

ellate species (ca. 15%; *Head*, 1996) produce organic walled cysts that are deposited and fossilize in sediments. These fossil remains are referred to as dinoflagellate cysts, or dinocysts.

The morphology of virtually all dinocysts is species-specific. Identification of different dinocyst species is usually conducted under light microscopy. The dinocysts have a series of characteristics that allow their taxonomic identification. Firstly, the presence of an archeopyle (Figure 3.4B) and any traces of tabulation (Figure 3.4D) are key features typical for dinocysts. An archeopyle is the opening in the dinocyst formed by the release of a single plate or group of plates. Tabulation is the pattern according to which the dinoflagellates external plates are arranged (*Evitt*, 1985). Careful microscopical observation of minute morphological details may allow identification onto species level even if the archeopyle and tabulation cannot unequivocally be identified. Morphological features such as color, size and shape of the cyst body, number of wall layers, structure, and ornamentation (Figure 3.4E) of cyst wall, and form and length of processes (Figure 3.4C, F) may also be highly diagnostic so that even a crumpled specimen, with no obviously signs of tabulation, can be identified (*Evitt*, 1985; *Matthiessen et al.*, 2005).

3.3.2 Paleo-ecology of dinoflagellate cysts

Dinocyst assemblages maintain relatively high taxonomic diversity across both inner neritic–oceanic and glacial–interglacial transitions even at relatively high latitudes. Dinoflagellates employ a range of trophic strategies including phototrophy, heterotrophy and mixotrophy (*Jeong et al.*, 2010), resulting in different ecological constraints. Thus, upon sedimentation, the cysts generally reflect the distribution of their respective motile stages in the upper water column which reflects the interplay between temperature, salinity, nutrients, sea ice cover, and light availability. A number of extensive surface sediment studies have established the relationship between dinocyst assemblage distribution and upper water mass properties in the Northern latitudes (e.g. *Rochon et al.*, 1999; *Marret et al.*, 2004; *Matthiessen et al.*, 2005; *Zonneveld et al.*, 2013; *de Vernal et al.*, 2020).

Among the phototrophic taxa, the most commonly found dinocysts in the high northern latitude surface sediment (n=1968) database from *de Vernal et al.* (2020) are *Operculodinium centrocarpum, Nematosphaeropsis labyrinthus, Spiniferites elongatus, Spiniferites ramosus* and cysts of *Pentapharsodinium dalei*. Where *O. centrocarpum* is unquestionably cosmopolitan, *N. labyrinthus* and *S. ramosus* appear rarely in the Arctic Ocean, and the cyst of *P. dalei* and *S. elongatus* have boreal–polar distributions. Among other common phototrophic taxa, *Impagidinium pallidum* is boreal–Subarctic, *Bitectatodinium tepikiense* and *Impagidinium sphaericum* occur mostly

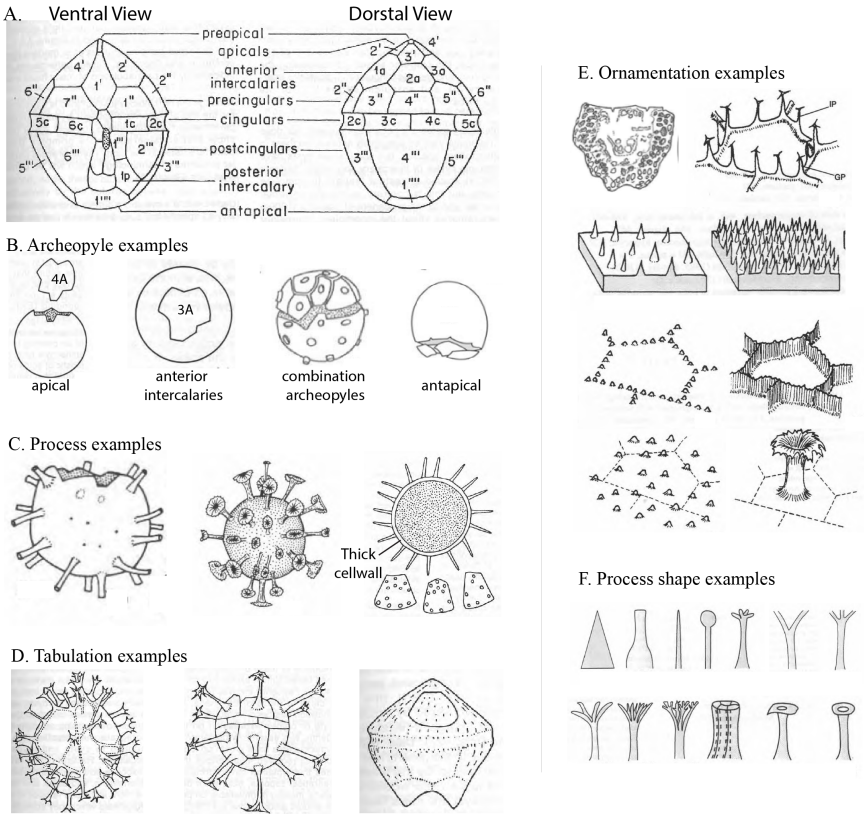

Figure 3.4: Schematic of the characteristics of a dinoflagellate cyst that can be used to identify the species; A) location and name of the different plate rows in two opposing views of the orientation of a dinoflagellate, ventral and dorsal, B) examples of different archeopyles, C) examples of processes on the cyst wall, D) examples of tabulation of the cyst wall, E) examples of ornamentation, F) examples of different processes. All figures are from *Evitt* (1985) and *Williams et al.* (2000).

at mid-latitudes of the North Atlantic, and taxa in abundant in low to middle latitudes include *Spiniferites mirabilis, Impagidinium aculeatum, Impagidinium patulum* and *Lingulodinium machaerophorum*. Examples of species found in the LIG sediments of the subpolar Labrador Sea (Core 22CC-B) are shown in Figure 3.5.

The above phototrophic dinocysts require seasonally open water for photosynthesis. Conversely, heterotrophic taxa are influenced by biotic factors including prey availability. This leads to the highest proportions of heterotrophic taxa in the coastal zones of the eastern North Pacific marked by upwelling, and in the circum-Arctic where sea ice cover develops seasonally (*de Vernal et al.*, 2020). Among the heterotrophic taxa the genus *Brigantedinum* spp. is the most cosmopolitan. In surface sediments, it is not very diagnostic as it is an opportunistic genus, but nevertheless, its recovery from bottom

sediments may indicate good preservation since it is sensitive to degradation by oxidation (*Zonneveld et al.*, 2008). Sea ice and productivity are two of the factors most strongly linked with heterotopic taxa distribution (*de Vernal et al.*, 2020). Many subpolar and polar species occur in regions that are characterized by a variable seasonal duration of sea ice cover, with a distinct relationship to sea ice cover proven for some species. *Islandinium minutum* is the polar species that probably withstands the most adverse conditions with respect to sea-ice cover (*Rochon et al.*, 1999). This species occurs in sediment traps within the maximum limit of sea ice cover (*Harland and Pudsey*, 1999). Some species also have a direct relationship to sea ice which is the case for *Polarella glacialis*, one of the only cyst-forming species that thrive in land fast and pack ice. Thus, the cyst of *P. glacialis* may be a good qualitative indicator for sea ice cover in both polar regions (*Montresor et al.*, 2003). While its use as a paleo sea-ice indicator has been questioned due to its small size (>15 μm) in combination with poor preservation potential (*Matthiessen et al.*, 2005), more recent studies have shown a tight connection between (the cysts of) *P. glacialis* with seasonal sea ice, demonstrating a promising potential as a new paleo sea-ice proxy (*Limoges et al.*, 2018; *Harardóttir et al.*, 2024).

3.3.3 Challenges with the approach

When doing dinocyst-based palaeoceanographic interpretation, it is important to consider that several processes may bias the fossil dinocyst assemblage as it is identified under the microscope. A first bias comes from the fact that only ca. 10–15% from the known (∼2000) dinoflagellates produce fossilizable organic-walled cysts during their life cycle (e.g. *Head*, 1996). Thus, a fossil assemblage can inherently only provide an estimate for the diversity of the living assemblage from which it originated. Dinocysts have a sedimentary behavior comparable to fine silt and can therefore be subject to transport as they sink to the seafloor. However, laboratory experiments indicate that cysts sink relatively rapidly in the water column (e.g. *Anderson et al.*, 1985; *Zonneveld and Brummer*, 2000), and it is generally believed that transport by currents over long distances has only minor influences. Hence, the environmental conditions of the overlying surface water are well reflected by the assemblages in sediments (*Marret and Zonneveld*, 2003; *Matthiessen et al.*, 2005; *Marret et al.*, 2020; *de Vernal et al.*, 2020). If not completely *in situ*, the dinocysts can at least give insight into the prevailing currents and their physical parameters that might have brought the cysts into the area where they eventually settled. Palynomorphs, including dinocysts, in general have a high preservation potential. For organic matter, oxygen is generally the most destructive agent, and it has been shown that well-oxygenated bottom sediments can cause species-selective degradation of dinocysts (*Zonneveld et al.*, 2008; *Gray et al.*, 2017). Whereas the cysts of phototrophic

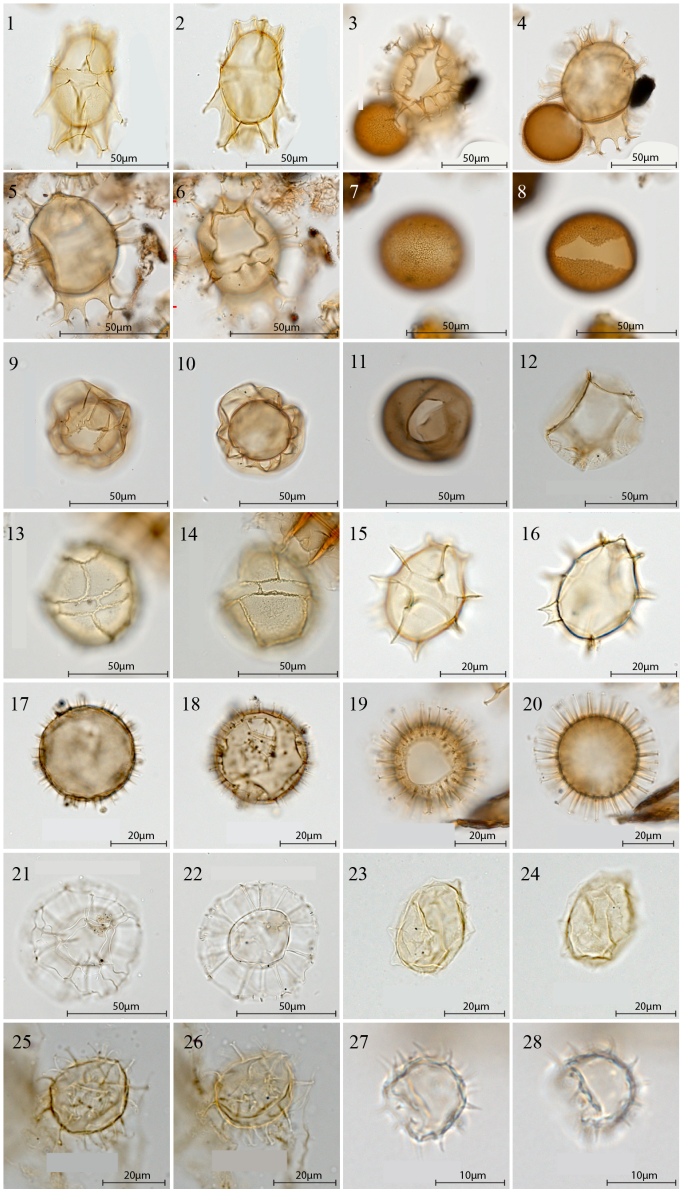

Figure 3.5: Light microscopy photographs of the typical species identified throughout the LIG from the subpolar Labrador Sea, Core 22CC-B. 1–2: *Spiniferites elongatus*, 3–6: *Spiniferites mirabilis*, 7–8: *Bitectatodinium tepikiense*, 9–10: *Ataxiodinium choane*, 11: *Brigantedinium simplex* (round brown cyst), 12: *Impagidinium pallidum*, 13–14: *Impagidinium sphaericum*, 15–16: *Impagidinium aculeatum*, 17–18: *Islandinium minutum*, 19–20: *Operculodinium centrocarpum* sensu Wall and Dale 1966, 21–22: *Nematosphaeropsis labyrinthus*, 23–24: cyst of *Scrippsiella trifida*, 25–26: cyst of *Pentapharsodinium dalei*, 27–28: cyst of *Polarella glacialis?*

taxa are fairly resistant to oxidation, cysts produced by heterotrophic taxa appear to be very sensitive to the presence of oxygen and are likely to be removed rapidly from the assemblages under well-oxygenated conditions (*Kodrans-Nsiah et al.*, 2008). An additional bias can come from microbial degradation and species-selective grazing by benthic deposit feeders. These processes, however, appear to be of minor importance for the common fossil cysts, as the benthic grazers seem to prefer naked, non-fossilizable and thus easily degradable cysts (*Persson and Rosenberg*, 2003).

Because of potential biases that occur for all biologically derived proxies, it is always important to apply a multiproxy approach. Such approaches will reveal potential biasing factors within one of the proxies, but may also reveal a larger picture of the surface ocean. For example, *De Schepper* (2013) brings up an example where an ocean site is located beneath a warm surface-water current. When a proxy records a cooling, what does that temperature drop really mean? We can question whether the current is still active but cooler, or if the current has shifted away from the site and cooler water taken its place. Geochemical proxies alone cannot answer these questions. Microfossil assemblages are, in this case, a major asset because assemblages provide information about fundamental water mass changes in the surface ocean, including shifts in ocean currents that are not necessarily picked up by a single geochemical proxy. This example highlights both the importance of dinocysts, and more generally microfossil assemblages, for reconstructions, and the use of multiproxy studies.

3.4 Dinoflagellate cyst laboratory preparation

Slides for dinocyst analysis under a microscope were prepared using a standard palynological preparation procedure (e.g. *De Schepper et al.*, 2017). The slides for this PhD thesis were prepared at Palynological Laboratory Services (Wales, UK) by Malcolm Jones. First, the mineral fraction was removed with cold hydrochloric and hydrofluoric acid. The palynological residue was sieved over a 10 μm polymer mesh before mounting on slides with glycerine jelly. One tablet of *Lycopodium clavatum* spores was added to each sample before the chemical treatment which allows calculation of dinocyst concentrations and associated errors (*Stockmarr*, 1971). The palynological slides were counted at x400 magnification for dinocyst assemblage analyses until a minimum of 300 in situ dinocysts were identified. If the dinocyst concentration was too low to reach this minimum threshold, the entire slide (ca. 20 non-overlapping traverses) was counted. Dinoflagellate cyst taxonomy and nomenclature followed *Williams et al.* (2017) (DINOFLAJ3).

More methodological details on dinocyst analyses and statistical analyses is given in the

manuscripts (Papers I-II).

3.5 Last Interglacial chronology

In this thesis, we define the LIG as the MIS 5e "plateau" of low benthic δ^{18}O values (Figure 3.6) which are assumed to mainly reflect the sea level high stand associated with ice sheet melting (*Shackleton et al.*, 2003). We base the age models of our studied sites on the alignment of δ^{18}O measured primarily on benthic foraminiferas to the reference core MD95-2042 δ^{18}O values (*Shackleton et al.*, 2002; *Shackleton et al.*, 2003) which is a high-resolution and commonly used chronology for the North Atlantic. For core MD95-2042, *Shackleton et al.* (2003) developed an age chronology for MIS 5e by constraining the low benthic isotopic plateau to 116.1 ka and 128 ka based on Uranium/Thorium dates of fossil coral reefs of the LIG sea level high stand (*Stirling et al.*, 1998). While this is only one reference chronology, a high consistency is evident with other chronologies that are orbitally tuned like the benthic δ^{18}O stacks "LR04" (*Lisiecki and Raymo*, 2005), NEAP18k (*Chapman and Shackleton*, 1999), and the benthic δ^{18}O stack of *Pisias et al.* (1984) and *Martinson et al.* (1987). This, provides independent validation of the individual reference chronologies. Additionally, the benthic δ^{18}O stacks are overall consistent with independent global ice volume chronology (*ngrip community members*, 2004) and insolation (*Laskar et al.*, 2004) (Figure 3.6), and thus provide workable floating timetables with a reasonably high resolution. For further details on how the chronologies for Core KH-14 and 22CC-B were constructed see papers I and II.

Nevertheless, the LIG chronology remains rather ambiguous. The LIG is a period that lies beyond the reach of radiocarbon dating, where a scarcity of radiometric dating techniques, and lack of precise absolute age constraints such as dated tephra layers and magnetic excursions, make dating of geological records across the LIG difficult. A detailed review of challenges related to LIG chronologies was provided by *Govin et al.* (2015).

Overall, a variety of existing time scales from different archives (i.e. sediment cores, ice cores, pollen, speleothems and corals) and record alignment techniques has lead to some confusion and a general lack of awareness of how chronologies are defined across the T II transition and the LIG. As a result, *Govin et al.* (2015) brings up examples where age uncertainties and discrepancies between the reference records have often been overlooked or even completely ignored in data compilations and subsequent model-data comparison. In addition, apparent age differences are generated by a lack of rigor in the way the LIG time periods are referred to. One example is the term "Eemian" which has been

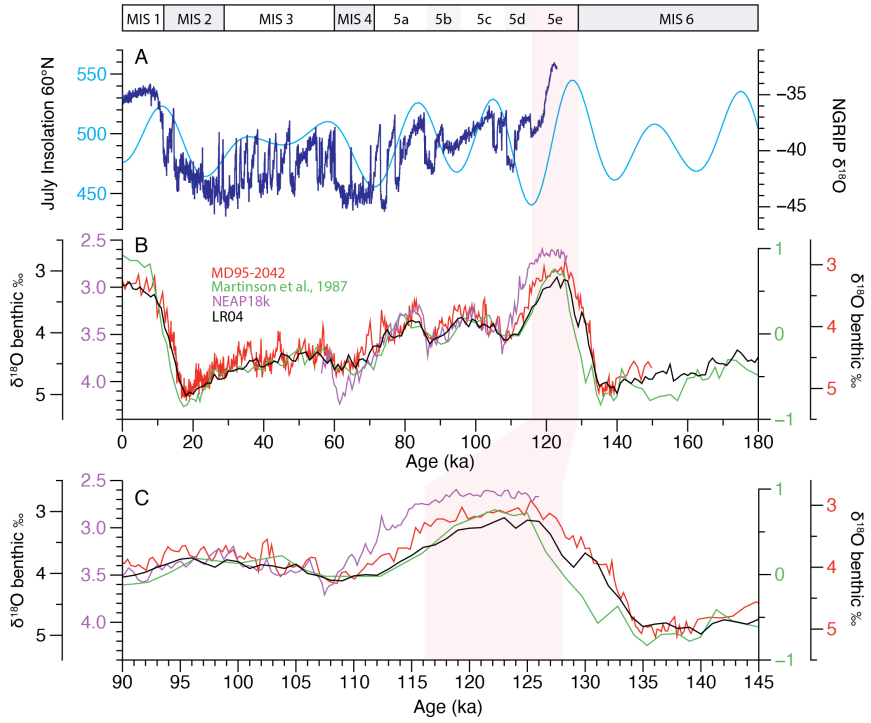

Figure 3.6: Late Pleistocene records of a) July northern hemisphere summer insolation (*Laskar et al.*, 2004), and the NGRIP ice core from Greenland (*ngrip community members*, 2004), B) reference chronologies of benthic foraminiferal δ^{18}O from MD95-2042 (*Shackleton et al.*, 2003), "LR04" (*Lisiecki and Raymo*, 2005), the δ^{18}O stack by *Pisias et al.* (1984) and *Martinson et al.* (1987), and NEAP18k (*Chapman and Shackleton*, 1999) for the last 180,000 years, C) Zoom-in on the LIG and its glacial transitions. Marine Isotope Stages (MIS) are numbered at the top and peak glacial stages are shaded in dark grey. MIS 5e is shaded in pink. All records are plotted on the age scale from the original publications.

frequently used interchangeably with "Last Interglacial" (e.g. *cape last interglacial project members*, 2006; *neem community members*, 2013). However, the Eemian is based on vegetation changes due to climate change, is a terrestrial stratigraphic concept (*Harting*, 1875), and is not synchronous with marine archives. These challenges are important to be aware of when working with LIG chronologies.

Due to the LIG ambiguity, to avoid misunderstanding, and in order to discuss LIG internal climate variability, it is crucial to be able to accurately compare individual records between sites. In reality, recognizing the LIG global climate from individual geologic records and the assignment of interglacial/glacial boundaries is often difficult. This is especially true for the high northern latitudes (e.g. the Nordic Seas, Fram Strait, the Labrador Sea) where deglacial overprints during early MIS 5e (e.g. *Bauch*, 1996;

Van Nieuwenhove et al., 2011; *Govin et al.*, 2012), and often sparse benthic foraminifera in sediments, makes core-to-core correlations challenging. Especially during T II, both benthic and planktonic isotopic records are affected by highly depleted $\delta^{18}O$ (e.g. *Rasmussen et al.*, 2003; *Risebrobakken et al.*, 2006). These negative $\delta^{18}O$ anomalies make the beginning of the LIG very difficult to identify in sediment cores from the high northern latitudes.

In some cases, when benthic foraminiferal $\delta^{18}O$ records are discontinuous or not available, it is necessary to align planktic foraminiferal $\delta^{18}O$ records to reference $\delta^{18}O$ stacks (e.g. *Bianchi and Gersonde*, 2002; *de Vernal and Hillaire-Marcel*, 2008). However, planktic $\delta^{18}O$ is even more sensitive than benthic $\delta^{18}O$ to local changes in sea surface temperature and non-glacioeustatic seawater $\delta^{18}O$ (e.g. meltwater input, local changes in precipitation and evaporation). Thus, uncertainties related to heterogeneous hydrographical changes in the ocean are even higher when aligning planktonic $\delta^{18}O$ records to reference $\delta^{18}O$ stacks. It is critical to overcome these challenges in order to decipher the nature and pattern of the LIG (*Govin et al.*, 2015). For further discussion on LIG chronologies, and some recommendations for future work see chapter 6.2.4.

Chapter 4

Summary of papers

Paper I: *Sea ice variability in the North Atlantic subpolar gyre throughout the Last Interglacial*

In paper I we investigate the nature and timing of sea ice variability in the subpolar Labrador Sea, a region influenced by the SPG and where deep water formation occurs. We aim to asses what role sea ice may have played in influencing the flow of the SPG circulation, ultimately to evaluate the potential of sea ice to drive or amplify ocean variability. For this purpose, we present new centennial-scale resolution sea ice algae biomarker IP_{25}, open-water phytoplankton sterols (brassicasterol and dinosterol), and dinoflagellate cyst assemblages from core GS16-204-22CC-B covering the LIG period and its glacial transitions, a total timespan of ca. 145–110 ka. Our results show that the late MIS 6 (145–135 ka) was overall characterized by extensive to perennial sea ice which started to break up occasionally during T II (135–128 ka). During the first phase of MIS 5e, the hydrography was highly variable. The initial 1,500 years (128–126.5 ka) were characterized by the presence of a seasonal Marginal Ice Zone (MIZ) accompanied by subsurface warmth. As the sea ice retreated, cool, likely polar-sourced water dominated the surface and subsurface ocean (126.5–124 ka) until an abrupt surge of sea ice marked the final pulse of the remnants of the deglaciation. The second half of MIS 5e (124–116 ka) was characterized by a persistent inflow of warm water, only interrupted by incursions of cold water as summer insolation declined. Seasonal sea ice returned to the Eirik Drift during MIS 5d. We show that sea ice variability throughout MIS 5e was coupled with the variability of the SPG circulation. Especially, the location of a proximal MIZ to the convection region in the Labrador Sea may have been important for SPG strengthening in the earliest MIS 5e (128–126.5 ka). Together with the sea ice return during the start of MIS 5d, we show that the presence of sea ice at the major transitions into

and out of MIS 5e may point to its important role in modulating and enhancing the magnitude and coherence of climate signals at major climatic transitions. Nevertheless, we also demonstrate that sea ice is not a prerequisite SPG variability. Other factors, like cryospheric reconfiguration, and their influence on freshwater export and rerouting to the North Atlantic, may be important mechanisms for the climate and hydrographic variability within the LIG, and the transitions associated with glacial termination and inception.

Paper II: *Sea ice variability throughout the Penultimate Deglaciation and Last Interglacial in the eastern Fram Strait*

In paper II we investigate the nature and timing of sea ice and surface ocean hydrography in the eastern Fram Strait (sediment core KH14-GPC-02), throughout the LIG, and its glacial transitions when the ocean underwent profound environmental changes. The Fram Strait is the only deep-water passage connecting the Arctic and North Atlantic Oceans, and its dynamic environment leads to a sea ice cover highly sensitive to changes in climate. We investigate the connection between the variability of Atlantic water influence to the surface ocean, coupled with ice sheet dynamics and sea ice in the eastern Fram Strait. The sea ice proxy-reconstructions are based on the sea ice biomarker IP_{25} and the related phytoplankton, PIP_{25} sea ice index, in combination with dinoflagellate cysts. Furthermore, interpretations are supported by XRF, stable oxygen isotope, and Total Organic Carbon measurements. Our findings demonstrate an evolution of sea ice from extensive, and variable, late Marine Isotope Stage (MIS) 6 sea ice cover, to a Marginal Ice Zone during T II, and to open ocean conditions during MIS 5e. The sea ice variability was likely linked to the extent of the Svalbard Barents Sea Ice Sheet (SBIS) and fluctuations of Atlantic water influence on the surface ocean. A unique environment is recorded during T II where the highest concentrations of sea ice, marine and terrigenous biomarkers point to a high-productivity ocean and an efficient biological pump associated with the sedimentary influx from the retreating SBIS and marginal ice zone establishment. During the LIG, when there was no sea ice at our core location, we recorded peak interglacial optimal conditions with maximum Atlantic water influence in the late MIS 5e, ca. 120 ka, consistent with several previous findings from cores located both upstream and downstream in the Western Spitsbergen Current. Throughout MIS 5d–b, oligotrophic conditions may have occurred due to an eastward advance of Arctic waters and a lower, but still present influence of Atlantic waters. Here, low concentrations, and potential poor biomarker preservation make any interpretation of sea ice conditions during this time challenging, and further studies are needed to asses the variability of sea ice during MIS 5d-b in the eastern Fram Strait

Paper III: *Proxy signals for sea ice, hydrography and deep convection in the subpolar gyre- a critical review of the Last Interglacial*

In paper III we revisit sediment Core GS16-204-22CC-B from Paper I, covering the LIG and its glacial transitions (ca. 145-108 ka). In the study, we firstly assessed the potential of stable oxygen isotopes (δ^{18}O) obtained from paired planktic and benthic foraminifers($\Delta\delta^{18}$O) in the subpolar Labrador Sea to serve as indicators of sea ice. Secondly, we reevaluated previous interpretations of ocean stratification, deep convection, and deep ocean currents in the subpolar Labrador Sea in connection to the different sea ice conditions. Thus, we assessed whether distinctive isotopic values can be identified for various hydrographic conditions and sea ice. The study suggests that combined isotopic measurements of benthic and planktic foraminifers may offer valuable insights into the potential presence of sea ice at the surface ocean. Specifically, we find that during the "cold" sea ice dominated periods (MIS 6, T II, and MIS 5d), distinct, similar isotopic values with ($\Delta\delta^{18}$O) around 0 occurred, which may be explained by similar cold temperatures throughout the water column from the surface to the deep ocean. Thus, we hypothesize that conditions cold enough to support sea ice may also lead to the production of near subsurface waters with temperatures dropping to levels close to those in the deep, similar to observations made from the modern Southern Ocean by *Lund et al.* (2021). However, we also demonstrate that unequivocal interpretations of isotopic offsets between planktic and benthic species are challenging, because competing influences on the isotope signal can, and have, intermittently overridden the signal related to sea ice and vertical stratification. Thus, other factors, such as intense deglacial freshwater fluxes, may complicate the univocal interpretation of the isotopes in the context of sea ice or other hydrographic conditions. Nevertheless, our results are promising, and we encourage further multiproxy studies involving a comparison of established sea ice proxies with planktic and benthic (δ^{18}O), combined with their collective $\Delta\delta^{18}$O, to assess the relationships between foraminiferal $\Delta\delta^{18}$O, sea ice, and ocean hydrographic conditions across a broader range of hydrographic settings. We suggest that when applied in conjunction with complementary sea ice and hydrographic proxies, the judicious use of $\Delta\delta^{18}$O could allow the vast body of available oxygen isotopic data to be brought to bear in filling key spatio-temporal gaps in our understanding of past sea ice variability.

Chapter 5

Scientific Results

I

Paper I

5.1 Sea ice variability in the North Atlantic subpolar gyre throughout the Last Interglacial

Kristine Steinsland, Danielle M. Grant, Ulysses S. Ninnemann, Kirsten Fahl, Ruediger Stein, Stijn De Schepper

Quaternary Science Reviews, **313/108198**, (2023)

Quaternary Science Reviews 313 (2023) 108198

Contents lists available at ScienceDirect

Quaternary Science Reviews

journal homepage: www.elsevier.com/locate/quascirev

Invited paper

Sea ice variability in the North Atlantic subpolar gyre throughout the Last Interglacial

Kristine Steinsland [a, *], Danielle M. Grant [a], Ulysses S. Ninnemann [b], Kirsten Fahl [c], Ruediger Stein [c, d, e], Stijn De Schepper [a]

[a] NORCE Climate and Environment, NORCE Norwegian Research Centre AS and Bjerknes Centre for Climate Research, Bergen, Norway
[b] University of Bergen, Department of Earth Science and Bjerknes Centre for Climate Research, Bergen, Norway
[c] Alfred Wegener Institute Helmholtz Centre for Polar and Marine Research, Bremerhaven, Germany
[d] University of Bremen, Faculty of Geosciences and Center for Marine Environmental Sciences, Bremen, Germany
[e] Ocean University of China, Frontiers Science Center for Deep Ocean Multispheres and Earth System and Key Laboratory of Marine Chemistry Theory and Technology, Qingdao, China

ARTICLE INFO

Article history:
Received 11 November 2022
Received in revised form
20 June 2023
Accepted 20 June 2023
Available online 9 July 2023

Handling Editor: A. Voelker

Keywords:
Sea ice
Labrador sea
Eirik drift
Ocean circulation
Dinoflagellate cysts
Biomarkers
IP_{25}
MIS 5e

ABSTRACT

The Last Interglacial period, Marine Isotope Stage 5e (MIS 5e ~116–128 ka), is thought to have had a warmer, but less stable climate than the present interglacial. One key factor that has the potential to influence the ocean and climate is sea ice, but its presence and extent throughout MIS 5e is poorly constrained. Here we reconstruct the sea surface hydrography and sea ice variability in the Labrador Sea, a region influenced by the subpolar gyre (SPG) and where deep water formation occurs, in order to evaluate the potential of sea ice to drive or amplify ocean variability. We analysed biomarkers (highly branched isoprenoids, HBIs, and sterols), dinoflagellate cyst assemblages and stable oxygen isotopes from the late stages of MIS 6, throughout MIS 5e, into MIS 5d. Our results show that the late glacial MIS 6 was likely characterised by a thick multiyear sea ice cover. During the first phase of MIS 5e, the hydrography was highly variable. The initial 1500 years (128–126.5 ka) were characterised by the presence of a seasonal Marginal Ice Zone (MIZ) accompanied by subsurface warmth. As the sea ice retreated, cool, likely polar-sourced water dominated the surface and subsurface ocean (126.5–124 ka), until an abrupt surge of sea ice marked the final pulse of the remnants of the deglaciation. The second half of MIS 5e (124–116 ka) was characterised by a persistent inflow of warm water, only interrupted by incursions of cold water as summer insolation declined. Seasonal sea ice returned to the Eirik Drift during MIS 5d. We infer that sea ice variability throughout MIS 5e was coupled with the variability of the SPG. Especially the location of a proximal MIZ to the Labrador Sea convection region could have been important for SPG dynamics. In addition, the presence of sea ice at the transitions into and out of MIS 5e could point to its important role in modulating and enhancing the magnitude and coherence of climate signals at major climatic transitions.

1. Introduction

The potential climatic implications of global warming can be understood by investigating past periods in Earth's history which were as warm or warmer than today. Although there is no perfect analogue, the Last Interglacial (LIG; 116–128 ka), Marine Isotope Stage 5e (MIS 5e), has many features in common with model projections of future climate. These features include a warmer than present global climate, a significantly reduced Greenland Ice Sheet (GIS), and a higher sea level (e.g. Otto-Bliesner et al., 2006; Kopp et al., 2009). For this reason, the LIG has sparked the interest of many studies, aiming to understand climate variability, instability, and their underlying mechanisms.

Sea ice has been proposed as a cause for variability and instability of the North Atlantic Ocean circulation during the LIG due to its potential effect on the subpolar gyre (SPG; Born et al., 2010; Galaasen et al., 2014; Li and Born, 2019; Kessler et al., 2020). Sea ice can change rapidly in response to relatively weak forcing and it can amplify climate change non-linearly, resulting in rapid and large

* Corresponding author.
E-mail address: stei@norceresearch.no (K. Steinsland).

https://doi.org/10.1016/j.quascirev.2023.108198
0277-3791/

climate shifts. The SPG has been suggested to be integrally connected to the larger scale circulation and the Atlantic Meridional Overturning Circulation (AMOC; e.g. Hátún et al., 2005; Thornalley et al., 2009; Yeager, 2015; Klockmann et al., 2020), and thus it serves as one link in the chain of global teleconnections that alters climate on a global scale. The SPG is sensitive to buoyancy and wind forcing (e.g. Born and Stocker, 2014; Levermann and Born, 2007; Montoya et al., 2011) whereas the extent of sea ice influences both these forcings. Furthermore, buoyancy forcing affects deep water formation in the North Atlantic, which in turn affects the strength of the AMOC. Thus, in the Labrador Sea where deep water formation occurs, the SPG could be especially sensitive to the extent of sea ice and its associated freshwater (Born et al., 2010; Li and Born, 2019). It has been suggested that a strong SPG may also tend to expand zonally (eastward), redirect Atlantic waters into the westward flowing Irminger Current (IC) and corresponds to a weak AMOC (Klockmann et al., 2020). In contrast, a weak SPG contracts to the west, directs Atlantic waters northeast into the Nordic Seas, contributing to persistent deep water formation there (Thornalley et al., 2009) and corresponds to a strong AMOC (Hátún et al., 2005; Häkkinen and Rhines, 2004). However, it does remain unclear exactly how tightly coupled gyre size and strength are (Foukal and Lozier, 2017), and how or if they contributed to recent changes in overturning circulation (Lozier, 2012; Lozier et al., 2019). Thus, based on the brief observational period, it is difficult to draw conclusions about how SPG geometry, strength, and the basin scale overturning circulation are linked. Despite the complex circulation coupling, the SPG's potential to alter mass, heat, and buoyancy, and alter climate across the North Atlantic, and beyond, makes it crucial to understand the mechanisms by, and timescales on, which the SPG can vary. In this study, we focus on the potential of sea ice and its associated feedbacks on SPG and North Atlantic Ocean variability during the LIG.

Fossil assemblages and biomarkers preserved in marine sediments are frequently used for sea ice reconstructions (e.g. de Vernal et al., 2013). While several proxies are indirectly related to sea ice, the biomarker IP_{25} is exclusively biosynthesized by a few diatom species living in Arctic sea ice (Brown et al., 2014; Limoges et al., 2018) and provides a sensitive and reliable sea ice indicator. LIG sea ice reconstructions based on biomarkers are restricted to the Arctic Ocean (Stein et al., 2017, 2022; Kremer et al., 2018a, 2018b). No biomarker records exist from the LIG subpolar North Atlantic. Specifically for the Labrador Sea, biomarker-based sea ice reconstructions are only available for part of MIS 3 (Scoto et al., 2022) and the last Glacial to Holocene (You et al., 2023). For the LIG time interval from this area, on the other hand, sea ice reconstructions are mainly based on dinoflagellate cyst (*hereafter* dinocyst) transfer functions and assemblages (e.g. Eynaud et al., 2004; Hillaire-Marcel et al., 2001; de Vernal and Hillaire-Marcel, 2008; Penaud et al., 2008; Van Nieuwenhove et al., 2011), and indirect inferences based on foraminifer assemblages (e.g. Irvali et al., 2012, 2016). A compilation of sea ice records by Kageyama et al. (2021) demonstrates that north of 79°N the LIG sea ice concentrations range from minimal to substantial (>75%) all year around. South of 79°N, the Atlantic and Nordic Seas were sea ice free during the LIG. This partly contrasts previous studies suggesting that sea ice and its associated melt in the Labrador Sea could modulate SPG circulation on centennial timescales within the LIG (Galaasen et al., 2014), and during the last glacial inception (Born et al., 2010). These authors speculate and/or infer sea ice presence from indirect proxies and modelling experiments but biomarker data that can unequivocally document sea ice presence is lacking. This highlights our limited knowledge about sea ice extent and variability in the North Atlantic SPG region, which is crucial in order to evaluate its role in modulating ocean circulation and the SPG on glacial-interglacial timescales.

Here we reconstruct sea ice occurrence, marginal ice zone (MIZ; transition between open ocean and sea ice) extent, and surface ocean hydrography from the late glacial stage of MIS 6 throughout MIS 5e, and into MIS 5d using dinocyst assemblages, biomarkers (IP_{25}) and stable oxygen isotopes from an Eirik Drift sediment core. We combine our data with previously published foraminifer records from the same region, and with other North Atlantic records to gain a broader understanding of the Labrador Sea surface hydrography, the surface currents of the SPG and the larger scale North Atlantic surface ocean variability.

2. Site location and oceanography

The Eirik Drift is a sediment drift located off the southern tip of the Greenland margin and is well situated to monitor changes in the northwest SPG that dominates the hydrography of the North Atlantic (Hátún et al., 2005). It is characterised by high sedimentation rates sustained by eroded sediments imported primarily by Denmark Strait Overflow Water and deposited here along the most offshore portion of the Deep Western Boundary Current (DWBC) (Wold, 1994; Hunter et al., 2007), leading to expanded sedimentary interglacial intervals (Hillaire-Marcel et al., 1994). The surface ocean hydrography at the Eirik Drift is characterised by the cyclonic circulation of the SPG, which is fed by the North Atlantic Current (NAC) from the south, and the East Greenland Current (EGC) from the north (Fig. 1). The NAC transports warm and salty Atlantic waters northward as an extension of the Gulf Stream, branching into the Norwegian Atlantic Current (NwAC) flowing northward, and the IC flowing west and forming the east part of the SPG circulation pattern. The EGC flows southward from the Arctic Ocean, via the Denmark Strait, into the North Atlantic and is a major contributor of cold, fresh surface water to the vicinity of the study area (Bacon et al., 2002).

3. Material and methods

In 2016, calypso Core GS16-204-22CC-B (*hereafter* 22CC-B; 58°02.83′N, 47°02.36′W; 3160 m water depth) was collected from the Eirik Drift with the research vessel G.O. Sars. Based on lithological description of this core, and a preliminary correlation (oxygen isotopes, colour scan) to the well-dated Core MD03-2664 (57°26.34′N, 48°36.35′W; 3440 m water depth; Irvali et al., 2012, 2016), we first estimated MIS 5e to occur between 14.5 and 18.5 m core depth. The samples for this study were collected at different times and for different purposes. During the initial sampling, we collected 1.5 cm thick sediment samples at 4 cm resolution for sedimentary ancient DNA (*sed*aDNA), palynology, foraminifers and biomarkers for the entire study interval (1456–1852 cm). In the second sampling phase, we sampled in-between the first sample set at higher resolution and with thinner sediment samples (0.7–0.8 cm) for part of the core (1556–1753.5 cm).

Dinocyst assemblages were analysed every 4 cm, except in MIS 6 (1756–1852 cm) where we analysed every 12 cm. Biomarkers and foraminifers were prioritised for a higher resolution sampling at obvious transitions in the core. Biomarkers were analysed at every ~2 cm between 1555 and 1648 cm, and at every ~1 cm between 1648 and 1756 cm. Foraminifers were analysed at the same resolution as the biomarkers (every ~1 cm) between 1704 and 1756 cm. For the rest of the core, sampling was done every 4 cm. For exact sampling depths, and intervals, see Supplementary Data.

3.1. Stable isotopes

Stable oxygen isotope analyses ($\delta^{18}O$) were performed on the planktic foraminifer *Neogloboquadrina pachyderma* (sinistral) and

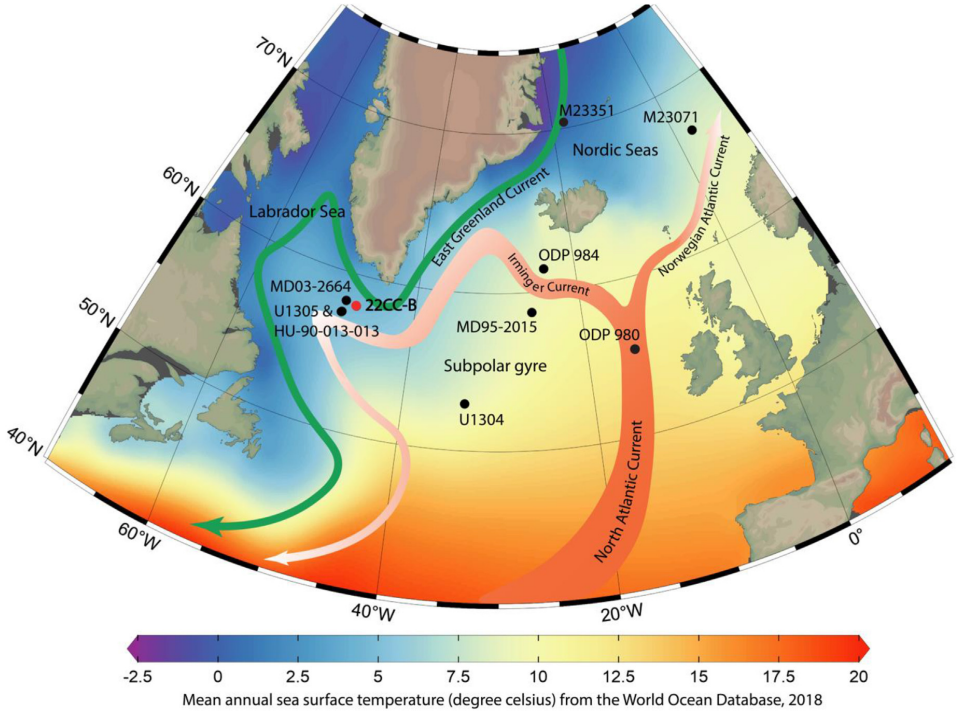

Fig. 1. Mean annual sea surface temperatures from WOA 2018 (Locarnini et al., 2019) and major surface ocean currents relative to our studied Core GS16-204-22CC-B (red dot). Other sediment records (black dots) discussed in the text are from MD03-2664 (Irvali et al., 2012, 2016; Galaasen et al., 2014), IODP Sites U1304 and U1305 (Channell et al., 2006), ODP Sites 984 (Mokeddem et al., 2014) and 980 (Oppo et al., 2006), HU-90-013-013 (Hillaire-Marcel et al., 1994), MD95-2015 (Eynaud et al., 2004), M23071 (Van Nieuwenhove et al., 2008), and M23351 (Zhuravleva et al., 2017).

benthic foraminifer *Cibicidoides wuellerstorfi* in order to constrain the chronology of MIS 5e. *N. pachyderma* (s) was identified in all samples, while *C. wuellerstorfi* was absent in ~1/3 of the samples (see Supplementary Data). A Finnigan MAT253 mass spectrometer with an online Kiel IV, located at FARLAB, University of Bergen, was used for the stable isotope analysis. Values are reported relative to Vienna Pee Dee Belemnite. Two working standards (CM12 and Riedel) along with 2 international standards (NBS-18 and NBS-19) were analysed each day interspersed with samples. The external precision for samples between 10 and 100 μg was better than 0.08 and 0.04‰ for $\delta^{18}O$ and $\delta^{13}C$, respectively, based on the long-term reproducibility (1σ) of the working standard CM12.

3.2. Total organic carbon, biomarkers and their ecological significance

A total of 187 samples were analysed for biomarkers (HBIs and sterols) and 254 samples for Total Organic Carbon (TOC)%. Biomarkers and TOC were measured and analysed at the Alfred Wegener Institute in Bremerhaven, Germany. To determine the TOC (%), 100 μg of freeze-dried and homogenised sediments were measured (per sample) using an ELTRA CS2000 Carbon Sulfur Detector. For biomarker analysis preparation, 5 g of freeze-dried sediments was homogenised using an agate mortar. Prior to extraction, the internal standards 7-hexylnonadecane (7-HND: 0.0038 μm/ml), androstanol (0.05 μm/ml), 9-octylheptadec (9-OHD: 0.005 μm/ml), and squalane (0.032 μm/ml) were added to the sediments to allow for later stage quantification. Biomarkers were extracted by sonication (3 × 15 min) using dichloromethane:methanol (2:1 v/v; 30 ml) as solvent. The extract was separated into hydrocarbon and sterol fractions through open-column chromatography (5 ml *n*-hexane for hydrocarbons and 9 ml ethylacetate:*n*-hexane (4:1) for sterols) with silica gel (SiO_2) as the stationary phase. The sterol fraction was silyated with 200 μl BSTFA (bis-trimethylsilyl-trifluoracet-amide; 60 °C for 2 h). Biomarker analysis was performed by gas chromatography-mass-spectrometry (GC-MS). Hydrocarbon concentrations were determined with a gas chromatograph Agilent Technologies 7890 GC (30 m HP-1MS column, 0.25 mm in diameter and 0.25 μm film thickness) coupled to an Agilent Technologies 5977 A mass selective detector. Sterol concentrations were measured with a gas chromatograph Agilent Technologies 6850 GC (30 m HP-1MS column, 0.25 mm in diameter and 0.25 μm film thickness) coupled to an Agilent Technologies 5975 A mass selective detector. HBIs (IP_{25}, HBI II, HBI III (Z), HBI III (E)) and sterols were identified by comparing their retention times to those of reference compounds (IP_{25}: Belt et al., 2007; HBI II: Johns et al., 1999; HBI III: Belt et al., 2000; sterols: Boon et al., 1979; Volkman, 1986). IP_{25}, HBI II, HBI III (Z), and HBI III (E) (IP_{25}: m/z 350; HBI II: m/z 348; HBI III (Z) and (E): m/z 346) were quantified by the abundant fragment ion m/z 266 of the internal standard 7-HND. Sterols were quantified as trimethylsilyl ethers (brassicasterol: m/z 470, campesterol: m/z 472, sitosterol: m/z 486, dinosterol: m/z 500) in regard to the molecular ion of androstanol (ion m/z 348). The different responses

of all these ions were balanced by external calibration. Instrument stability was controlled by reruns of external standards and replicate analyses for random samples. All biomarker concentrations have been normalised to the TOC.

The sea ice proxy IP_{25} (Ice Proxy with 25 carbon atoms) is a molecule produced by a relatively small number of diatoms that inhabit the base of Arctic sea ice (Brown et al., 2014; Limoges et al., 2018) and is predominantly found in areas covered by seasonal sea ice (Belt et al., 2007; Xiao et al., 2015; Kolling et al., 2020; for review see Belt, 2018). In this study, we consider the occurrence of IP_{25} as a sea ice indicator. A difficulty with IP_{25} is that both permanent sea ice environments and open water conditions are characterised by IP_{25} concentrations of zero. Under permanent sea ice conditions, IP_{25} is absent due to limited light and nutrient availability which are required for the growth of sea ice phytoplankton. Likewise, in open waters, the habitat for the ice algae is missing, and IP_{25} concentrations are zero. The ambiguity of the signal from permanent sea ice *vs* open ocean requires that IP_{25} is analysed in combination with open-water phytoplankton biomarkers like brassicasterol and dinosterol (cf. Müller et al., 2009, 2011). These are produced by a variety of phytoplankton genera like dinoflagellates, diatoms and haptophytes (Boon et al., 1979; Robinson et al., 1984; Volkman et al., 1998). Alongside IP_{25}, several other biomarkers are related to sea ice. HBI III (Z) is a common constituent of marine settings (Belt et al., 2000) but shows a more direct association with MIZ productivity (Collins et al., 2013; Belt et al., 2015). HBI II is produced by sea ice/land-fast ice-dwelling diatoms in the Southern Ocean (Belt et al., 2016). Although its origin and potential as an environmental proxy in the Northern Hemisphere is unclear, it is often observed together with IP_{25}. Thus, Belt et al. (2018) postulate that HBI II might represent an "even better" sea ice proxy than IP_{25} or at least be a useful substitute in cases where IP_{25} is absent. Terrigenous influence can be inferred by sitosterol and campesterol (Pryce, 1971; Huang and Meinschein, 1979). Although these biomarkers are found in a few microalgae species, the main contributors are higher land plants (Volkman, 1986; Jaffé et al., 1995; Rontani et al., 2014).

3.3. Dinoflagellate cyst assemblages and ecological significance

A total of 85 samples were selected for dinocyst assemblage analysis and prepared using a standard palynological preparation procedure (e.g. De Schepper et al., 2017). To remove the mineral fraction, cold hydrochloric and hydrofluoric acid was used. The palynological residue was sieved over a 10 μm polymer mesh before mounting on slides with glycerine jelly. One tablet of *Lycopodium clavatum* spores (batch #140119321, n = 19,855 ± 521 spores per tablet) was added to each sample before chemical treatment to allow calculation of dinocyst concentrations and errors following Stockmarr (1971). The palynological slides were counted at 400× magnification for dinocyst assemblage analyses until a minimum of 300 *in situ* dinocysts were identified. If the dinocyst concentration was too low to reach the minimum threshold, the entire slide (ca. 20 non-overlapping traverses) was counted. We identified 38 dinocyst taxa in total. The major dinocyst taxa consist of *Bitectatodinium tepikiense*, *Operculodinium centrocarpum* sensu Wall and Dale (1966) (hereafter *O. centrocarpum*), *Nematosphaeropsis labyrinthus* and the group of Round Brown cysts (RBC). *Brigantedinium* specimens were grouped together as RBC because folding or orientation of specimens often limited identification to species level. *Spiniferites* spp. includes all *Spiniferites* cysts except *S. elongatus* and *S. mirabilis*. All *Impagidinium* species identified were grouped together with the exception of *I. pallidum*. These grouped species include *I. aculeatum, I. sphaericum, I. paradoxum, I. patulum* and *I. plicatum*.

The distribution of dinoflagellates depends on physical and chemical sea surface parameters such as currents, temperature, salinity, irradiance, nutrients and sea ice (e.g. de Vernal et al., 2020). Their different environmental preferences make them suited for surface ocean reconstructions.

B. tepikiense is linked to the subpolar-temperate transition in the North-Atlatic (Dale, 1996) and also enhanced water stratification (Rochon et al., 1999; de Vernal et al., 2005; de Vernal and Marret, 2007; Hennissen et al., 2014). The species has a high tolerance to a wide range of salinities and temperatures and it can be observed in regions that are seasonally covered by sea ice for less than 4 months a year (de Vernal et al., 1997). In modern sediments from the Labrador Sea and North Atlantic, *B. tepikiense* rarely exceeds >10% of the assemblage (e.g. de Vernal et al., 2005, 2020). During the Last Glacial Maximum, *B. tepikiense* makes up more than 50% of the assemblage in the northern North Atlantic (de Vernal et al., 2005). Thus, the species is characteristic for conditions different than present and is not common in warm interglacial periods. *N. labyrinthus* is another subpolar-temperate species (Rochon et al., 1999; Marret and Zonneveld, 2003) that has been linked to climate transitions (i.e. glacial–interglacial) when profound changes in water mass composition occurred (Hennissen et al., 2017, and references therein).

The distribution of *O. centrocarpum* in modern surface sediments of the North Atlantic reveals that high relative abundances are linked to warm Atlantic Water (e.g. NAC/NwAC), although it is generally a cosmopolitan taxon (e.g. Marret and Zonneveld, 2003). In fossil records from the Arctic and sub-Arctic, *O. centrocarpum* is often regarded as an indicator for interglacial intervals with Atlantic water advection (e.g. Rochon et al., 1999; Matthiessen et al., 2001; Matthiessen and Knies, 2001; Grøsfjeld et al., 2006). Also *S. mirabilis* is an indicator of warm temperate to temperate environments. Previous studies have linked this species to interglacial optima in the northern North Atlantic during MIS 5 (Sánchez Goñi et al., 1999; Eynaud et al., 2004; Penaud et al., 2008; Van Nieuwenhove et al., 2008, 2011).

Other environmentally significant species in our record include the RBC and the cysts of *Pentapharsodinium dalei* indicating sea ice and surface ocean stratification respectively. The RBC are a group of heterotrophic taxa that strongly relate to the trophic state of the surface waters in addition to temperature and salinity (e.g. de Vernal et al., 2000). In environments with increased nutrient availability like frontal zones and sea ice margins, RBC and heterotrophic dinocyst taxa commonly outnumber other dinocysts (e.g. de Vernal et al., 2020). In our record, the cysts of *P. dalei* are found in combination with the RBC. In the Arctic and sub-Arctic oceans high proportions of cysts of *P. dalei* are found in stratified and productive waters at a distance from the multiyear sea-ice zone (Radi et al., 2001; Marret et al., 2004; Solignac et al., 2009) and in fjords receiving a spring freshet of glacier meltwater (Dale, 2001; Grøsfjeld et al., 2009).

4. Results

4.1. Chronology

The age model for Site 22CC-B (Fig. 2) is based on aligning our benthic (*C. wuellerstorfi*) $\delta^{18}O$ record with the benthic $\delta^{18}O$ isotopic record from the nearby Core MD03-2664 (Irvali et al., 2012, 2016), using AnalySeries (Paillard et al., 1996). Previous studies (Irvali et al., 2012, 2016; Galaasen et al., 2014) tuned Core MD03-2664 to MD95-2042 on the Iberian Margin (Shackleton et al., 2002, 2003) where the MIS 5e boundaries are set by the benthic isotopic low plateau to 116.1 ± 0.9 ka and 128 ± 1 ka based on fossil coral reef U-series dates of the LIG sea level high stand (Stirling et al.,

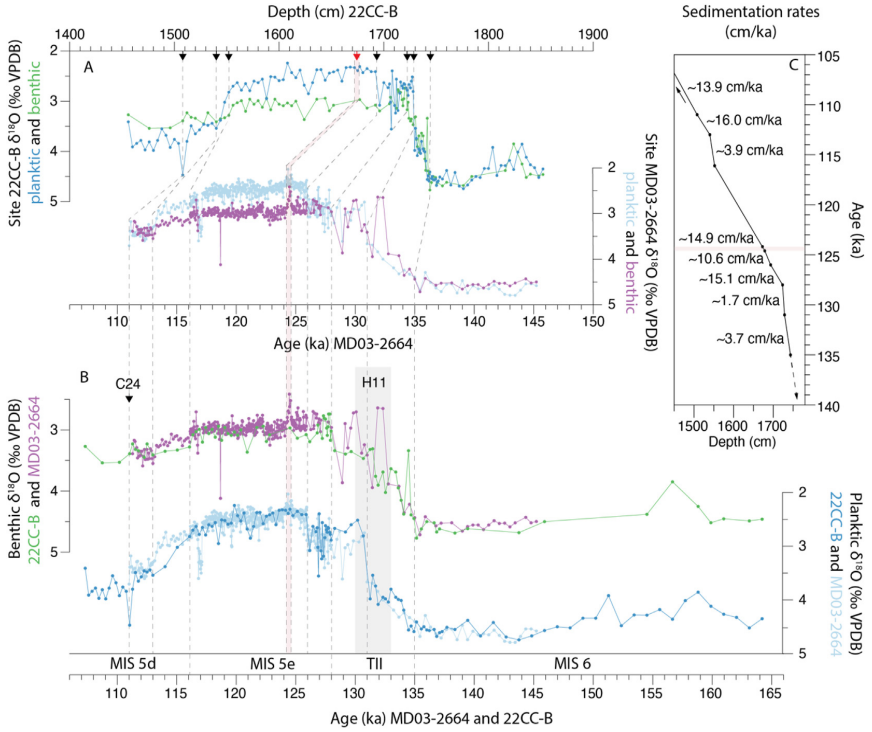

Fig. 2. Age model for Core 22CC-B. A) Core 22CC-B planktic and benthic $\delta^{18}O$ plotted on depth, and Core MD03-2664 planktic and benthic $\delta^{18}O$ record plotted on age (ka) (Irvali et al., 2012, 2016). B) Benthic $\delta^{18}O$ of Cores 22CC-B and MD03-2664 plotted on the age scale (ka) of MD03-2664 with the tie points (dashed lines), and planktic $\delta^{18}O$ of Cores 22CC-B and MD03-2664 plotted on age (ka). The red layer is represented by the red arrow and pink shaded area. The grey shaded area represents H11 within TII. C) Depth (cm) versus age (ka) plot for Core 22CC-B, showing tie points and approximate sedimentation rates. The red layer is represented in the pink shaded area.

1998). We identified these MIS 5e boundaries at 22CC-B in our benthic $\delta^{18}O$ record, as well as the onset of Termination II (TII) at the top of MIS 6 (135 ka) and the base of MIS 5d (113 ka) (Fig. 2A).

Additional tie points in our age model are based on the planktic $\delta^{18}O$ record and colour scan. We associate one planktic $\delta^{18}O$ tie point with the distinct isotopic minimum during TII at 131 ka during Henrich event 11 (H11) (Irvali et al., 2016). An abrupt shift in planktic $\delta^{18}O$ recognised in Core 22CC-B and also in Cores MD95-2042 and MD03-2664 (Shackleton et al., 2002, 2003; Irvali et al., 2012) provides an additional tie point at 126 ka (Fig. 2B), that is associated with the start of the Eemian interglacial on land (Shackleton et al., 2003). A distinct "red layer" was observed in both Core 22CC-B and MD03-2664 based on sediment colour properties (Supplementary Fig. 1). The top and bottom of this layer were used as tie points for our age model with the ages of 124.2 and 124.6 ka, respectively (Galaasen et al., 2014). A similar red layer is also documented at the Integrated Ocean Drilling Program (IODP) Site U1305 on the Eirik Drift and was likely deposited by an outburst flood event associated with the final collapse of the Laurentide Ice Sheet (LIS) in the early part of the LIG (Nicholl et al., 2012). The final tie point is placed at the rapid increase of planktic $\delta^{18}O$ at 111.0 ka in MIS 5d (Fig. 2B), which corresponds in Core MD03-2664 to a large IRD peak reflecting the C24 event (e.g. Hodell et al., 2009). In summary, our age model utilizes the same tie points that Irvali et al. (2012, 2016) and Galaasen et al. (2014) used to correlate their record to MD95-2042 of Shackleton et al. (2002, 2003). Additionally, in order to have some control on the ages of the upper MIS 5d, i.e. younger than 111 ka, we used a ^{14}C AMS age from a twin core on the Eirik Drift (46 ka at 602.7 cm core depth in hole 22CC-A; Griem et al., 2019). We transferred the ^{14}C age from Core 22CC-A to 22CC-B by aligning the red-green colour scan and magnetic susceptibility. The ages <111 ka are thus approximate and should not be considered as absolute ages. The base of MIS 6 is not constrained, and the ages >135 ka are based on a linear extrapolation of the sedimentation rate between 131 and 135 ka. Thus, the ages of an extended MIS 6 beyond 135 ka are imprecise and should be used cautiously.

4.2. Isotopes

The late MIS 6 planktic (*N. pachyderma* sinistral) and benthic (*C. wuellerstorfi*) $\delta^{18}O$ show typical glacial values of, on average, ~4.4‰ and ~4.5‰, respectively (Fig. 2B). From ~135 ka, both benthic and planktic $\delta^{18}O$ shift towards lower values, marking the initiation of TII. Within TII, the planktic $\delta^{18}O$ decreases from 4.0 to 2.7‰ at 131 ka, associated with H11. The onset of the MIS 5e low benthic $\delta^{18}O$ plateau at 128.0 ka is characterised by an increase in sedimentation rate from 1.7 cm/ka to 15.1 cm/ka (Fig. 2C). The lowest benthic $\delta^{18}O$ values occur between 128 and 126.5 ka. In this same period, the planktic $\delta^{18}O$ shows high variability, ending in a distinct increase at ~126.5 ka, followed directly by a decrease of 0.7‰. From the middle to late MIS 5e, the benthic and planktic $\delta^{18}O$ are

consistent with characteristic low values of interglacial periods. Both isotopic records show a general increasing trend throughout MIS 5e. The transition into MIS 5d is characterised by a gradual increase in planktic $\delta^{18}O$, and a more muted increase in benthic $\delta^{18}O$, suggesting a change in local surface water hydrography in excess of the change registered in the deep ocean.

4.3. Dinoflagellate cysts

In MIS 6 dinocyst counts (Fig. 3) are very low making reliable interpretations based on relative abundance difficult. Towards TII, concentrations are also very low (average of ~27 cysts/g sediment), yet they increase to an average of 110 cyst/g sediment. Here, we observe the onset and increase in the relative abundance of RBC which during TII reach up to ~30% of the dinocyst assemblage.

The dinocyst concentration increases at the onset of MIS 5e (Fig. 3A). *Spiniferites* spp., RBC, cysts of *P. dalei* and *N. labyrinthus* are among the species that contribute to the concentration increase (Fig. 3F–I). RBC reach, at maximum, 30% of the total assemblage in the earliest MIS 5e (128–126.5 ka). At 126.5 ka, the abundance and concentrations of RBC rapidly decrease and *B. tepikiense* becomes the dominant species (60%) (Fig. 3E).

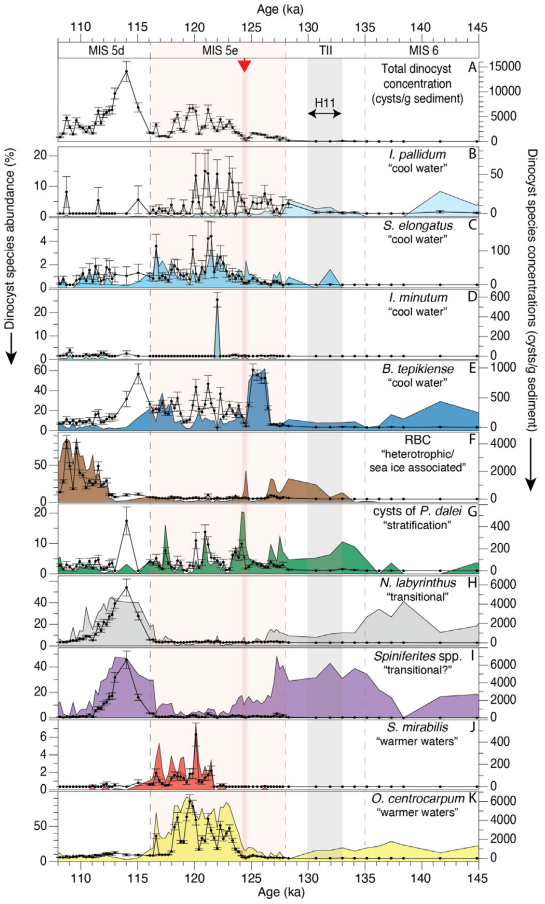

Fig. 3. Dinocyst relative abundances (%) represented with coloured curves and concentrations (cyst/g sediment) with errors represented with black lines for the most abundant species of Site 22CC-B plotted on age (ka). A) The total dinocyst concentration with errors, B–K) relative abundance and concentration with errors. The red shaded area and arrow represent the red layer. The grey shaded area represents H11, and the pink shaded area marks MIS 5e.

The "red layer" event (124.6–124.2 ka) is reflected by a decrease of dinocyst concentrations and marks the onset of a different dinocyst assemblage. *B. tepikiense* is first replaced at the "red layer" by the heterotrophic group of RBC (43%) and thereafter cysts of *P. dalei* (20%). Other noteworthy dinocyst taxa in the "red layer' include the cyst of *Scrippsiella trifida* which appears almost exclusively here. Shortly following the deposition of the red layer and cysts of *P. dalei*, overall cyst concentrations rise. In addition, the relative abundance of *O. centrocarpum* increases to an average of ~72%, while its concentration increases to maximum values and fluctuates between ~1000 and 5000 cyst/g sediment for the next 6000 years (Fig. 3K). In this interval, we also encounter the warm water indicator *S. mirabilis* between 121.5 and 115 ka (Fig. 3J). In a single sample (~122 ka), we encountered high relative abundances of the Arctic, cool water dinocyst *Islandinium minutum*, a species often associated with sea ice (Fig. 3D). Other sea ice proxies (see section 3.3) were not recorded associated with this sample. *O. centrocarpum* concentrations and abundances decrease at ~118 ka, when *B. tepikiense* and cysts of *P. dalei* increase.

The MIS 5d dinocyst assemblage is initially dominated by *N. labyrinthus* and *Spiniferites* spp., together representing up to 90% of the assemblage at its maximum. The dominance of these species corresponds with the highest overall dinocyst concentrations of the record reaching a maximum of 14,000 cyst/g sediment. When *N. labyrinthus*, *Spiniferites* spp., and dinocyst concentrations decrease at ~114 ka, RBC start dominating the assemblage for the remainder of MIS 5d.

4.4. Biomarkers

Through MIS 6, the sea ice (IP_{25}, HBI II) and MIZ (HBI III Z) HBI biomarkers are low or under the detection limit while the open ocean (brassicasterol, dinosterol) and terrestrial (sitosterol and campesterol) sterol biomarkers are low in concentration (Fig. 4D–G). In late TII all biomarkers, and especially the HBI biomarkers, increase in concentrations corresponding to the abrupt transition to the lower planktic $\delta^{18}O$ values at 131 ka. At the onset of MIS 5e (128 ka), all biomarker concentrations rapidly increase further with IP_{25} and HBI II reaching maximum values between 127.4 and 126.9 ka. Maximum values of HBI III (Z), brassicasterol, dinosterol, sitosterol, and campesterol remain until ~126.4 ka. Subsequently, all biomarker concentrations decrease from 126.4 ka, only to briefly increase in the red layer. Here, the sea ice and other biomarkers peak except for HBI III (Z), and we record the highest concentration of the terrestrial biomarker sitosterol at 49 μg/gTOC in this red layer. For the remainder of MIS 5e, all biomarker concentrations decline and sea ice biomarkers are not detected. At the start of MIS 5d, the biomarker concentrations increase and IP_{25} is detected again from ~114 ka and remains present throughout MIS 5d.

5. Discussion

5.1. Late MIS 6 and Termination II: the perennial sea ice cover breaks up

During our studied interval of MIS 6, the Eirik Drift was likely covered by an extensive perennial sea ice cover. This interpretation is based on the very low dinocyst concentrations (Fig. 4A) and low to absent IP_{25} concentrations in our samples (Fig. 5E). IP_{25}

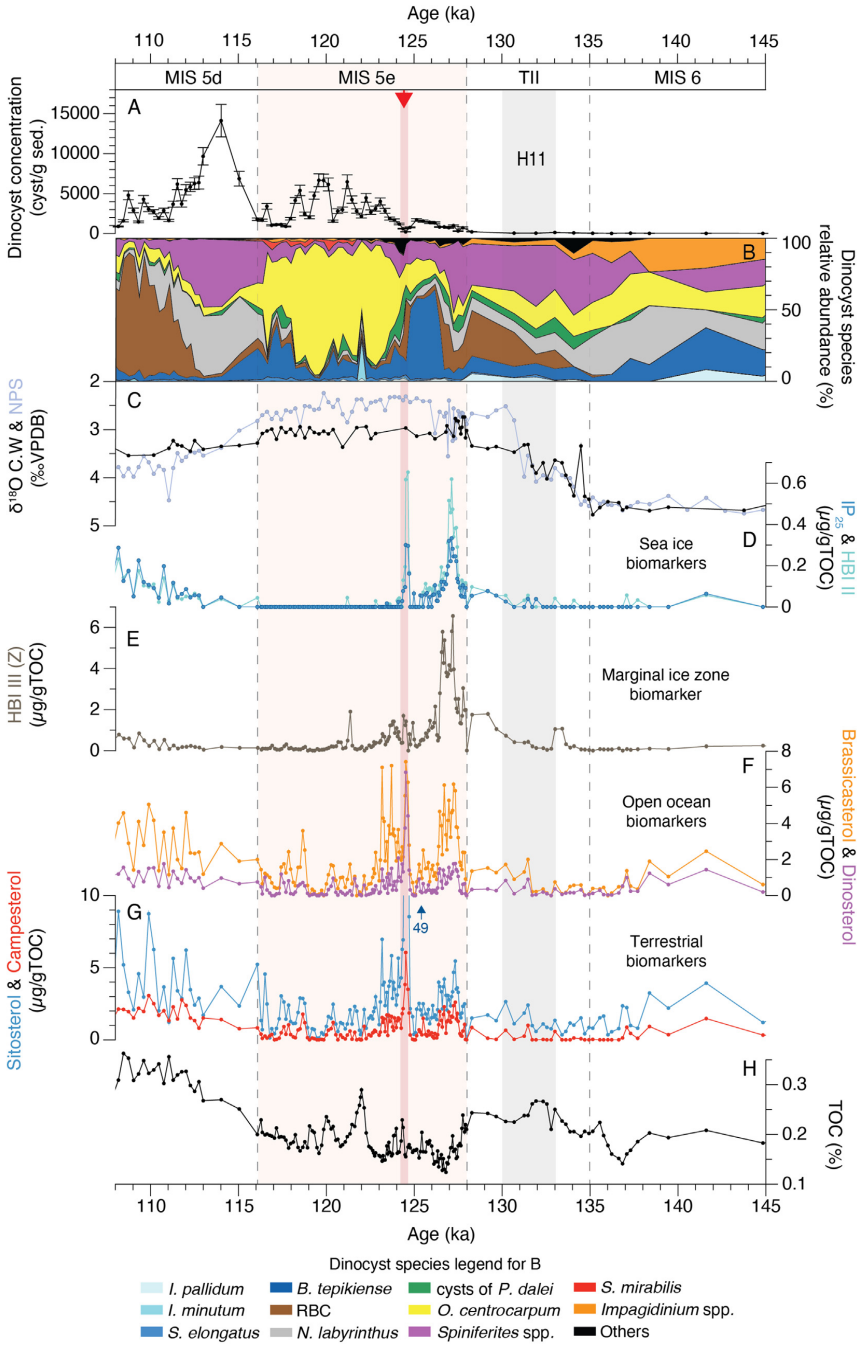

Fig. 4. Dinocyst, stable oxygen isotope, and biomarker results plotted on age (ka). A) Dinocyst total concentrations with errors, B) dinocyst species relative abundances, C) $\delta^{18}O$ of *C. wuellerstorfi* and *N. pachyderma* (s), D) concentrations of sea ice and sea ice associated biomarkers IP_{25} and HBI II, E) concentration of the marginal ice zone biomarker HBI III (Z), F) concentrations of the open ocean biomarkers brassicasterol and dinosterol, G) concentrations of the terrestrial biomarkers sitosterol and campesterol and H) TOC %. The red shaded area and arrow represent the red layer. The grey shaded area represents H11, and the pink shaded area marks MIS 5e.

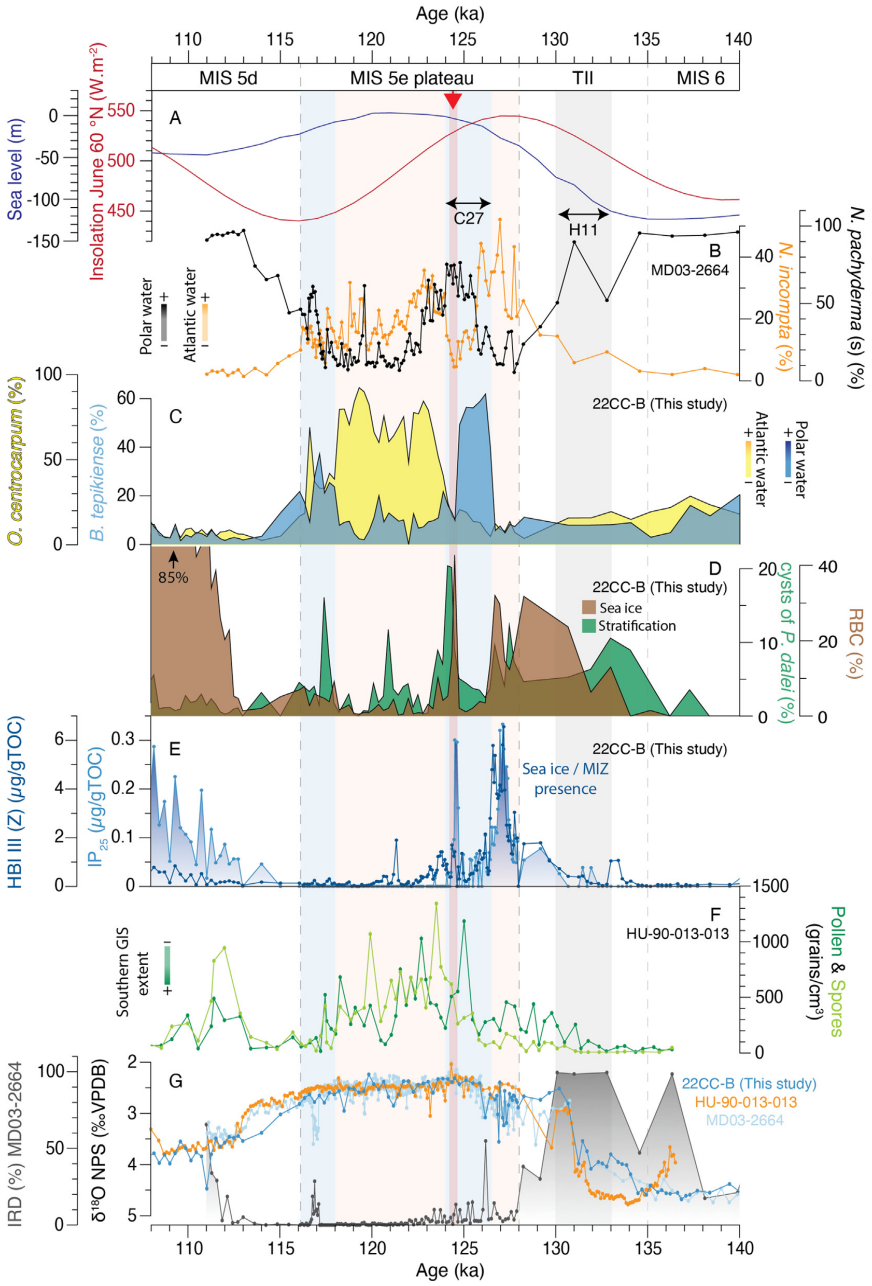

Fig. 5. A) June insolation at 60°N (Berger and Loutre, 1991) and sea level in meters relative to modern (Spratt and Lisiecki, 2016), B) relative abundance of the cold water *N. pachyderma* (s) and the Atlantic water indicator *N. incompta* from Core MD03-2664 (Irvali et al., 2012, 2016), C) relative abundance of *O. centrocarpum* and *B. tepikiense* from Core 22CC-B, D) relative abundance of the round brown cysts (RBC), an indicator for high nutrient availability and sea ice, and cysts of *P. dalei* which are often linked to stratified waters, E) concentrations of the sea ice (IP_{25}) and marginal ice zone (HBI III (Z)) biomarker, F) pollen and spore records from Core HU-90-013-013 and estimated ice cover on Greenland (de Vernal and Hillaire-Marcel, 2008), G) Eirik Drift planktic foraminifer $\delta^{18}O$ records, and IRD from Core MD03-2664 (black). The Heinrich Event 11 (H11) is marked by the grey shaded area. Periods within MIS 5e characterised by warm water inflow to the Eirik Drift via the Irminger Current (IC) are marked by the pink shaded area; the cold event C27 and the cooler conditions with enhanced pulses of EGC at the end of MIS 5e are marked by the blue shaded areas. The red layer is marked by the red arrow and red shaded area.

concentrations of (almost) zero can reflect open water conditions but combined with low open water biomarkers (brassicasterol, dinosterol, and HBI III (Z)), we interpret these records to reflect a perennial sea ice cover with minimal open-water phytoplankton production. A thick sea ice cover limits light penetration in the surface ocean and nutrient availability, both of which are essential for phytoplankton and sea ice algae productivity (Müller et al., 2011; Fahl and Stein, 2012; Xiao et al., 2015). The Core MD03-2664 foraminifer assemblage and stable isotopes have been interpreted to reflect an extended sea ice margin occurring south of our core location and increased polar water influence via the EGC (Irvali et al., 2012). However, the low but present dinocysts and biomarkers and the infrequent occurrence of foraminifers at Site 22CC-B may suggest that the perennial sea ice cover was interrupted by short intervals with restricted open water conditions during summer that allowed phytoplankton reproduction. Indeed, Mokeddem and McManus (2016) demonstrate with foraminifer records from the Ocean Drilling Program (ODP) Site 984 that a baseline of full glacial conditions was interrupted by short-lived retreats of the polar front northward that allowed warm and saline water inflow to the northwest Atlantic.

At the onset of TII the perennial sea ice likely started to break up more frequently when summer insolation increased (Fig. 5A). The dinocyst counts and concentrations are very low (Fig. 3), yet the relative abundances are statistically significant, as determined using the method of Heslop et al. (2011) (Supplementary Fig. 2). RBC, a group of heterotrophic dinocysts often associated with seasonal sea ice, occur for the first time in our record and increase in relative abundance. At ~130 ka, as local summer insolation neared its peak, the perennial sea ice broke up more frequently and we record increased IP_{25} and HBI III (Z) concentrations. The sea ice was still extensive but less so than in MIS 6 and early TII. A drop in IRD % (Fig. 5G) and in the abundance of polar foraminifers in Core MD03-2664 at 130 ka (Fig. 5B) suggests a general retreat of polar conditions as TII came to an end.

The dinocyst assemblage at the Eirik Drift shows no indications of Atlantic water inflow during TII, similar to the assemblage from the South Icelandic Basin Core MD95-2015 (Eynaud et al., 2004). In contrast, the Nordic Seas were influenced by warm Atlantic water, as indicated by the dominance of the Atlantic water tracer *O. centrocarpum* at the Vøring Plateau (Core M23071; Van Nieuwenhove et al., 2008). Together, this could point to a contracted SPG to the west. A contracted or weakened SPG would allow for warm and saline Atlantic waters to flow northward into the Nordic Seas, while the western North Atlantic is cut off from warm water inflow (Hátún et al., 2005; Thornalley et al., 2009; Bauch et al., 1999, 2012; Van Nieuwenhove et al., 2011). Such a scenario of a contracted or weakened SPG is also proposed by Zhuravleva et al. (2017) who indicate cold surface water conditions, high meltwater input from the GIS and/or enhanced sea ice in East Greenland Margin Core M23351. Taken together, the break-up of perennial sea ice, and a highly fresh and stratified upper ocean in the North Atlantic is consistent with a contracted/weak SPG during TII (Fig. 6).

5.2. MIS 5e

5.2.1. Earliest MIS 5e (128–126.5 ka): marginal ice zone and (sub) surface warming

Coincident with peak summer insolation in the earliest MIS 5e, we record the first evidence of a MIZ at the Eirik Drift. We interpret a MIZ due to the simultaneous increase of the sea ice biomarkers IP_{25} and HBI III (Z) (Fig. 5E). While IP_{25} alone could indicate sea ice transport via the EGC, HBI III (Z) is found to be strongly enhanced in MIZ environments in the Antarctic (Collins et al., 2013) and the Arctic (Belt et al., 2015). Further corroborating evidence for MIZ conditions comes from increased concentrations and abundances of the heterotrophic RBC, which are often abundant in highly productive sea ice environments (e.g. de Vernal et al., 1997, 2005, 2020), and cysts of *P. dalei*, a species associated with stratified waters (Fig. 5D; see section 3.3). Contemporaneously, sea surface productivity increased as indicated by the open-water phytoplankton biomarkers dinosterol and, especially, brassicasterol (Fig. 4F). The environment during the first 1500 years of MIS 5e at the Eirik Drift was thus an environment with sea ice, high productivity and stratification.

Interestingly, several data records and modelling experiments highlight this earliest part of MIS 5e to be the warmest part of the entire interglacial. Foraminifer-based temperature reconstructions from Core MD03-2664 demonstrate peak MIS 5e temperatures at the Eirik Drift (Irvali et al., 2012). Furthermore, in Core MD03-2664, the shift in the foraminifer assemblage from dominance of *N. pachyderma* (s) during MIS 6/TII to an assemblage with the subpolar-transitional species *N. incompta* (Fig. 5B), and *T. quinqueloba*, *G. bulloides* and *G. glutinata*, suggest an increased Atlantic water influence (Irvali et al., 2012). Similarly, foraminifer records from Core HU-90-013-013 on the Eirik Drift (Seidenkrantz et al., 1995, 1996), ODP 984 south of Iceland (Mokeddem et al., 2014) and isotope records from IODP Site U1304 on the Gardar Drift (Hodell et al., 2009) point to early MIS 5e warmth and provide broad evidence for warm Atlantic waters. Peak early MIS 5e warmth is further corroborated by several model experiments (e.g. Otto-Bliesner et al., 2006; Bakker et al., 2014). The higher surface ocean temperatures at the Eirik Drift are likely related to an active and west-east oriented SPG drawing in water from the IC as it does today (Fig. 6; e.g. Irvali et al., 2012, 2016; Bauch et al., 2011). This potentially zonally extended SPG configuration appears to have coincided with active dense water formation and ventilation in the Nordic Seas. This is evidenced by high values of benthic carbon isotopes on the Eirik Drift where the deep waters are influenced by the dense overflows from the Nordic Seas (Galaasen et al., 2014). Thus, in this scenario, a seemingly extended SPG is related to a strong AMOC, or at least well-ventilated dense overflows from the Nordic Seas, and not a weak AMOC as suggested by Klockmann et al. (2020). This highlights the complexity of the interaction between SPG dynamics and North Atlantic circulation, and that SPG geometry and strength are by no means the sole modulator of Nordic Seas ventilation.

Taken at face value, it seems difficult to reconcile a MIZ with peak warm MIS 5e near-surface ocean conditions. Discrepancies between reconstructions with different proxies are not uncommon, and have been linked to both habitat difference (i.e. water depth) and/or seasonality (e.g. de Vernal et al., 2020; Van Nieuwenhove et al., 2016; Andersson et al., 2010; Cortese et al., 2005; Risebrobakken et al., 2011; Leduc et al., 2010). Here, taking the habitat into account, biomarkers and dinocysts likely record changes in the uppermost part of the water column, where cold, sea ice laden surface waters occur. The planktic foraminifers would occupy the slightly deeper, warmer waters sourced by the IC. It is well known that planktic foraminifers occur in a sub-surface, slightly deeper habitat (e.g. Simstich et al., 2003; Kozdon et al., 2009; Jonkers et al., 2010; Pados and Spielhagen, 2014). Alternatively, the proxies reflect different seasons, with biomarkers/dinocysts reflecting more spring and autumn conditions and the planktic foraminifers reflecting the summer. For this reason, caution must always be taken when looking at a single proxy. Assuming that the subsurface habitat of *N. pachyderma* (s) also reflects surface ocean conditions, can lead to misinterpretation under some circumstances as pointed out by e.g. Hillaire-Marcel et al. (1994) and Dokken et al. (2013). Indeed, the subsurface

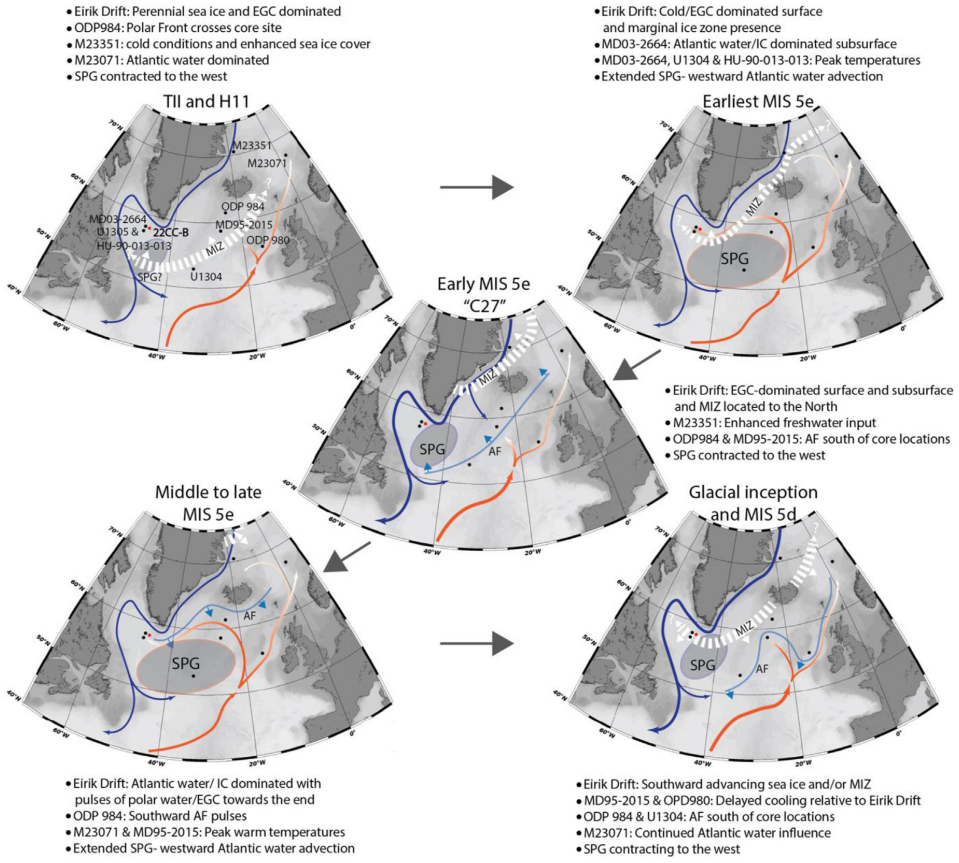

Fig. 6. Schematic North Atlantic surface hydrography during the late TII and H11, MIS 5e, and the last glacial inception and early MIS 5d. Surface ocean currents are indicated by dark blue (polar waters) and orange arrows (Atlantic waters). Thicker blue lines (polar water) mark periods with increased EGC dominance and potential increased freshwater by rerouting. The most likely position during each of the time intervals of the marginal ice zone (MIZ; white dashed lines), the Arctic Front (AF; light blue lines), and the subpolar gyre (SPG; grey shaded circles) are shown. The retreat or advance of the AF and MIZ are indicated by arrows.

habitat of *N. pachyderma* (s) may be particularly well-suited for recording warming events in the subsurface during episodes of stratification and surface cooling (e.g. Max et al., 2022). Viewed in this light, the warm foraminifer-based temperatures of the early MIS 5e could be caused by warm Atlantic waters circulating beneath a fresh surface layer and sea ice. This is similar to what occurs today when warm Atlantic water meets, and subducts beneath, fresh polar water in regions where a strong halocline is maintained by sea ice (Rudels et al., 2015). The presence of sea ice would, in turn, hinder ocean to atmosphere heat flux and cooling locally, potentially further contributing to a warm subsurface IC.

We speculate whether the MIZ location in the Labrador Sea could have played a role in maintaining or strengthening the SPG circulation and influenced the transport of warm and saline waters to the Eirik Drift. Although sea ice can inhibit local deep water formation, its proximity to the Labrador Sea convection regions may have stimulated heat and buoyancy loss, and therefore dense water formation that would affect the SPG strength. Near the polar MIZ today, Cold Air Outbreaks (CAOs) occur where strong winds off the sea ice edge play an important role for water mass transformation (Smedsrud et al., 2022). Thus, a MIZ immediately north of convection regions in the Labrador Sea might have stimulated water mass transformation in the subpolar region, altering the density structure and strength of the SPG (Born and Stocker, 2014). While more data will be necessary to test this concept, if correct, it could point to the MIZ being a critical factor to invigorate or maintain the SPG circulation during the earliest MIS 5e. Independent of the actual gyre configuration, our data indicate that when a MIZ was present at the northern margin of the SPG, a relatively cool surface and a halocline was maintained over a warmer subsurface layer of Atlantic Water (IC origin) at peak summer insolation. By analogy with today's Arctic, where similar configurations exist where Atlantic Water meets the sea ice edge (e.g. Årthun et al., 2012; Rudels et al., 2015), the presence of sea ice may have been a critical factor in maintaining this mode of stratification.

5.2.2. Early MIS 5e (126.5–124 ka): hydrographic shift and subsurface cooling

The surface ocean hydrography profoundly shifted at ~126.5 ka and the influence of Atlantic water to the subsurface was replaced by a stronger EGC influence. At the same time, the MIZ retreated north, away from the Eirik Drift. The EGC influence is inferred from

the rapid increase in abundance of the polar front associated dinocyst, *B. tepikiense* (Fig. 5C). IP_{25} concentrations decrease considerably, reflecting reductions in spring sea ice cover. However, HBI III (Z), HBI II, and IP_{25} do remain present in several samples, indicating the occasional occurrence of sea ice in the area (Fig. 5E). Cold, stratified surface waters characterised by large seasonal temperature variations and occasional sea ice cover is consistent with the high abundance of *B. tepikiense* (de Vernal et al., 2005, 2020) that is recorded here and similarly in the South Icelandic Basin (Eynaud et al., 2004). Seasonally open waters with increased sea surface productivity are recorded on the East Greenland margin which suggests a MIZ retreat far north of the Eirik Drift (Zhuravleva et al., 2017). At the Eirik Drift the foraminifer assemblage changes from a dominance of *N. incompta* to *N. pachyderma* (s) (Fig. 5B; Core MD03-2664; Irvali et al., 2012). This is also observed in Core HU-90-013-013 (Seidenkrantz et al., 1995) and suggests that Atlantic water influence decreased and cooler EGC conditions dominated.

This increasing EGC influence occurs during the C27 cooling event that is recognised in several North Atlantic proxy records (e.g. Oppo et al., 2006; Mokeddem et al., 2014; Irvali et al., 2016; Mokeddem and McManus, 2016; Tzedakis et al., 2018). A cooling event around this time is also observed in numerous locations across the North Atlantic and has been described as "stepwise deglaciation" or "reversal in deglacial warming trend" (e.g. Seidenkrantz et al., 1995, 1996; Risebrobakken et al., 2006; Bauch and Erlenkeuser, 2008; Van Nieuwenhove et al., 2011; Bauch et al., 2011, 2012; Zhuravleva et al., 2017).

In the light of this widespread North Atlantic cooling, it may seem incongruous that we record a northward retreat and decline in sea ice at the Eirik Drift. Sea ice retreat, despite continued polar water export, may simply be due to high summer insolation (Fig. 5A) and atmospheric CO_2 (Lüthi et al., 2008) at the time, which would have made it hard for sea ice to survive at the Eirik Drift, even in a cool surface ocean. Indeed, despite the evidence of cooler conditions and enhanced EGC in the early MIS 5e, the conditions on Greenland itself were mild. On the Eirik Drift (Core HU-90-013-013), de Vernal and Hillaire-Marcel (2008) show increased pollen and spore concentrations indicating a rapid expansion of vegetation in southern Greenland (Fig. 5F) and implying a retreat of the GIS. Simultaneously, intensified melting from the northeastern GIS is demonstrated by the isotopic record of Core M23351 (Zhuravleva et al., 2017) and sediment chemistry (Carlson et al., 2008; Colville et al., 2011), consistent with a widespread cryospheric decline at this time.

It has been proposed that increased freshwater input from a melting GIS and/or sea ice is a driving mechanism behind surface ocean cooling and changes in SPG circulation during the early LIG (e.g. Irvali et al., 2012, 2016; Mokeddem et al., 2014; Galaasen et al., 2014; Tzedakis et al., 2018). According to model simulations (Born et al., 2010), increased freshwater input to the Labrador Sea could weaken the SPG by altering the surface water salinity and density, and the rate of dense water formation in the Labrador Sea. It has been suggested that a weakened and contracted SPG (Fig. 6) allows for warmer subtropical waters to penetrate farther to the northeast and into the Nordic Seas (Hátún et al., 2005; Thornalley et al., 2009; Bauch et al., 1999, 2012; Van Nieuwenhove et al., 2011) invigorating deep water formation in the Nordic Seas, while Atlantic water transport westward to the Labrador Sea decreases. While such a shift in gyre dynamics could help explain the reduced input of IC water to the Eirik Drift at this time and the prevalence of cold, fresh, polar-like conditions, it does not readily explain the coeval decrease in deep water ventilation at the site. Deep water formation in the Nordic Seas seems to have been weakened during this time, as evidenced in depleted benthic $\delta^{13}C$ values on the Eirik Drift (Galaasen et al., 2014), since this site is influenced today by dense (Denmark Strait) overflow waters. Supporting a reduced ventilation of Nordic Seas deep water at this time, low $\delta^{13}C$ values have been recorded around 126.5 ka on the East Greenland margin (Zhuravleva et al., 2017) and in the Nordic Seas (Bauch et al., 2012). Although the Nordic Seas depletions appear smaller and shorter (~1000 years) compared to the Labrador Sea (~2500 years), they first occur together with the C27 cooling phase.

Another factor contributing to increasing EGC and polar-like conditions could be the potential rerouting of freshwater caused by the presence of an ice sheet over the Canadian Arctic Archipelago (CAA; Condron and Winsor, 2012; Lofverstrom et al., 2022). As sea level rose coming out of the glacial period and the Bering Strait opened, freshwater could once again flow from the Pacific to the Atlantic via the Arctic Ocean. If a remnant LIS remained in the CAA, all freshwater that today can flow freely through the Davis Strait west of Greenland would be rerouted through the Fram Strait, into the EGC and onwards into the North Atlantic deep convection regions. Previous studies have also shown that AMOC strength and North Atlantic climate is sensitive to the status of gateways in the Arctic (Otto-Bliesner et al., 2006; Hu et al., 2010; Karami et al., 2021). We hypothesise that Arctic rerouting of Pacific freshwater remains a potential contributor to the enhanced influence of the relatively cool and fresh EGC in the early MIS 5e. Condron and Winsor (2012) and Lofverstrom et al. (2022) suggest such rerouting as a potential feedback mechanism behind the Younger Dryas cooling late in the last deglaciation. Interestingly, the C27 event associated with the EGC expansion south of Greenland and the surface ocean cooling in the North Atlantic, have often been compared to the Younger Dryas (e.g. Sarnthein and Tiedemann, 1990; Seidenkrantz et al., 1996; Sánchez Goñi et al., 2005). Two prerequisites are necessary for this EGC focused freshwater routing to be plausible. One, sea level must have been high enough for the Bering Strait to be open, and two, enough glacial ice must have persisted to block freshwater export routes west of Greenland (Lofverstrom et al., 2022). The first condition seems to have been met: sea level was high enough during this period (Fig. 5A; Spratt and Lisiecki, 2016) to allow freshwater transport across Bering Strait. For the second condition to be met, the LIS must have remained sufficiently large early in MIS 5e to have blocked freshwater export through the CAA, despite the orbitally modulated high summer insolation.

An interesting sedimentological feature in our core is the red layer at the end of the C27 cooling. It is associated with a sudden rapid re-occurrence of sea ice at the Eirik Drift which is distinctly marked by the occurrence of IP_{25}, and RBC, followed by cysts of *P. dalei*. Taken together they indicate a short event of rapid sea ice discharge, meltwater and stratification. This signal was likely transported and does not represent a reappearance of the MIZ at our site, which is further supported by the low MIZ marker HBI III (Z). Furthermore, cysts of *S. trifida* have been linked to LIS-sourced meltwater input around southern Greenland and south-eastern Canada for early Holocene sediments (Head et al., 2006; Van Nieuwenhove et al., 2018), and its occurrence here in the LIG may equally suggest an origin from Canadian waters. The red layer found in our core, and in Cores MD03−2664 and U1304, has been linked to an outburst flood event through the Hudson Strait (Nicholl et al., 2012; Shaw and Lesemann, 2003) akin to the 8.2 ka event early in the Holocene when the southern margin of the LIS retreated enough that proglacial lake Agassiz broke through the ice dam blocking its drainage through Hudson Straight (Hillaire-Marcel et al., 2007) and deposited a similar red layer (Kerwin, 1996; St-Onge and Lajeunesse, 2007; Lajeunesse and St-Onge, 2008). The similarity between the sediment deposits and their relative timings, early in both interglacials, suggests similar mechanisms behind the events. This implies that like during the Holocene, there

could have been a residual LIS presence even after peak summer insolation during early MIS 5e. Such a remnant large ice mass would be consistent with the recent suggestion of an early MIS 5e sea level high stand related to Antarctic melting, whereas the GIS contribution rather played a larger role later in MIS 5e (Rohling et al., 2019). Regarding the freshwater rerouting theory, a remnant LIS could hint that ice cap remnants occurred also further north in the CAA; however this remains indirect, inconclusive evidence that ice restricted or blocked the CAA freshwater route.

5.2.3. Middle to late MIS 5e (124–116 ka): Atlantic water advection and occasional cold-water events

For the remainder of MIS 5e, the surface waters at the Eirik Drift are characterised mainly by Atlantic water inflow via the IC and an extended and/or strong SPG. This is evident from the dominance of the Atlantic water indicator *O. centrocarpum* and the absence of sea ice biomarkers, demonstrating open waters. From ca. 122 ka, a low but notable and sustained occurrence of *S. mirabilis* (Fig. 3J) indicates warm-temperate waters (see section 3.3). This species characterises interglacial optima in the northern North Atlantic and is known in late MIS 5e from the Gardar Drift (Core MD95-2015; Eynaud et al., 2004), Nordic Seas (Core M23071; Van Nieuwenhove et al., 2008), and even Fram Strait (Van Nieuwenhove et al., 2011). While its occurrence is used to interpret a late glacial optimum for these areas (e.g. Van Nieuwenhove et al., 2011), we find that at the Eirik Drift the influence of warm Atlantic water via the IC was interrupted by episodes of cold Arctic water outflow through the EGC. These intermittent incursions of EGC influence occur against a background of declining sea surface temperature (Irvali et al., 2016) and summer insolation (Fig. 5A). Similar late MIS 5e cooling events have been documented in the central (ODP 984; Mokeddem et al., 2014) and eastern subpolar North Atlantic (ODP 980; Oppo et al., 2006). In our study, peaks of the cysts of *P. dalei* and *B. tepikiense* indicate these incursions of cold water masses and southward pulses of the Arctic Front, especially since *B. tepikiense* is a frontal zone indicator reflecting cold, stratified surface waters characterised by large seasonal temperature variability (de Vernal et al., 2005, 2020). The largest cold water excursions at the Eirik Drift are around 118–117 ka where the cysts of *P. dalei* and *B. tepikiense* increase in abundance, and the Atlantic water indicator *O. centrocarpum* decreases (Fig. 5C and D). In Core MD03-2664, the 117 ka cooling is marked by a peak in IRD, a large anomaly in the planktic oxygen isotopes (Fig. 5G), and an increase in *N. pachyderma* (s) (Fig. 5B; Irvali et al., 2016). These data together reflect enhanced GIS activity and growth, and colder surface ocean conditions towards the end of MIS 5e. Additionally, expanded GIS extent is inferred from a decrease in the pollen and spore concentrations (Fig. 5F; de Vernal and Hillaire-Marcel, 2008) from the Eirik Drift indicating a deterioration of the vegetation in the south of Greenland. On the East Greenland margin short-term, pronounced depletions in both planktic and benthic $\delta^{18}O$ (Core M23351; Zhuravleva et al., 2017) are associated with enhanced freshwater pulses that could be related to the cooling events and increased GIS activity. These cold anomalies indicate that even during the warm LIG, incursions of cold and fresh Arctic water masses influenced the Labrador Sea.

5.3. MIS 5d (116–108 ka): glacial inception and the return of seasonal sea ice

As summer insolation reached a minimum at the transition into MIS 5d, the return of cool conditions led to the return of sea ice at the Eirik Drift. Prior to the return of sea ice, a transitional phase from MIS 5e to 5d is characterised by *N. labyrinthus* and high dinocyst concentrations, indicating increased surface ocean productivity, typically seen at frontal zones. Following the transitional phase, the Arctic front migrated southwards again and EGC-like conditions returned. The EGC likely transported sea ice to the Labrador Sea, as one can interpret from the increased IP_{25} concentrations. The low HBI III (Z) concentrations could suggest that the Eirik Drift is not in the marginal ice zone, however, a readvance of the MIZ towards the Eirik Drift is likely, given the dominance of RBC (Fig. 5D and E).

When examining the North Atlantic on a broader scale, there are differences in the dinocyst assemblages between the western and eastern regions during MIS 5d. While cold conditions are evident at the Eirik Drift, dinocyst assemblages from the southern Icelandic Basin suggest sea ice free conditions and rather warm Atlantic (IC) waters persisted (Core MD95-2015; Eynaud et al., 2004). Furthermore, Eirik Drift sea surface temperature records (Core MD03-2664; Irvali et al., 2016) indicate a larger cooling compared to the central Atlantic ODP 980 (Oppo et al., 2006). The temperature difference and/or delayed cooling response in the east *vs* west is likely explained by the ocean frontal zones, and sea ice expanding south of the Eirik Drift prior to reaching the more eastern site. The frontal zone and/or MIZ was likely located north of the Iceland Basin in a SW-NE orientation, consistent with a weak SPG contracted to the northwest (Fig. 6; e.g. Mokeddem et al., 2014). A contracted SPG allows warmer and more saline water to enter the eastern subpolar North Atlantic and Nordic Seas, while Atlantic water transport via the IC towards the west would decrease (see section 5.2.2). The cooling-fostered return of sea ice could have amplified or even triggered reductions in SPG strength by freshening the surface ocean during the last glacial inception, consistent with model findings (Born et al., 2010). However, it is important to note that the SPG is sensitive not only to buoyancy forcing (e.g. Levermann and Born, 2007; Mengel et al., 2012; Born and Stocker, 2014) but also to atmospheric circulation patterns (e.g. Lohmann et al., 2009).

It is also possible that the glacial inception itself may have played a key role in cooling by influencing pathways of Arctic freshwater and sea ice export to the North Atlantic. Initial ice sheet growth at the last glacial inception was so rapid and substantial that global sea level decreased by as much as 30–50 m between ~120 and 110 ka (Kopp et al., 2009; Spratt and Lisiecki, 2016; Waelbroeck et al., 2002; Lambeck and Chappell, 2001), which is demonstrated by increased IRD at the Eirik Drift (Fig. 5G) and across the North Atlantic (e.g. Risebrobakken et al., 2007; Zhuravleva et al., 2017; Oppo et al., 2006). Lofverstrom et al. (2022) suggested that the low summer insolation at 116 ka was sufficient to grow an ice sheet to once again block the CAA ocean gateways, similar to other modelling studies (Vettoretti and Peltier, 2003; Birch et al., 2017; Born et al., 2010). In addition, the global sea level remained high enough (Fig. 5A) to allow Pacific water inflow through the Bering Strait within the first phase of glacial inception. Similar to what we speculate might have happened in the early MIS 5e (see section 5.2.2), an ice sheet-blocked CAA would have rerouted Arctic freshwater into the EGC, and, via the EGC, south to the Labrador Sea where the increased freshwater could weaken convection and the gyre circulation. Uncertainty remains about whether the potential ice sheet could completely or partly block the CAA due to the depth of the two main export routes, Nares Strait and Lancaster Sound. However, Lofverstrom et al. (2022) argue that due to highly stratified waters in the Nares Strait and Lancaster Sound (Münchow et al., 2015; Prinsenberg and Hamilton, 2005), the formation of a thick floating ice shelf could be sufficient to inhibit freshwater flux through the archipelago. Another challenge is that direct proxy evidence of the ice sheet configuration in the CAA is not available, since ice sheets in later glacial stages have removed evidence of earlier glaciations (Svendsen et al., 2004; Stokes et al., 2012; Batchelor et al., 2019; Kleman et al., 2010; Dalton et al., 2022).

Reliable ice sheet reconstructions in the CAA region and additional evidence of changes in freshwater transport routes are crucial to better evaluate this scenario, and to what extent it ultimately could have impacted the SPG, AMOC and North Atlantic circulation.

6. Summary and conclusions

Based on new sea ice and surface ocean hydrographical data from the Eirik Drift in the Labrador Sea we interpret the paleoceanographic evolution from the penultimate glacial throughout MIS 5e and into MIS 5d as follows.

- MIS 6 (>~135 ka) was characterised by a thick and extensive perennial sea ice cover at the Eirik Drift. The sea ice cover started to break up episodically during TII (135–128 ka), as northern hemisphere summer insolation increased toward its maximum.
- From the onset of MIS 5e (128–126.5 ka), the Eirik Drift surface waters were characterised by a MIZ and the EGC, while the subsurface was influenced by warm Atlantic waters via the IC and an active/extended SPG circulation. It can be hypothesized that the proximity of the MIZ to the Labrador Sea convection regions could have maintained or invigorated SPG circulation during the earliest MIS 5e.
- The MIZ retreated northwards (126.5–124 ka) and both the surface and subsurface were dominated by strong EGC and polar water conditions. High insolation and atmospheric CO_2 probably did not allow for sea ice to survive as far south as the Eirik Drift. This setting is consistent with a weak/contracted SPG circulation coincident with the C27 (cooling) event and/or "deglacial pause" that is observed across the North Atlantic. The interval ended with an outburst flood event, likely from the Hudson Strait region, which is documented by a distinct red layer, and a short-lived surge of sea ice and stratification of the upper water column.
- The second half of MIS 5e (124–116 ka) was characterised by a strong influence (inflow) of Atlantic water via the IC, potentially indicating an extended/strong SPG at this time. This state was interrupted by episodes of cold Arctic water through the EGC, as summer insolation decreased towards the end of MIS 5e.
- At the transition into MIS 5d (116 ka) the Eirik Drift was again dominated by the EGC and a readvance of the Arctic front to the south of the Eirik Drift before sea ice reappeared. The sea ice presence could have played an important role in amplifying the cooling of last glacial inception by diminishing the strength and lateral extension of the SPG.
- We note that intervals of marked increase in EGC influence at both the start (126.5–124 ka) and termination (116 ka) of MIS 5e occur at times when sea level was high enough for the Bering Strait to be open. At the same time, the residual or proto LIS may have been sufficiently expanded to restrict export pathways west of Greenland resulting in a focusing, and intensification of the EGC route for freshwater transport to the SPG. If such a scenario were to be corroborated by future findings, it underlines the possibly important role of cryosphere reconfigurations, and their influence on freshwater export and rerouting to the North Atlantic, for understanding the climate and hydrographic transitions associated with glacial termination and inception.

Finally, our combined dinocyst and biomarker data are the first to unequivocally demonstrate the presence of sea ice during TII, the earliest MIS 5e and MIS 5d as well as indirectly in MIS 6. During the late MIS 5e, cold events were recorded but sea ice was not present as far south as the Eirik Drift. Nevertheless, it appears clear that sea ice played a role in the SPG circulation during glacial termination and inception.

Author contributions

KS and SDS designed the study. KS generated and analysed all data with the help of KF, SDS, RS and USN. USN generated the stable isotope data. KS wrote the manuscript with input from all authors.

Declaration of competing interest

The authors declare that they have no known competing financial interests or personal relationships that could have appeared to influence the work reported in this paper.

Data availability

Raw data is available from www.pangaea.de at https://doi.org/10.1594/PANGAEA.955398

Acknowledgements

This study is part of the AGENSI project, which is funded by the European Research Council (ERC) under the European Union's Horizon 2020 research and innovation program (grant agreement n° 818449). We like to thank the researchers and crew on board RV G.O. Sars during the 2016 cruise of the Ice2Ice project, which was funded by the European Research Council under the European Union's Seventh Framework Programme (FP7/2007–2013, ERC grant agreement n° 610055). We thank Walter Luttmer in the biomarker laboratory, Dag Inge Blindheim for technical support and Malcolm Jones at Palynological Laboratory Service Ltd.

Appendix A. Supplementary data

Supplementary data to this article can be found online at https://doi.org/10.1016/j.quascirev.2023.108198.

References

Andersson, C., Pausata, F.S.R., Jansen, E., Risebrobakken, B., Telford, R.J., 2010. Holocene trends in the foraminifer record from the Norwegian Sea and the North Atlantic Ocean. Clim. Past 6, 179–193.

Årthun, M., Eldevik, T., Smedsrud, L.H., Skagseth, Ø., Ingvaldsen, R.B., 2012. Quantifying the influence of atlantic heat on barents Sea Ice variability and retreat. J. Clim. 25, 4736–4743. https://doi.org/10.1175/JCLI-D-11-00466.1.

Bacon, S., Reverdin, G., Rigor, I.G., Snaith, H.M., 2002. A freshwater jet on the east Greenland shelf. J. Geophys. Res.: Oceans 107. https://doi.org/10.1029/2001JC000935, 5-1-5-16.

Bakker, P., Masson-Delmotte, V., Martrat, B., Charbit, S., Renssen, H., Gröger, M., Krebs-Kanzow, U., Lohmann, G., Lunt, D.J., Pfeiffer, M., Phipps, S.J., Prange, M., Ritz, S.P., Schulz, M., Stenni, B., Stone, E.J., Varma, V., 2014. Temperature trends during the Present and Last Interglacial periods – a multi-model-data comparison. Quat. Sci. Rev. 99, 224–243. https://doi.org/10.1016/j.quascirev.2014.06.031.

Batchelor, C.L., Margold, M., Krapp, M., Murton, D.K., Dalton, A.S., Gibbard, P.L., Stokes, C.R., Murton, J.B., Manica, A., 2019. The configuration of Northern Hemisphere ice sheets through the Quaternary. Nat. Commun. 10, 3713. https://doi.org/10.1038/s41467-019-11601-2.

Bauch, H.A., Erlenkeuser, H., 2008. A "critical" climatic evaluation of last interglacial (MIS 5e) records from the Norwegian Sea. Polar Res. 27, 135–151. https://doi.org/10.3402/polar.v27i2.6172.

Bauch, H.A., Erlenkeuser, H., Fahl, K., Spielhagen, R.F., Weinelt, M.S., Andruleit, H., Henrich, R., 1999. Evidence for a steeper Eemian than Holocene sea surface temperature gradient between Arctic and sub-Arctic regions. Palaeogeogr. Palaeoclimatol. Palaeoecol. 145, 95–117. https://doi.org/10.1016/S0031-0182(98)00104-7.

Bauch, H.A., Kandiano, E.S., Helmke, J., Andersen, N., Rosell-Mele, A., Erlenkeuser, H., 2011. Climatic bisection of the last interglacial warm period in the Polar North Atlantic. Quat. Sci. Rev. 30, 1813–1818. https://doi.org/10.1016/j.quascirev.2011.05.012.

Bauch, H.A., Kandiano, E.S., Helmke, J.P., 2012. Contrasting ocean changes between the subpolar and polar North Atlantic during the past 135 ka. Geophys. Res. Lett. 39. https://doi.org/10.1029/2012GL051800.

Belt, S.T., 2018. Source-specific biomarkers as proxies for Arctic and Antarctic sea ice. Org. Geochem. 125, 277–298. https://doi.org/10.1016/

j.orggeochem.2018.10.002.
Belt, S.T., Allard, W.G., Massé, G., Robert, J.-M., Rowland, S.J., 2000. Highly branched isoprenoids (HBIs): identification of the most common and abundant sedimentary isomers. Geochem. Cosmochim. Acta 64, 3839–3851. https://doi.org/10.1016/S0016-7037(00)00464-6.
Belt, S.T., Massé, G., Rowland, S.J., Poulin, M., Michel, C., LeBlanc, B., 2007. A novel chemical fossil of palaeo sea ice: IP25. Org. Geochem. 38, 16–27. https://doi.org/10.1016/j.orggeochem.2006.09.013.
Belt, S.T., Cabedo-Sanz, P., Smik, L., Navarro-Rodriguez, A., Berben, S., Knies, J., Husum, K., 2015. Identification of paleo Arctic winter sea ice limits and the marginal ice zone: optimised biomarker-based reconstructions of late Quaternary Arctic sea ice. Earth Planet Sci. Lett. 431, 127–139. https://doi.org/10.1016/j.epsl.2015.09.020.
Belt, S.T., Smik, L., Brown, T., Kim, J.-H., Rowland, S., Allen, C., Gal, J.-K., Shin, K.-H., Lee, J., Taylor, K., 2016. Source identification and distribution reveals the potential of the geochemical Antarctic sea ice proxy IPSO25. Nat. Commun. 7, 12655. https://doi.org/10.1038/ncomms12655.
Belt, S.T., Brown, T.A., Smik, L., Assmy, P., Mundy, C.J., 2018. Sterol identification in floating Arctic sea ice algal aggregates and the Antarctic sea ice diatom Berkeleya adeliensis. Org. Geochem. 118, 1–3. https://doi.org/10.1016/j.orggeochem.2018.01.008.
Berger, A., Loutre, M.F., 1991. Insolation values for the climate of the last 10 million years. Quat. Sci. Rev. 10, 297–317. https://doi.org/10.1016/0277-3791(91)90033-Q.
Birch, L., Cronin, T., Tziperman, E., 2017. Glacial inception on baffin island: the role of insolation, meteorology, and topography. J. Clim. 30, 4047–4064. https://doi.org/10.1175/JCLI-D-16-0576.1.
Boon, J.J., Rijpstra, W.I.C., De Lange, F., De Leeuw, J.W., Yoshioka, M., Shimizu, Y., 1979. Black Sea sterol—a molecular fossil for dinoflagellate blooms. Nature 277, 125–127. https://doi.org/10.1038/277125a0.
Born, A., Stocker, T.F., 2014. Two stable equilibria of the atlantic subpolar gyre. J. Phys. Oceanogr. 44, 246–264. https://doi.org/10.1175/JPO-D-13-073.1.
Born, A., Nisancioglu, K.H., Braconnot, P., 2010. Sea ice induced changes in ocean circulation during the Eemian. Clim. Dynam. 35, 1361–1371. https://doi.org/10.1007/s00382-009-0709-2.
Brown, T.A., Belt, S.T., Tatarek, A., Mundy, C.J., 2014. Source identification of the Arctic sea ice proxy IP25. Nat. Commun. 5, 4197. https://doi.org/10.1038/ncomms5197.
Carlson, A.E., Stoner, J.S., Donnelly, J.P., Hillaire-Marcel, C., 2008. Response of the southern Greenland Ice Sheet during the last two deglaciations. Geology 36, 359–362. https://doi.org/10.1130/G24519A.1.
Channell, J.E.T., Kanamatsu, T., Sato, T., Stein, R., Alvarez Zarikian, C.A., Malone, M.J., and the Expedition 303/306 Scientists, 2006. In: Proceedings of the IODP, 303/306, Proceedings of the IODP. Integrated Ocean Drilling Program. https://doi.org/10.2204/iodp.proc.303306.2006.
Collins, L.G., Allen, C.S., Pike, J., Hodgson, D.A., Weckström, K., Massé, G., 2013. Evaluating highly branched isoprenoid (HBI) biomarkers as a novel Antarctic sea-ice proxy in deep ocean glacial age sediments. Quat. Sci. Rev. 79, 87–98. https://doi.org/10.1016/j.quascirev.2013.02.004.
Colville, E.J., Carlson, A.E., Beard, B.L., Hatfield, R.G., Stoner, J.S., Reyes, A.V., Ullman, D.J., 2011. Sr-Nd-Pb isotope evidence for ice-sheet presence on southern Greenland during the last interglacial. Science 333, 620–623. https://doi.org/10.1126/science.1204673.
Condron, A., Winsor, P., 2012. Meltwater routing and the younger Dryas. Proc. Natl. Acad. Sci. USA 109, 19928–19933. https://doi.org/10.1073/pnas.1207381109.
Cortese, G., Dolven, J.K., Bjørklund, K.R., Malmgren, B.A., 2005. Late Pleistocene–Holocene radiolarian paleotemperatures in the Norwegian Sea based on artificial neural networks. Palaeogeogr. Palaeoclimatol. Palaeoecol. 224, 311–332. https://doi.org/10.1016/j.palaeo.2005.04.015.
Dale, B., 1996. Chapter 31. Dinoflagellate cyst ecology: modeling and geological applications. In: Jansonius, J., McGregor, D.C. (Eds.), Palynology: Principles and Applications, vol. 3. American Association of Stratigraphic Palynologists Foundation, Dallas, TX, pp. 1249–1275.
Dale, B., 2001. The sedimentary record of dinoflagellate cysts: looking back into the future of phytoplankton blooms. Sci. Mar. 65, 257–272. https://doi.org/10.3989/scimar.2001.65s2257.
Dalton, A.S., Stokes, C.R., Batchelor, C.L., 2022. Evolution of the Laurentide and innuitian ice sheets prior to the last glacial maximum (115 ka to 25 ka). Earth Sci. Rev. 224, 103875. https://doi.org/10.1016/j.earscirev.2021.103875.
de Schepper, S., Beck, K.M., Mangerud, G., 2017. Late neogene dinoflagellate cyst and acritarch biostratigraphy for Ocean Drilling program hole 642B, Norwegian sea. Rev. Palaeobot. Palynol. https://doi.org/10.1016/j.revpalbo.2016.08.005.
de Vernal, A., Hillaire-Marcel, C., 2008. Natural variability of Greenland climate, vegetation, and ice volume during the past million years. Science 320, 1622–1625. https://doi:10.1126/science.1153929.
de Vernal, A., Marret, F., 2007. Organic-walled dinoflagellate cysts: tracers of sea-surface conditions. In: Hillaire-Marcel, C., de Vernal, A. (Eds.), Proxies in Late Cenozoic Paleoceanography, vol. 1. Elsevier, Rotterdam, pp. 371–408. https://doi.org/10.1016/S1572-5480(07)01014-7.
de Vernal, A., Rochon, A., Turon, J.-L., Matthiessen, J., 1997. Organic-walled dinoflagellate cysts: palynological tracers of sea-surface conditions in middle to high latitude marine environments. Geobios 30, 905–920. https://doi.org/10.1016/S0016-6995(97)80215-X.
de Vernal, A., Hillaire-Marcel, C., Turon, J.-L., Matthiessen, J., 2000. Reconstruction of sea-surface temperature, salinity, and sea-ice cover in the northern North Atlantic during the last glacial maximum based on dinocyst assemblages. Can. J. Earth Sci. 37, 725–750. https://doi.org/10.1139/e99-091.
de Vernal, A., Eynaud, F., Henry, M., Hillaire-Marcel, C., Londeix, L., Mangin, S., Matthiessen, J., Marret, F., Radi, T., Rochon, A., Solignac, S., Turon, J.-L., 2005. Reconstruction of sea-surface conditions at middle to high latitudes of the Northern Hemisphere during the Last Glacial Maximum (LGM) based on dinoflagellate cyst assemblages. Quat. Sci. Rev. 24, 897–924. https://doi.org/10.1016/j.quascirev.2004.06.014.
de Vernal, A., Gersonde, R., Goosse, H., Seidenkrantz, M.-S., Wolff, E.W., 2013. Sea ice in the paleoclimate system: the challenge of reconstructing sea ice from proxies – an introduction. Quat. Sci. Rev. 79, 1–8. https://doi.org/10.1016/j.quascirev.2013.08.009.
de Vernal, A., Radi, T., Zaragosi, S., Van Nieuwenhove, N., Rochon, A., Allan, E., De Schepper, S., Eynaud, F., Head, M.J., Limoges, A., Londeix, L., Marret, F., Matthiessen, J., Penaud, A., Pospelova, V., Price, A., Richerol, T., 2020. Distribution of common modern dinoflagellate cyst taxa in surface sediments of the Northern Hemisphere in relation to environmental parameters: the new n=1968 database. Mar. Micropaleontol. 159, 101796. https://doi.org/10.1016/j.marmicro.2019.101796.
Dokken, T.M., Nisancioglu, K.H., Li, C., Battisti, D.S., Kissel, C., 2013. Dansgaard-Oeschger cycles: interactions between ocean and sea ice intrinsic to the Nordic seas. Paleoceanography 28, 491–502. https://doi.org/10.1002/palo.20042.
Eynaud, F., Turon, J.L., Duprat, J., 2004. Comparison of the Holocene and eemian palaeoenvironments in the South Icelandic basin: dinoflagellate cysts as proxies for the North atlantic surface circulation. Rev. Palaeobot. Palynol. 128, 55–79. https://doi.org/10.1016/S0034-6667(03)00112-X.
Fahl, K., Stein, R., 2012. Modern seasonal variability and deglacial/Holocene change of central Arctic Ocean sea-ice cover: new insights from biomarker proxy records. Earth Planet Sci. Lett. 351 (352), 123–133. https://doi.org/10.1016/j.epsl.2012.07.009.
Foukal, N.P., Lozier, M.S., 2017. Assessing variability in the size and strength of the North Atlantic subpolar gyre. J. Geophys. Res. 122, 6295–6308. https://doi.org/10.1002/2017JC012798.
Galaasen, E.V., Ninnemann, U.S., Irvali, N., Kleiven, H.F., Rosenthal, Y., Kissel, C., Hodell, D.A., 2014. Rapid reductions in North Atlantic deep water during the peak of the last Interglacial period. Science 343, 1129–1132. https://doi.org/10.1126/science.1248667.
Griem, L., Voelker, A.H.L., Berben, S.M.P., Dokken, T.M., Jansen, E., 2019. Insolation and glacial meltwater influence on sea-ice and circulation variability in the northeastern Labrador Sea during the last glacial period. Paleoceanogr. Paleoclimatol. 34, 1689–1709. https://doi.org/10.1029/2019PA003605.
Grøsfjeld, K., Funder, S., Seidenkrantz, M.-S., Glaister, C., 2006. Last Interglacial marine environments in the White Sea region, northwestern Russia. Boreas 35, 493–520. https://doi.org/10.1080/03009480600781917.
Grøsfjeld, K., Harland, R., Howe, J., 2009. Dinoflagellate cyst assemblages inshore and offshore Svalbard reflecting their modern hydrography and climate. Norw. J. Geol. 89, 129–134.
Häkkinen, S., Rhines, P.B., 2004. Decline of subpolar North Atlantic circulation during the 1990s. Science 304, 555–559.
Hátún, H., Sandø, A.B., Drange, H., Hansen, B., Valdimarsson, H., 2005. Influence of the atlantic subpolar gyre on the thermohaline circulation. Science 309, 1841–1844.
Head, M.J., Lewis, J., de Vernal, A., 2006. The cyst of the calcareous dinoflagellate Scrippsiella trifida: resolving the fossil record of its organic wall with that of Alexandrium tamarense. J. Paleontol. 80, 1–18. https://doi.org/10.1666/0022-3360(2006)080[0001:TCOTCD]2.0.CO;2.
Hennissen, J.A.I., Head, M.J., de Schepper, S., Groeneveld, J., 2014. Palynological evidence for a southward shift of the North atlantic current at 2.6 ma during the intensification of late cenozoic northern hemisphere glaciation. Paleoceanography 29, 564–580. https://doi.org/10.1002/2013PA002543.
Hennissen, J.A.I., Head, M.J., de Schepper, S., Groeneveld, J., 2017. Dinoflagellate cyst paleoecology during the pliocene–pleistocene climatic transition in the North atlantic. Palaeogeogr. Palaeoclimatol. Palaeoecol. 470, 81–108. https://doi.org/10.1016/j.palaeo.2016.12.023.
Heslop, D., de Schepper, S., Proske, U., 2011. Diagnosing the uncertainty of taxa relative abundances derived from count data. Mar. Micropaleontol. 79, 114–120. https://doi.org/10.1016/j.marmicro.2011.01.007.
Hillaire-Marcel, de Vernal, A., Bilodeau, G., Wu, G., 1994. Isotope stratigraphy, sedimentation rates, deep circulation, and carbonate events in the Labrador Sea during the last ~200ka. Can. J. Earth Sci. 31, 63–89. https://doi.org/10.1139/e94-007.
Hillaire-Marcel, C., de Vernal, A., Bilodeau, G., Weaver, A., 2001. Absence of deep-water formation in the Labrador Sea during the last Interglacial period. Nature 410, 1073–1077. https://doi.org/10.1038/35074059.
Hillaire-Marcel, C., de Vernal, A., Piper, D.J.W., 2007. Lake Agassiz final drainage event in the northwest North Atlantic. Geophys. Res. Lett. 34. https://doi.org/10.1029/2007GL030396.
Hodell, D.A., Minth, E.K., Curtis, J.H., McCave, I.N., Hall, I.R., Channell, J.E.T., Xuan, C., 2009. Surface and deep-water hydrography on Gardar Drift (Iceland Basin) during the last interglacial period. Earth Planet Sci. Lett. 288, 10–19. https://doi.org/10.1016/j.epsl.2009.08.040.
Hu, A., Meehl, G.A., Otto-Bliesner, B.L., Waelbroeck, C., Han, W., Loutre, M.-F., Lambeck, K., Mitrovica, J.X., Rosenbloom, N., 2010. Influence of Bering Strait flow and North Atlantic circulation on glacial sea-level changes. Nat. Geosci. 3, 118–121. https://doi.org/10.1038/ngeo729.

Huang, W.-Y., Meinschein, W.G., 1979. Sterols as ecological indicators. Geochem. Cosmochim. Acta 43, 739–745. https://doi.org/10.1016/0016-7037(79)90257-6.
Hunter, S., Wilkinson, D., Louarn, E., Nick McCave, I., Rohling, E., Stow, D.A.V., Bacon, S., 2007. Deep western boundary current dynamics and associated sedimentation on the Eirik Drift, Southern Greenland Margin. Deep Sea Res. Oceanogr. Res. Pap. 54, 2036–2066. https://doi.org/10.1016/j.dsr.2007.09.007.
Irvali, N., Ninnemann, U.S., Galaasen, E.V., Rosenthal, Y., Kroon, D., Oppo, D.W., Kleiven, H.F., Darling, K.F., Kissel, C., 2012. Rapid switches in subpolar North Atlantic hydrography and climate during the Last Interglacial (MIS 5e). Paleoceanography 27. https://doi.org/10.1029/2011PA002244.
Irvali, N., Ninnemann, U.S., Kleiven, H.F., Galaasen, E.V., Morley, A., Rosenthal, Y., 2016. Evidence for regional cooling, frontal advances, and East Greenland Ice Sheet changes during the demise of the last interglacial. Quat. Sci. Rev. 150, 184–199. https://doi.org/10.1016/j.quascirev.2016.08.029.
Jaffé, R., Wolff, G.A., Cabrera, A.C., Chitty, H.C., 1995. The biogeochemistry of lipids in rivers of the Orinoco Basin. Geochem. Cosmochim. Acta 59, 4507–4522. https://doi.org/10.1016/0016-7037(95)00246-V.
Johns, L., Wraige, E.J., Belt, S.T., Lewis, C.A., Massé, G., Robert, J.-M., Rowland, S.J., 1999. Identification of a C25 highly branched isoprenoid (HBI) diene in Antarctic sediments, Antarctic sea-ice diatoms and cultured diatoms. Org. Geochem. 30, 1471–1475. https://doi.org/10.1016/S0146-6380(99)00112-6.
Jonkers, L., Brummer, G.-J.A., Peeters, F.J.C., van Aken, H.M., De Jong, M.F., 2010. Seasonal stratification, shell flux, and oxygen isotope dynamics of left-coiling N. pachyderma and T. quinqueloba in the western subpolar North Atlantic. Paleoceanography 25. https://doi.org/10.1029/2009PA001849.
Kageyama, M., Sime, L.C., Sicard, M., Guarino, M.-V., de Vernal, A., Stein, R., Schroeder, D., Malmierca-Vallet, I., Abe-Ouchi, A., Bitz, C., Braconnot, P., Brady, E.C., Cao, J., Chamberlain, M.A., Feltham, D., Guo, C., LeGrande, A.N., Lohmann, G., Meissner, K.J., Menviel, L., Morozova, P., Nisancioglu, K.H., Otto-Bliesner, B.L., O'ishi, R., Ramos Buarque, S., Salas y Melia, D., Sherriff-Tadano, S., Stroeve, J., Shi, X., Sun, B., Tomas, R.A., Volodin, E., Yeung, N.K.H., Zhang, Q., Zhang, Z., Zheng, W., Ziehn, T., 2021. A multi-model CMIP6-PMIP4 study of Arctic sea ice at 127: sea ice data compilation and model differences. Clim. Past 17, 37–62. https://doi.org/10.5194/cp-17-37-2021.
Karami, M.P., Myers, P.G., de Vernal, A., Tremblay, L.B., Hu, X., 2021. The role of Arctic gateways on sea ice and circulation in the Arctic and North Atlantic Oceans: a sensitivity study with an ocean-sea-ice model. Clim. Dynam. 57, 2129–2151. https://doi.org/10.1007/s00382-021-05798-6.
Kerwin, M.W., 1996. A regional stratigraphic isochron (ca. 800014C yr B.P.) from final deglaciation of Hudson Strait. Quat. Res. 46, 89–98. https://doi.org/10.1006/qres.1996.0049.
Kessler, A., Bouttes, N., Roche, D.M., Ninnemann, U.S., Galaasen, E.V., Tjiputra, J., 2020. Atlantic meridional overturning circulation and δ13C variability during the last interglacial. Paleoceanogr. Paleoclimatol. 35, e2019PA003818. https://doi.org/10.1029/2019PA003818.
Kleman, J., Jansson, K., De Angelis, H., Stroeven, A.P., Hättestrand, C., Alm, G., Glasser, N., 2010. North American Ice Sheet build-up during the last glacial cycle, 115–21kyr. Quat. Sci. Rev. 29, 2036–2051. https://doi.org/10.1016/j.quascirev.2010.04.021.
Klockmann, M., Mikolajewicz, U., Kleppin, H., Marotzke, J., 2020. Coupling of the subpolar gyre and the overturning circulation during abrupt glacial climate transitions. Geophys. Res. Lett. 47, e2020GL090361. https://doi.org/10.1029/2020GL090361.
Kolling, H.M., Stein, R., Fahl, K., Sadatzki, H., de Vernal, A., Xiao, X., 2020. Biomarker distributions in (Sub)-Arctic surface sediments and their potential for Sea Ice reconstructions. G-cubed 21, e2019GC008629. https://doi.org/10.1029/2019GC008629.
Kopp, R.E., Simons, F.J., Mitrovica, J.X., Maloof, A.C., Oppenheimer, M., 2009. Probabilistic assessment of sea level during the last interglacial stage. Nature 462, 863–867. https://doi.org/10.1038/nature08686.
Kozdon, R., Eisenhauer, A., Weinelt, M., Meland, M.Y., Nürnberg, D., 2009. Reassessing Mg/Ca temperature calibrations of Neogloboquadrina pachyderma (sinistral) using paired δ44/40Ca and Mg/Ca measurements. G-cubed 10, Q03005. https://doi.org/10.1029/2008GC002169.
Kremer, A., Stein, R., Fahl, K., Bauch, H., Mackensen, A., Niessen, F., 2018a. A 190-ka biomarker record revealing interactions between sea ice, Atlantic Water inflow and ice sheet activity in eastern Fram Strait. Arktos 4, 22. https://doi.org/10.1007/s41063-018-0052-0.
Kremer, A., Stein, R., Fahl, K., Ji, Z., Yang, Z., Wiers, S., Matthiessen, J., Forwick, M., Löwemark, L., O'Regan, M., Chen, J., Snowball, I., 2018b. Changes in sea ice cover and ice sheet extent at the Yermak Plateau during the last 160 ka – reconstructions from biomarker records. Quat. Sci. Rev. 182, 93–108. https://doi.org/10.1016/j.quascirev.2017.12.016.
Lajeunesse, P., St-Onge, G., 2008. The subglacial origin of the Lake Agassiz–Ojibway final outburst flood. Nat. Geosci. 1, 184–188. https://doi.org/10.1038/ngeo130.
Lambeck, K., Chappell, J., 2001. Sea level change through the last glacial cycle. Science 292, 679–686. https://doi.org/10.1126/science.1059549.
Leduc, G., Schneider, R., Kim, J.-H., Lohmann, G., 2010. Holocene and Eemian sea surface temperature trends as revealed by alkenone and Mg/Ca paleothermometry. Quat. Sci. Rev. 29, 989–1004. https://doi.org/10.1016/j.quascirev.2010.01.004.
Levermann, A., Born, A., 2007. Bistability of the Atlantic subpolar gyre in a coarse-resolution climate model. Geophys. Res. Lett. 34. https://doi.org/10.1029/2007GL031732.
Li, C., Born, A., 2019. Coupled atmosphere-ice-ocean dynamics in Dansgaard-Oeschger events. Quat. Sci. Rev. 203, 1–20. https://doi.org/10.1016/j.quascirev.2018.10.031.
Limoges, A., Ribeiro, S., Weckström, K., Heikkilä, M., Zamelczyk, K., Andersen, T.J., Seidenkrantz, M.S., 2018. Linking the modern distribution of biogenic proxies in high Arctic Greenland shelf sediments to sea ice, primary production, and Arctic-Atlantic inflow. J. Geophys. Res.: Biogeosciences 123, 760–786. https://doi.org/10.1002/2017JG003840.
Locarnini, R.A., Mishonov, A.V., Baranova, O.K., Boyer, T.P., Zweng, M.M., Garcia, H.E., Reagan, J.R., Seidov, D., Weathers, K., Paver, C.R., Smolyar, I., 2019. In: Mishonov Technical, A. (Ed.), World Ocean Atlas 2018, Volume 1: Temperature, NOAA Atlas NESDIS, vol. 81, p. 52pp.
Lofverstrom, M., Thompson, D.M., Otto-Bliesner, B.L., Brady, E.C., 2022. The importance of Canadian Arctic Archipelago gateways for glacial expansion in Scandinavia. Nat. Geosci. 15, 482–488. https://doi.org/10.1038/s41561-022-00956-9.
Lohmann, K., Drange, H., Bentsen, M., 2009. Response of the North Atlantic subpolar gyre to persistent North Atlantic oscillation like forcing. Clim. Dynam. 32, 273–285. https://doi.org/10.1007/s00382-008-0467-6.
Lozier, M.S., 2012. Overturning in the North atlantic. Ann. Rev. Mar. Sci 4, 291–315. https://doi.org/10.1146/annurev-marine-120710-100740.
Lozier, M.S., Li, F., Bacon, S., Bahr, F., Bower, A.S., Cunningham, S.A., de Jong, M.F., de Steur, L., deYoung, B., Fischer, J., Gary, S.F., Greenan, B.J.W., Holliday, N.P., Houk, A., Houpert, L., Inall, M.E., Johns, W.E., Johnson, H.L., Johnson, C., Karstensen, J., Koman, G., Le Bras, I.A., Lin, X., Mackay, N., Marshall, D.P., Mercier, H., Oltmanns, M., Pickart, R.S., Ramsey, A.L., Rayner, D., Straneo, F., Thierry, V., Torres, D.J., Williams, R.G., Wilson, C., Yang, J., Yashayaev, I., Zhao, J., 2019. A sea change in our view of overturning in the subpolar North Atlantic. Science 363, 516–521. https://doi.org/10.1126/science.aau6592.
Lüthi, D., Le Floch, M., Bereiter, B., Blunier, T., Barnola, J.-M., Siegenthaler, U., Raynaud, D., Jouzel, J., Fischer, H., Kawamura, K., Stocker, T.F., 2008. High-resolution carbon dioxide concentration record 650,000–800,000 years before present. Nature 453, 379–382. https://doi.org/10.1038/nature06949.
Marret, F., Zonneveld, K.A.F., 2003. Atlas of modern organic-walled dinoflagellate cyst distribution. Rev. Palaeobot. Palynol. 125, 1–200. https://doi.org/10.1016/S0034-6667(02)00229-4.
Marret, F., Eiríksson, J., Knudsen, K.L., Turon, J.-L., Scourse, J.D., 2004. Distribution of dinoflagellate cyst assemblages in surface sediments from the northern and western shelf of Iceland. Rev. Palaeobot. Palynol. 128, 35–53. https://doi.org/10.1016/S0034-6667(03)00111-8.
Matthiessen, J., Knies, J., 2001. Dinoflagellate cyst evidence for warm interglacial conditions at the northern Barents Sea margin during marine oxygen isotope stage 5. J. Quat. Sci. 16, 727–737. https://doi.org/10.1002/jqs.656.
Matthiessen, J., Knies, J., Nowaczyk, N.R., Stein, R., 2001. Late Quaternary dinoflagellate cyst stratigraphy at the Eurasian continental margin, Arctic Ocean: indications for Atlantic water inflow in the past 150,000 years. Global Planet. Change 31, 65–86. https://doi.org/10.1016/S0921-8181(01)00113-8.
Max, L., Nürnberg, D., Chiessi, C.M., Lenz, M.M., Mulitza, S., 2022. Subsurface ocean warming preceded Heinrich Events. Nat. Commun. 13, 4217. https://doi.org/10.1038/s41467-022-31754-x.
Mengel, M., Levermann, A., Schleussner, C.-F., Born, A., 2012. Enhanced Atlantic subpolar gyre variability through baroclinic threshold in a coarse resolution model. Earth System Dynamics 3, 189–197. https://doi.org/10.5194/esd-3-189-2012.
Mokeddem, Z., McManus, J.F., 2016. Persistent climatic and oceanographic oscillations in the subpolar North Atlantic during the MIS 6 glaciation and MIS 5 interglacial. Paleoceanography 31, 758–778. https://doi.org/10.1002/2015PA002813.
Mokeddem, Z., McManus, J.F., Oppo, D.W., 2014. Oceanographic dynamics and the end of the last interglacial in the subpolar North Atlantic. Proc. Natl. Acad. Sci. USA 111, 11263–11268. https://doi.org/10.1073/pnas.1322103111.
Montoya, M., Born, A., Levermann, A., 2011. Reversed North Atlantic gyre dynamics in present and glacial climates. Clim. Dynam. 36, 1107–1118. https://doi.org/10.1007/s00382-009-0729-y.
Müller, J., Massé, G., Stein, R., Belt, S.T., 2009. Variability of sea-ice conditions in the Fram Strait over the past 30,000 years. Nat. Geosci. 2, 772–776. https://doi.org/10.1038/ngeo665.
Müller, J., Wagner, A., Fahl, K., Stein, R., Prange, M., Lohmann, G., 2011. Towards quantitative sea ice reconstructions in the northern North Atlantic: a combined biomarker and numerical modelling approach. Earth Planet Sci. Lett. 306, 137–148. https://doi.org/10.1016/j.epsl.2011.04.011.
Münchow, A., Falkner, K.K., Melling, H., 2015. Baffin island and west Greenland current systems in northern baffin bay. Prog. Oceanogr. 132, 305–317. https://doi.org/10.1016/j.pocean.2014.04.001.
Nicholl, J.A.L., Hodell, D.A., Naafs, B.D.A., Hillaire-Marcel, C., Channell, J.E.T., Romero, O.E., 2012. A Laurentide outburst flooding event during the last interglacial period. Nat. Geosci. 5, 901–904. https://doi.org/10.1038/ngeo1622.
Oppo, D.W., McManus, J.F., Cullen, J.L., 2006. Evolution and demise of the last interglacial warmth in the subpolar North Atlantic. Quat. Sci. Rev. 25, 3268–3277. https://doi.org/10.1016/j.quascirev.2006.07.006.
Otto-Bliesner, B.L., Marshall, S.J., Overpeck, J.T., Miller, G.H., Hu, A., Members of CAPE Last Interglacial Project, 2006. Simulating arctic climate warmth and icefield retreat in the last interglaciation. Science 311, 1751–1753.
Pados, T., Spielhagen, R.F., 2014. Species distribution and depth habitat of recent planktic foraminifera in Fram Strait, Arctic Ocean. Polar Res. 33, 22483. https://doi.org/10.3402/polar.v33.22483.
Paillard, D., Labeyrie, L., Yiou, P., 1996. Macintosh Program performs time-series

analysis. Eos, Transactions American Geophysical Union 77, 379. https://doi.org/10.1029/96EO00259, 379.
Penaud, A., Eynaud, F., Turon, J.L., Zaragosi, S., Marret, F., Bourillet, J.F., 2008. Interglacial variability (MIS 5 and MIS 7) and dinoflagellate cyst assemblages in the bay of biscay (North Atlantic). Mar. Micropaleontol. 68, 136–155. https://doi.org/10.1016/j.marmicro.2008.01.007.
Prinsenberg, S.J., Hamilton, J., 2005. Monitoring the volume, freshwater and heat fluxes passing through Lancaster sound in the Canadian arctic archipelago. Atmos.-Ocean 43, 1–22. https://doi.org/10.3137/ao.430101.
Pryce, R.J., 1971. The occurrence of bound, water-soluble squalene, 4,4-dimethyl sterols, 4α-methyl sterols and sterols in leaves of Kalanchoe blossfeldiana. Phytochemistry 10, 1303–1307. https://doi.org/10.1016/S0031-9422(00)84332-0.
Radi, T., Vernal, A. de, Peyron, O., 2001. Relationships between dinoflagellate cyst assemblages in surface sediment and hydrographic conditions in the Bering and Chukchi seas. J. Quat. Sci. 16, 667–680. https://doi.org/10.1002/jqs.652.
Risebrobakken, B., Balbon, E., Dokken, T., Jansen, E., Kissel, C., Labeyrie, L., Richter, T., Senneset, L., 2006. The penultimate deglaciation: high-resolution paleoceanographic evidence from a north–south transect along the eastern Nordic Seas. Earth Planet Sci. Lett. 241, 505–516. https://doi.org/10.1016/j.epsl.2005.11.032.
Risebrobakken, B., Dokken, T., Otterå, O.H., Jansen, E., Gao, Y., Drange, H., 2007. Inception of the Northern European ice sheet due to contrasting ocean and insolation forcing. Quat. Res. 67, 128–135. https://doi.org/10.1016/j.yqres.2006.07.007.
Risebrobakken, B., Dokken, T., Smedsrud, L.H., Andersson, C., Jansen, E., Moros, M., Ivanova, E.V., 2011. Early Holocene temperature variability in the Nordic Seas: the role of oceanic heat advection versus changes in orbital forcing. Paleoceanography 26. https://doi.org/10.1029/2011PA002117.
Robinson, N., Eglinton, G., Brassell, S.C., Cranwell, P.A., 1984. Dinoflagellate origin for sedimentary 4α-methylsteroids and 5α(H)-stanols. Nature 308, 439–442. https://doi.org/10.1038/308439a0.
Rochon, A., de Vernal, A., Turon, J.-L., Matthiessen, J., Head, M.J., 1999. Distribution of recent dinoflagellate cysts in surface sediments from the North Atlantic Ocean and adjacent seas in relation to sea-surface parameters. Am. Assoc. Stratigr. Palynol. Contrib. Ser. 35, 1–146.
Rohling, E.J., Hibbert, F.D., Grant, K.M., Galaasen, E.V., Irvalı, N., Kleiven, H.F., Marino, G., Ninnemann, U., Roberts, A.P., Rosenthal, Y., Schulz, H., Williams, F.H., Yu, J., 2019. Asynchronous Antarctic and Greenland ice-volume contributions to the last interglacial sea-level highstand. Nat. Commun. 10, 5040. https://doi.org/10.1038/s41467-019-12874-3.
Rontani, J.-F., Charrière, B., Sempéré, R., Doxaran, D., Vaultier, F., Vonk, J.E., Volkman, J.K., 2014. Degradation of sterols and terrigenous organic matter in waters of the Mackenzie Shelf, Canadian Arctic. Org. Geochem. 75, 61–73. https://doi.org/10.1016/j.orggeochem.2014.06.002.
Rudels, B., Korhonen, M., Schauer, U., Pisarev, S., Rabe, B., Wisotzki, A., 2015. Circulation and transformation of atlantic water in the eurasian basin and the contribution of the Fram Strait inflow branch to the Arctic Ocean heat budget. Prog. Oceanogr. 132, 128–152. https://doi.org/10.1016/j.pocean.2014.04.003.
Sánchez Goñi, M.F., Eynaud, F., Turon, J.L., Shackleton, N.J., 1999. High resolution palynological record off the Iberian margin: direct land-sea correlation for the Last Interglacial complex. Earth Planet Sci. Lett. 171, 123–137. https://doi.org/10.1016/S0012-821X(99)00141-7.
Sánchez Goñi, M.F., Loutre, M.F., Crucifix, M., Peyron, O., Santos, L., Duprat, J., Malaizé, B., Turon, J.-L., Peypouquet, J.-P., 2005. Increasing vegetation and climate gradient in Western Europe over the Last Glacial Inception (122–110 ka): data-model comparison. Earth Planet Sci. Lett. 231, 111–130. https://doi.org/10.1016/j.epsl.2004.12.010.
Sarnthein, M., Tiedemann, R., 1990. Younger dryas-style cooling events at glacial terminations I-vi at ODP site 658: associated benthic δ13C anomalies constrain meltwater hypothesis. Paleoceanography 5, 1041–1055. https://doi.org/10.1029/PA005i006p01041.
Scoto, F., Sadatzki, H., Maffezzoli, N., Barbante, C., Gagliardi, A., Varin, C., Vallelonga, P., Gkinis, V., Dahl-Jensen, D., Kjaer, H.A., Burgay, F., Saiz-Lopez, A., Stein, R., Spolaor, A., 2022. Sea ice fluctuations in the Baffin Bay and the Labrador Sea during glacial abrupt climate changes. Proc. Natl. Acad. Sci. USA 119, e2203468119. https://doi.org/10.1073/pnas.2203468119.
Seidenkrantz, M.-S., Kristensen, P., Knudsen, K.L., 1995. Marine evidence for climatic instability during the last interglacial in shelf records from northwest Europe. J. Quat. Sci. 10, 77–82. https://doi.org/10.1002/jqs.3390100108.
Seidenkrantz, M.-S., Bornmalm, L., Johnsen, S.J., Knudsen, K.L., Kuijpers, A., Lauritzen, S.-E., Leroy, S.A.G., Mergeal, I., Schweger, C., Van Vliet-Lanoë, B., 1996. Two-step deglaciation at the oxygen isotope stage 6/5E transition: the Zeifen-Kattegat climate oscillation. Quat. Sci. Rev. 15, 63–75. https://doi.org/10.1016/0277-3791(95)00086-0.
Shackleton, N., Chapman, M., Sanchez Goñi, M., Pailler, D., Lancelot, Y., 2002. The Classic Marine Isotope Substage 5e. Quat. Res. 58, 14–16. https://doi.org/10.1006/qres.2001.2312.
Shackleton, N.J., Sánchez-Goñi, M.F., Pailler, D., Lancelot, Y., 2003. Marine Isotope Substage 5e and the Eemian Interglacial. Global Planet. Change 36, 151–155. https://doi.org/10.1016/S0921-8181(02)00181-9.
Shaw, J., Lesemann, J.-E., 2003. Subglacial outburst floods and extreme sedimentary events in the Labrador Sea. In: Chan, M.A., Archer, A.W. (Eds.), Extreme Depositional Environments: Mega End Members in Geologic Time. Geological Society of America. https://doi.org/10.1130/0-8137-2370-1.25, 0.
Simstich, J., Sarnthein, M., Erlenkeuser, H., 2003. Paired δ18O signals of Neogloboquadrina pachyderma (s) and Turborotalita quinqueloba show thermal stratification structure in Nordic Seas. Mar. Micropaleontol. 48, 107–125. https://doi.org/10.1016/S0377-8398(02)00165-2.
Smedsrud, L.H., Muilwijk, M., Brakstad, A., Madonna, E., Lauvset, S.K., Spensberger, C., Born, A., Eldevik, T., Drange, H., Jeansson, E., Li, C., Olsen, A., Skagseth, Ø., Slater, D.A., Straneo, F., Våge, K., Årthun, M., 2022. Nordic seas heat loss, atlantic inflow, and arctic Sea Ice cover over the last century. Rev. Geophys. 60, e2020RG000725. https://doi.org/10.1029/2020RG000725.
Solignac, S., Grøsfjeld, K., Giraudeau, J., de Vernal, A., 2009. Distribution of recent dinocyst assemblages in the western Barents Sea. Norw. J. Geol. 11.
Spratt, R., Lisiecki, L., 2016. A Late Pleistocene sea level stack. Clim. Past 12, 1079–1092. https://doi.org/10.5194/cpd-11-3699-2015.
St-Onge, G., Lajeunesse, P., 2007. Flood-Induced turbidites from northern Hudson bay and western Hudson Strait: a two-pulse record of lake Agassiz final outburst flood?. In: Lykousis, V., Sakellariou, D., Locat, J. (Eds.), Submarine Mass Movements and Their Consequences. Advances in Natural and Technological Hazards Research, vol. 27. Springer, Dordrecht. https://doi.org/10.1007/978-1-4020-6512-5_14.
Stein, R., Fahl, K., Gierz, P., Niessen, F., Lohmann, G., 2017. Arctic Ocean sea ice cover during the penultimate glacial and the last interglacial. Nat. Commun. 8, 1–13. https://doi.org/10.1038/s41467-017-00552-1.
Stein, R., Kremer, A., Fahl, K., 2022. Past glacial-interglacial changes in Arctic Ocean sea-ice conditions. Past Global Changes Magazine 30, 90–91. https://doi.org/10.22498/pages.30.2.90.
Stirling, C.H., Esat, T.M., Lambeck, K., McCulloch, M.T., 1998. Timing and duration of the Last Interglacial: evidence for a restricted interval of widespread coral reef growth. Earth Planet Sci. Lett. 160, 745–762. https://doi.org/10.1016/S0012-821X(98)00125-3.
Stockmarr, J., 1971. Tablets with spores used in absolute pollen analysis. Pollen Spores 13, 615–621.
Stokes, C.R., Tarasov, L., Dyke, A.S., 2012. Dynamics of the North American ice sheet complex during its inception and build-up to the last glacial maximum. Quat. Sci. Rev. 50, 86–104. https://doi.org/10.1016/j.quascirev.2012.07.009.
Svendsen, J.I., Alexanderson, H., Astakhov, V.I., Demidov, I., Dowdeswell, J.A., Funder, S., Gataullin, V., Henriksen, M., Hjort, C., Houmark-Nielsen, M., Hubberten, H.W., Ingólfsson, Ó., Jakobsson, M., Kjær, K.H., Larsen, E., Lokrantz, H., Lunkka, J.P., Lyså, A., Mangerud, J., Matiouchkov, A., Murray, A., Möller, P., Niessen, F., Nikolskaya, O., Polyak, L., Saarnisto, M., Siegert, C., Siegert, M.J., Spielhagen, R.F., Stein, R., 2004. Late Quaternary ice sheet history of northern Eurasia. Quat. Sci. Rev. 23, 1229–1271. https://doi.org/10.1016/j.quascirev.2003.12.008.
Thornalley, D.J.R., Elderfield, H., McCave, I.N., 2009. Holocene oscillations in temperature and salinity of the surface subpolar North Atlantic. Nature 457, 711–714. https://doi.org/10.1038/nature07717.
Tzedakis, P.C., Drysdale, R.N., Margari, V., Skinner, L.C., Menviel, L., Rhodes, R.H., Taschetto, A.S., Hodell, D.A., Crowhurst, S.J., Hellstrom, J.C., Fallick, A.E., Grimalt, J.O., McManus, J.F., Martrat, B., Mokeddem, Z., Parrenin, F., Regattieri, E., Roe, K., Zanchetta, G., 2018. Enhanced climate instability in the North atlantic and southern europe during the last interglacial. Nat. Commun. 9, 4235. https://doi.org/10.1038/s41467-018-06683-3.
Van Nieuwenhove, N., Bauch, H.A., Matthiessen, J., 2008. Last interglacial surface water conditions in the eastern Nordic Seas inferred from dinocyst and foraminiferal assemblages. Mar. Micropaleontol. 66, 247–263. https://doi.org/10.1016/j.marmicro.2007.10.004.
Van Nieuwenhove, N., Bauch, H.A., Eynaud, F., Kandiano, E., Cortijo, E., Turon, J.-L., 2011. Evidence for delayed poleward expansion of North Atlantic surface waters during the last interglacial (MIS 5e). Quat. Sci. Rev. 30, 934–946. https://doi.org/10.1016/j.quascirev.2011.01.013.
Van Nieuwenhove, N., Baumann, A., Matthiessen, J., Bonnet, S., de Vernal, A., 2016. Sea surface conditions in the southern Nordic Seas during the Holocene based on dinoflagellate cyst assemblages. Holocene 26, 722–735. https://doi.org/10.1177/0959683615618258.
Van Nieuwenhove, N., Pearce, C., Knudsen, M.F., Røy, H., Seidenkrantz, M.-S., 2018. Meltwater and seasonality influence on subpolar gyre circulation during the Holocene. Palaeogeogeography, Palaeoclimatology, Palaeoecology. 502, 104–118. https://doi.org/10.1016/j.palaeo.2018.05.002.
Vettoretti, G., Peltier, W., 2003. Post-eemian glacial inception. Part I: the impact of summer seasonal temperature bias. J. Clim. 16, 889–911. https://doi.org/10.1175/1520-0442(2003)016<0889:PEGIPI>2.0.CO;2.
Volkman, J.K., 1986. A review of sterol markers for marine and terrigenous organic matter. Org. Geochem. 9, 83–99. https://doi.org/10.1016/0146-6380(86)90089-6.
Volkman, J.K., Barrett, S.M., Blackburn, S.I., Mansour, M.P., Sikes, E.L., Gelin, F., 1998. Microalgal biomarkers: a review of recent research developments. Org. Geochem. 29, 1163–1179. https://doi.org/10.1016/S0146-6380(98)00062-X.
Waelbroeck, C., Labeyrie, L., Michel, E., Duplessy, J.C., McManus, J.F., Lambeck, K., Balbon, E., Labracherie, M., 2002. Sea-level and deep water temperature changes derived from benthic foraminifera isotopic records. Quat. Sci. Rev. 21, 295–305. https://doi.org/10.1016/S0277-3791(01)00101-9.
Wall, D., Dale, B., 1966. "Living fossils" in western atlantic plankton. Nature 211, 1025–1026. https://doi.org/10.1038/2111025a0.
Wold, C.N., 1994. Cenozoic sediment accumulation on drifts in the northern North Atlantic. Paleoceanography 9, 917–941. https://doi.org/10.1029/94PA01438.
Xiao, X., Fahl, K., Müller, J., Stein, R., 2015. Sea-ice distribution in the modern Arctic Ocean: biomarker records from trans-Arctic Ocean surface sediments.

Geochem. Cosmochim. Acta 155, 16–29. https://doi.org/10.1016/j.gca.2015.01.029.
Yeager, S., 2015. Topographic coupling of the atlantic overturning and gyre circulations. J. Phys. Oceanogr. 45, 1258–1284. https://doi.org/10.1175/JPO-D-14-0100.1.
You, D., Stein, R., Fahl, K., Williams, M.C., Schmidt, D.N., McCave, I.N., Barker, S., Niu, L., Kuhn, G., Niessen, F., 2023. Last deglacial abrupt climate changes caused by meltwater pulses in the Labrador Sea. Communications Earth & Environments 4. https://doi.org/10.1038/s43247-023-00743-3.
Zhuravleva, A., Bauch, H.A., Van Nieuwenhove, N., 2017. Last Interglacial (MIS5e) hydrographic shifts linked to meltwater discharges from the East Greenland margin. Quat. Sci. Rev. 164, 95–109. https://doi.org/10.1016/j.quascirev.2017.03.026.

Supplementary information to “Sea ice variability in the North Atlantic subpolar gyre throughout the Last Interglacial”

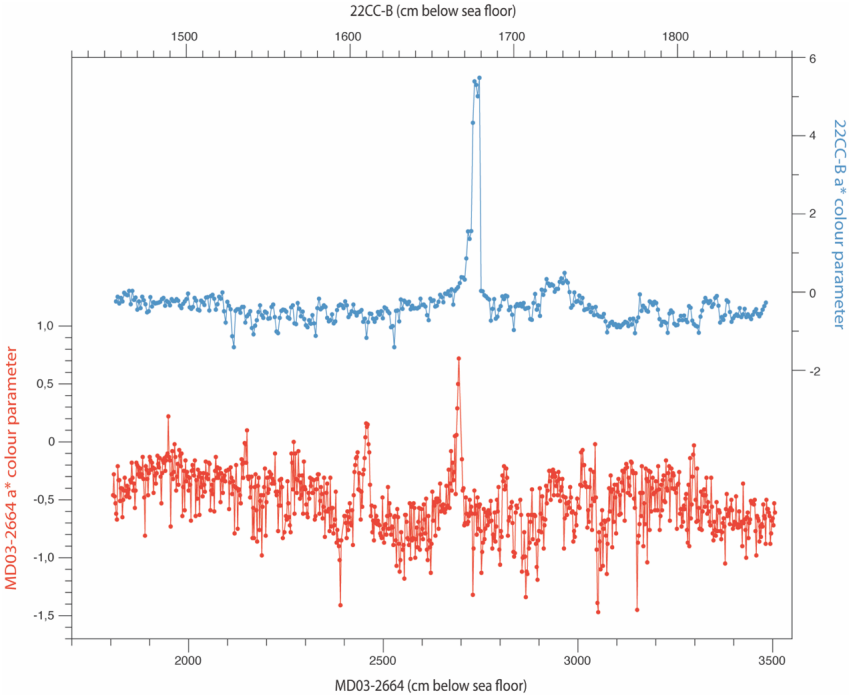

Supplementary Figure 1: a* colour parameter from cores 22CC-B (this study; blue curve) and MD03-2664 (Galaasen et al., 2014; red curve) plotted on their respective depth scales (cm below sea floor). Higher a* values reflect more red colour of the sediment. The “red layer” is identified between ca. 1678.5–1673.0 cm in 22CC-B.

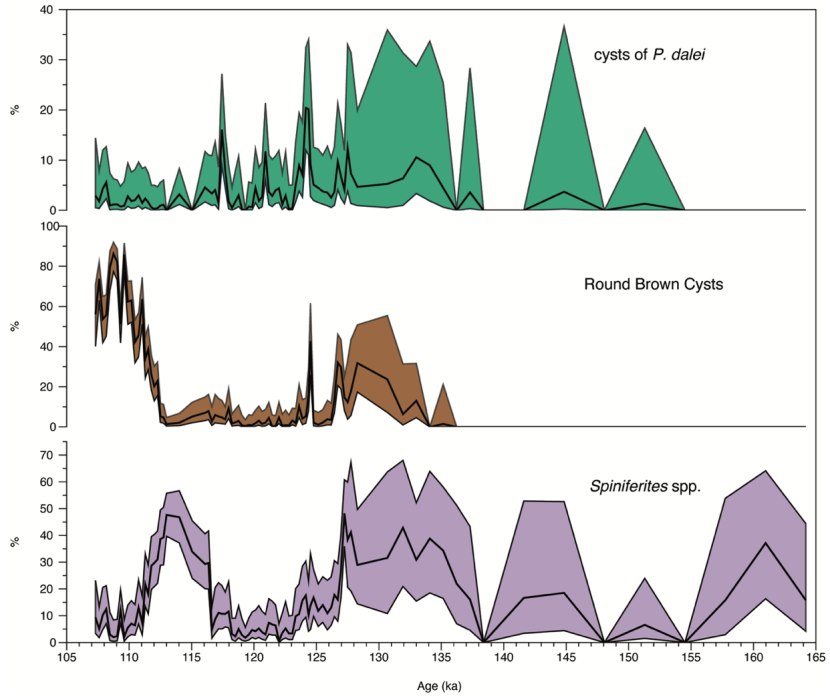

Supplementary Figure 2: Uncertainty of the relative abundance (%) calculated using the method of Heslop et al. (2011) for three dinoflagellate cyst taxa discussed in text (cysts of *P. dalei*, Round Brown Cysts and *Spiniferites* spp.). The black lines represent the relative abundance (%) and the shaded areas represent the minimum and maximum percentage values at 0.05 significance level. The uncertainty intervals are largest in the older part of the record (> ca. 127 ka) because the number of counted dinoflagellate cyst specimens was considerably lower than in the rest of the record.

References:

Heslop, D., de Schepper, S., Proske, U., 2011. Diagnosing the uncertainty of taxa relative abundances derived from count data. Marine Micropaleontology. 79, 114–120. Doi: 10.1016/j.marmicro.2011.01.007.

Galaasen, E.V., Ninnemann, U.S., Irvali, N., Kleiven, H.F., Rosenthal, Y., Kissel, C., Hodell, D.A., 2014. Rapid Reductions in North Atlantic Deep Water During the Peak of the Last Interglacial Period. Science. 343, 1129–1132. doi:10.1126/science.1248667

Chapter 6

Synthesis and Outlook

This thesis presents new insights into past sea ice conditions and the significance of sea ice in the context of ocean and climate variability. I generated centennial-scale sea ice biomarker and dinoflagellate cyst assemblage records from the subpolar Labrador Sea and the Fram Strait, covering the time interval between 140 and 90 thousand years ago. During this time interval, Earth's climate underwent profound glacial-interglacial changes from the late MIS 6 glacial throughout T II, the warmer-than-present LIG (MIS 5e; 128–116 ka), the last glacial inception into MIS 5d. The three integrated papers of this PhD thesis contribute new insights into the paleoceanographic history of the Arctic to Subarctic regions, providing comprehensive and empirical evidence on 1) the nature, timing and extent of (sub)Arctic sea ice throughout MIS 5e its glacial transitions, 2) the broader interactions between sea ice, ocean currents and ice sheet evolution, and 3) insights into the application of foraminiferal oxygen isotopes to indicate sea ice coupled with vertical stratification, and deep convection in the subpolar Labrador Sea.

6.1 Synthesis of papers

In Paper I, we documented the sea ice variability in the subpolar Labrador Sea (Objective I), and found that extensive/perennial sea ice cover existed starting with the late MIS 6 (145–135). The sea ice cover started to break up occasionally during T II (135–128 ka) and the marginal ice zone gradually retreated northward. In the earliest MIS 5e (128–126.5 ka), the marginal ice zone was likely located directly over the core location on the Eirik Drift. Subsequently, sea ice-free conditions occurred in the latter MIS 5e (126.5–116 ka), and it re-advanced again to the Eirik Drift during MIS 5d ($<$ 114 ka). With this, our data are the first to directly demonstrate the presence of sea ice in the

subpolar Labrador Sea during T II, the earliest MIS 5e and MIS 5d, and indirectly in late MIS 6. This contribution significantly advances our understanding of the LIG sea ice extent, addressing previously unresolved questions regarding the timing of sea ice retreat following the glacial MIS 6, its existence within the LIG, and its re-advance following the LIG in the context of insolation, Greenland Ice sheet extent, and the surface currents of the SPG (Objective II).

Our first hypothesis was that sea ice may have modulated the SPG circulation during the LIG and its glacial transitions. Indeed, our findings from the Labrador Sea revealed a strong connection between sea ice and SPG variability, especially in the earliest MIS 5e and MIS 5d, i.e., at the end of the glacial termination, and at the start of glacial inception. Thus, we conclude that sea ice played a role in modulating the SPG during these periods. Firstly, during the earliest MIS 5e, the marginal sea ice zone was likely positioned in the subpolar Labrador Sea. Given its proximity to the convection region in the Labrador Sea, the marginal ice zone, and its associated cooling feedbacks, may have sustained or enhanced convection in the subpolar Labrador Sea during a time when melting of deglacial ice remnants may otherwise have weakened the convection. Thus, the marginal ice zone may have played a role in maintaining or enhancing the SPG. Secondly, the return of sea ice during MIS 5d may have played a role in amplifying the cooling of the last glacial inception by diminishing the strength or lateral extension of the SPG. Thus, the presence of sea ice, both into and out of MIS 5e, may have played roles in amplifying climate signals of warming/cooling by influencing the flow of the SPG.

We also found that sea ice was not a prerequisite for SPG variability. Particularly in the early MIS 5e (126.5–124 ka), our study shows the sea ice had mostly retreated. But despite the retreat, the ocean experienced profound cooling. This likely corresponded with a reduction in SPG strength and/or lateral orientation. Based on previous studies by *Condron and Winsor* (2012) and *Lofverstrom et al.* (2022), we discussed whether Laurentide Ice Sheet remnants in the Canadian Arctic Archipelago (CAA) may have influenced the buoyancy forcing of the SPG. Specifically, the residual Laurentide Ice Sheet may have been sufficiently expanded to restrict export pathways for freshwater west of Greenland resulting in a focusing, and intensification of the EGC route for freshwater transport to the SPG. We also hypothesized a similar scenario for MIS 5d. Although our data remain inconclusive of such a scenario, if it were to be corroborated by future findings, it underlines the possibly important role of cryospheric reconfigurations, and their influence on freshwater export and rerouting to the North Atlantic, for understanding the climate and hydrography in the North Atlantic.

In Paper II, we documented the sea ice conditions in the eastern Fram Strait from the late glacial MIS 6, throughout the LIG (Objective I). Our data revealed a similar sea

ice trend as the subpolar Labrador Sea. Our study found that the sea ice cover evolved from a late MIS 6 extensive sea ice to a prominent marginal ice zone that persisted for nearly the entire 7000-year duration of T II, before completely retreating at the end of the deglaciation. We tested the second hypothesis that sea ice, Atlantic waters, and the surrounding ice sheets were important for shaping the ocean-climate variability in the eastern Fram Strait. Throughout MIS 6, the extensive sea ice cover likely experienced occasional melting and reductions. These reductions may have been due to the opening of local polynyas triggered by katabatic winds associated with the large extent of the Svalbard Barents Sea Ice Sheet (SBIS) and the inflow of sub-surfaced Atlantic water that may have occasionally outcropped at the surface ocean, similar to previous findings by *Matthiessen and Knies* (2001) and *Stein et al.* (2017).

During T II, we observed a unique sedimentary environment that may have increased the efficiency of the ocean biological pump. Processes associated with the marginal sea ice zone presence, and high sedimentary input from the disintegrating SBIS, likely led to increased primary productivity and efficient vertical transport of phytoplankton organic matter and storage in the sediments. The phytoplankton organic matter remineralizes and sequesters CO_2 into the deep ocean together with the sinking of CO_2-enriched brines, and thereby the environment during T II may have influenced the ocean biologic pump. Such an environment may suggest a potential importance of glacial termination phases and the interactions of sea ice and ice sheets for enhanced CO_2 capture in the oceans. Following T II, the eastern Fram Strait became sea ice-free, and a two-step warming of the surface ocean occurred throughout the LIG with a late interglacial optimum around ca. 120,000 years ago. During MIS 5d, summer insolation decreased (*Laskar et al.*, 2004) and the surrounding ice sheets expanded again (*Svendsen et al.*, 2004). Despite the apparent cooler conditions, we did not detect a reappearance of sea ice in the eastern Fram Strait. However, it remains unclear whether this is a true climate signal, or rather caused by poor biomarker preservation (see paper II and chapter 6.2.2).

When we compared our reconstruction alongside other published LIG records in the Fram Strait (*Stein et al.*, 2017; *Kremer et al.*, 2018a,b), it became clear that large spatial variability of the sea ice cover over relatively short distances occurred. The variability underscores the high sensitivity of sea ice in the Fram Strait to Atlantic water influence and ice sheet dynamics. While our findings contribute new knowledge to the complex sea ice interactions in the Fram Strait region, they also highlight that more records for this area are needed to precisely capture the magnitude of, and the causes for, the large variability. Especially during the glacial transitions where generally low resolution and uncertain chronologies make any precise comparisons of sea ice cover challenging.

In Paper III, we returned to the subpolar Labrador Sea, expanding the analysis from Pa-

per I, and reevaluated previous interpretations of ocean stratification, deep convection, and deep ocean currents in connection to the different sea ice conditions. The objective was to evaluate the potential of oxygen isotopes from paired planktic and benthic foraminifers to indicate sea ice cover (objective III). Our study suggests that combined isotopic measurements of benthic and planktic foraminifers, ($\triangle\delta^{18}$O), i.e., isotopic offset, may offer valuable insights into the presence of sea ice at the surface ocean in the subpolar Labrador Sea. This is evident throughout the cold periods of MIS 6, T II, and MIS 5d. During these periods, similar planktic and benthic isotopic values (i.e. isotopic offsets around zero) occurred, suggesting that similar temperatures persisted throughout the water column when there was sea ice. Based on these observations we hypothesized that conditions cold enough to support sea ice may lead to subsurface waters with temperatures dropping to levels close to those in the deep ocean, comparable to observations made from the modern Southern Ocean (*Lund et al.*, 2021).

However, we also demonstrate that unequivocal interpretations of isotopic offsets between planktic and benthic species are challenging, particularly evident during T II and the earliest MIS 5e. During T II anomalous decreases in benthic δ^{18}O indicate fluctuations in the deep ocean environment, which is a well-known feature in the high northern latitude oceans (e.g. *Rasmussen et al.*, 2003; *Risebrobakken et al.*, 2006). Brine formation, temperature anomalies, δ^{18}O-depleted meltwater bursts and/or deepening of the surface water layer have been suggested as possible mechanisms for the anomalies but ultimately the reason behind their depletions remains unresolved. Importantly, these anomalies are widespread, and they demonstrate that competing influences on the isotope signal can, and have, overridden the signal related to sea ice and vertical stratification associated with interpreting isotopes. Thus, the anomalies complicate a univocal interpretation of the isotopes in the context of sea ice or other hydrographic conditions. Additionally, during the earliest MIS 5e the "isotopic offset" does correspond to the sea ice documented at the surface ocean. Nevertheless, the offset here cannot be explained by the sea ice associated subsurface cooling like during the cold periods. During this time, proxy evidence suggests a warming of the subsurface ocean (*Irvali et al.*, 2012, 2016), which is clearly inconsistent with the hypothesis of subsurface cooling. Therefore the "isotopic offset" should always be used in association with other proxies, as alone, they may lead to wrong conclusions. A need for further multiproxy studies remains, involving a comparison of established sea ice proxies with planktic and benthic δ^{18}O to thoroughly assess the relationships between foraminiferal planktic and benthic isotopes, sea ice, and ocean hydrographic conditions in the wider subpolar North Atlantic.

6.2 Challenges and outlook

This thesis has provided new insights into the sea ice and paleoceanographic history of the (sub)Arctic Oceans. However, the reconstructions presented here are pieces of a bigger puzzle. Throughout the LIG and its glacial transitions, sea ice reconstructions are scarce but urgently needed. Additional records, with high resolution and robust chronologies, are essential to document, and elucidate the complex interactions of sea ice with ocean currents and ice sheets. Our investigations have identified both challenges and opportunities for future research, particularly in understanding the interplay between sea ice and the SPG, comprehending the complex sea ice conditions in the Fram Strait, understanding the potential of new proxies for sea ice reconstructions, and establishing robust chronologies. Addressing these aspects is essential for a more comprehensive understanding of climate variability throughout the LIG and, ultimately, for comprehending the implications of a future Arctic characterized by reduced sea ice cover.

6.2.1 Sea ice and the subpolar gyre

This thesis documents a strong connection between sea ice presence and the dynamics of the SPG. However, a limitation of our reconstruction is its predominant focus on the surface ocean, despite the complex nature of the SPG circulation and its intricate link with the AMOC. The generally limited availability of deep ocean data on high enough resolution to capture short-term variability and abrupt climate events presents an impediment to achieving a comprehensive understanding of the interconnections between sea ice and the SPG, and their potential larger-scale influences for the global ocean circulation via the AMOC.

Assessing phasing relationships between sea ice and the deep components of the SPG and the AMOC may be a crucial investigation to further understand their connections, and to understand the influence of sea ice on short-term variability and abrupt climate events. This requires higher-resolution studies that integrate proxy observations from both the surface and deep ocean. For establishing such a phasing relationship, a sea ice reconstruction on a very high sedimentation rate site such as Core MD99-2664 on the Eirik Drift (*Irvali et al.*, 2012, 2016; *Galaasen et al.*, 2014) which has the high-temporal resolution of 35 cm/thousand years (30 years per 1-cm sample) and well-preserved biogenic remains making it an optimal core for such multiproxy studies.

A sea ice reconstruction from core MD99-2664 may provide further insights into whether sea ice in the SPG region could have contributed to the abrupt instability in NADW

that was documented in rapid depletions in benthic $\delta^{13}C$ by *Galaasen et al.* (2014) in the latter MIS 5e. These short reductions of NADW occurred when climatic conditions favored ice mass expansion rather than rapid retreat, suggesting that decaying ice sheets was likely not the trigger of the transient NADW reductions and thus, the causes for the instability remains uncertain. Our data from Paper 1 suggests that sea ice could not have been a cause for these instabilities, because in our core we did not find evidence for sea ice, although cold events were recorded. Given the lower sedimentation rate at our site 22CC-B, we cannot exclude that our record lacked the high time-resolution required to capture potential short-lived sea ice expansions or transportation events, which may have contributed to the instabilities in the deep ocean circulation. Thus, a comprehensive suite of investigations, incorporating high temporal resolution and multiproxy approaches, including proxies for water mass distributions and AMOC structure ($\delta^{13}C$, ϵNd), and intensity of AMOC circulation, as indicated by reconstructing deep water export fluxes ($^{231}Pa/^{230}Th$), and bottom flow speeds (sediment grain sizes) from high-sedimentation locations in the subpolar Labrador Sea, North Atlantic, and Arctic regions, are indispensable for a better understanding of complex interactions of the surface to deep ocean.

6.2.2 Fram Strait complexity

This thesis underscores the importance of sea ice interactions with Atlantic water and ice sheet dynamics in shaping the environmental conditions of the Fram Strait region. Comparing with previously published LIG studies, it became evident that sea ice conditions differed between locations, demonstrating large variability within relatively small areas. A word of caution is necessary when directly comparing paleo-records between different locations in the Fram Strait and Arctic Ocean. Sediment cores in this region often have uncertain chronologies making alignment between records challenging (see section 6.2.4). In addition, several records are low-resolution, which makes it challenging to determine exactly how sea ice varied between regions during transitional periods when climate underwent severe changes. In the broader context, it is crucially important to understand how Fram Strait sea ice conditions responded to different internal and external influences to understand how changes here may propagate into the Arctic, and ultimately the central Arctic Ocean. For this, additional high-resolution reconstructions are essential to assess and align age models and proxy reconstructions, particularly from MIS 6 and T II into MIS 5e, and from MIS 5e into MIS 5d.

A particular challenge to our sea ice reconstructions was the peculiarly low biomarker concentrations following MIS 5e (MIS 5d-5b). We discussed in paper II whether the low

biomarker concentrations may have been due to poor preservation conditions, or due to extremely oligotrophic open water conditions. Because our temporal resolution was not high enough and the record was potentially affected by preservation, we could not resolve a sea ice MIS 5d-record from the Fram Strait. Nevertheless this period is important to understand, as MIS 5d can shed more light on the natural climate response during the terminal phase of an interglacial (*Govin et al.*, 2015), as our current interglacial is unconcluded. This is particularly relevant for understanding the climate sensitivity of the current late Holocene time interval, on millennial time scale characterized by orbitally-driven cooling (*Kaufman et al.*, 2009). To assess the viability of the biomarkers from this period and to evaluate its subjection to preservation one may test the nearby Core MD99-2303 (*Risebrobakken et al.*, 2005, 2007), or other nearby sites which may either confirm a peculiar oligotrophic environment during this time, or whether the biomarker signal may be due to poor preservation.

6.2.3 Proxy development

This thesis has illustrated that the stable oxygen isotopes in benthic and planktic foraminifers may serve as a proxy capable of inferring sea ice presence in the subpolar North Atlantic. However, a large challenge in this investigation lies in the absence of a contemporary analog for a sea-ice-dominated subpolar Labrador Sea. The hydrographic conditions, and the configuration of the SPG during periods of global/regional cooling, that allows substantial sea ice to occur in the Labrador Sea, lacks a present-day equivalent. Nevertheless, we hypothesized that during colder glacial climates, characterized by the presence of sea ice in the subpolar North Atlantic, the hydrographic conditions might have mirrored those observed in the modern Southern Ocean (*Lund et al.*, 2021).

We importantly acknowledge that our hypothesis is tested from only two cores in the subpolar Labrador Sea. This did show that the $\Delta\delta^{18}O$ signal is regionally consistent (on the Eirik Drift) but to truly test the potential of the $\Delta\delta^{18}O$ for sea ice reconstructions in the subpolar North Atlantic, an in-depth evaluation of the $\Delta\delta^{18}O$ coupled with sea ice reconstructions from several locations across a broader range of hydrographic settings is crucially necessary. We suggest that when applied in conjunction with complementary sea ice and hydrographic proxies, the judicious use of $\Delta\delta^{18}O$ gradients could allow the vast body of available oxygen isotopic data to be brought to bear in filling key spatio-temporal gaps in our understanding of past sea ice variability.

In the context of proxy developments, the biomarkers and dinocysts analyzed in this thesis provide the crucial sea ice and paleoceanographic context to evaluate the sedimentary ancient DNA (aDNA) records generated from the same samples (Grant et al.,

in review/contribution paper IV). It will allow to directly compare the aDNA based marine biodiversity with independent sea ice, ocean and climate reconstructions from the same location. With the development of aDNA, it will be possible to better understand the effect of sea ice and climate changes on marine biodiversity and plankton community assemblages, and improve reconstructions of past sea ice conditions (e.g. *Zimmermann et al.*, 2023).

6.2.4 Chronologies

LIG age models for sediment cores in the high latitude Northern Hemisphere ocean represent an ongoing yet crucial challenge. Particularly in the Fram Strait, the absolute dating of the glacial-interglacial climate transitions is challenging, and especially the transition from T II to MIS 5e. Several marine sediment cores in the high northern latitudes have substantial uncertainties associated with their age models, and it follows that comparison of paleoceanographic or climatic signals is not straightforward and can be questioned. While large efforts have been put into a unified definition and understanding of the LIG in the Arctic and North Atlantic (e.g. *Govin et al.*, 2015), there is still a way to go. For example, in our studied core, especially an absence of foraminifers and deglacial overprints makes core-to-core correlations challenging. The LIG age models may potentially be improved by developing a more detailed tephrachronology and paleointensity framework for the region.

Widescale efforts in extensive mapping and radiometric dating of tephra horizons (*Davies et al.*, 2014) could bring crucial age control points within the LIG and help improve LIG chronology uncertainties from the high northern latitudes (e.g. *Capron et al.*, 2014). To increase the potential for finding tephra, tomography (CT) scanning of the cores (*van der Bilt et al.*, 2021) may be one good option. Also, efforts on developing paleointensity records with a good temporal resolution into reference stacks have potential as synchronization tools in LIG marine sediments (*Govin et al.*, 2015). Paleointensity is strongly related to changes in cosmogenic isotope production rates in ice cores (e.g. *Mazaud et al.*, 1994; *Stoner et al.*, 2000; *Ménabréaz et al.*, 2014), and together they may provide a viable synchronization technique between sediment and ice core records.

6.2.5 The Last Interglacial

The scientific community is still divided about the state of the sea ice cover in the Arctic Ocean during the LIG. The sea ice cover may have been perennial throughout the entire MIS 5e (*Stein et al.*, 2017), although there are also claims that it was at least seasonally

sea ice-free (*Guarino et al.*, 2020; *Vermassen et al.*, 2023). What is clear from future predictions (*Stroeve et al.*, 2007; *Stroeve et al.*, 2012; *Notz and Stroeve*, 2018) is that as the global climate warms, the Arctic will be sea ice free during summers, possibly already by 2050 (*Collins et al.*, 2013b). Studying the LIG, gives valuable information about the implications of sea ice decline in the future. Nevertheless, it is important to acknowledge that the warm climate of the LIG was paced by high insolation rather than high atmospheric CO_2 concentrations, which characterizes modern warming. While past CO_2 levels have fluctuated over millions of years, the current rate of increase is exceptional. Thus, interglacial periods will never be perfect comparisons for a future climate. However, the documentation of Arctic sea-ice variability does provide very important information on the natural variability of the ocean and climate system, crucial to fully assess the effective role of anthropogenic versus natural forcing in the near future.

The LIG represents one unique interglacial period, and gaining insights from multiple such periods is likely important to enhance our broader understanding of interglacial climates. In this context, MIS 11, ca. 374–424 ka, is considered the best analog of a human-free Holocene amongst past interglacials (e.g. *Candy et al.*, 2014), owing to its similarities in orbital geometry (*Loutre and Berger*, 2003) and preindustrial atmospheric greenhouse gas conditions (*Raynaud et al.*, 2005). Even further back, MIS 31, ca. 1081–1062 ka (*Lisiecki and Raymo*, 2005), has been of interest due to the strong orbital forcing combined with relatively high CO_2 levels (*Hönisch et al.*, 2009; *Tripati et al.*, 2011) contributing to remarkable warmth in the high-latitudes and has been described as a "super interglacial" (*Melles et al.*, 2012; *Coletti et al.*, 2015). Consequently, prioritizing the collection and exploration of long sediment records spanning millions of years, and encompassing numerous warm periods from both the Arctic and Subarctic Oceans is imperative for future research initiatives.

6.3 Concluding remarks

The Arctic Ocean is gradually turning from white to blue, likely sooner rather than later, while we have yet to understand the vast implications of such a drastic change. We investigated the Arctic to Subarctic sea ice variability throughout the Last Interglacial and its glacial transitions to understand sea ice in the larger context of ocean and climate changes. Paleoclimate reconstructions are a fundamental pillar in our understanding of past and future climate change. To contribute to refining our understanding of past climate variability as well as improve the predictive capacity of climate models for the future it will be necessary to generate high-resolution sea ice records using multidisciplinary approaches and further develop our analytical tool for sea ice reconstructions.

As such, paleoclimate data can provide invaluable information for mitigation strategies for the impacts of climate change, one of the largest challenges and responsibilities for humankind in the 21st century.

Bibliography

Aagaard, K. (1981), On the deep circulation in the Arctic Ocean, *Deep Sea Research Part A. Oceanographic Research Papers*, *28*(3), 251–268, doi:10.1016/0198-0149(81)90066-2.

Aagaard, K. (1982), Inflow from the Atlantic Ocean to the Polar Basin, in *The Arctic Ocean: The Hydrographic Environment and the Fate of Pollutants*, edited by L. Rey, pp. 69–81, Palgrave Macmillan UK, London, doi:10.1007/978-1-349-05919-5_3.

Aagaard, K., and L. K. Coachman (1968), The East Greenland Current North of Denmark Strait: Part I, *ARCTIC*, *21*(3), 181–200, doi:10.14430/arctic3262.

Adl, S. M., A. G. B. Simpson, M. A. Farmer, R. A. Andersen, O. R. Anderson, J. R. Barta, S. S. Bowser, G. Brugerolle, R. A. Fensome, S. Fredericq, T. Y. James, S. Karpov, P. Kugrens, J. Krug, C. E. Lane, L. A. Lewis, J. Lodge, D. H. Lynn, D. G. Mann, R. M. McCourt, L. Mendoza, O. Moestrup, S. E. Mozley-Standridge, T. A. Nerad, C. A. Shearer, A. V. Smirnov, F. W. Spiegel, and M. F. J. R. Taylor (2005), The new higher level classification of eukaryotes with emphasis on the taxonomy of protists, *Journal of Eukaryotic Microbiology*, *52*(5), 399–451, doi:10.1111/j.1550-7408.2005.00053.x.

Anderson, D. M., J. J. Lively, E. M. Reardon, and C. A. Price (1985), Sinking characteristics of dinoflagellate cysts1, *Limnology and Oceanography*, *30*(5), 1000–1009, doi:10.4319/lo.1985.30.5.1000.

Arrigo, K. R., T. Mock, and M. P. Lizotte (2009), Primary Producers and Sea Ice, in *Sea Ice*, pp. 283–325, John Wiley & Sons, Ltd, doi:10.1002/9781444317145.ch8.

Arrigo, K. R., D. K. Perovich, R. S. Pickart, Z. W. Brown, G. L. van Dijken, K. E. Lowry, M. M. Mills, M. A. Palmer, W. M. Balch, F. Bahr, N. R. Bates, C. Benitez-Nelson, B. Bowler, E. Brownlee, J. K. Ehn, K. E. Frey, R. Garley, S. R. Laney, L. Lubelczyk, J. Mathis, A. Matsuoka, B. G. Mitchell, G. W. K. Moore, E. Ortega-Retuerta, S. Pal, C. M. Polashenski, R. A. Reynolds, B. Schieber, H. M. Sosik, M. Stephens,

and J. H. Swift (2012), Massive Phytoplankton Blooms Under Arctic Sea Ice, *Science*, *336*(6087), 1408–1408, doi:10.1126/science.1215065.

Bauch, H. A. (1996), Monitoring Termination II at high latitude: anomalies in the planktic foraminiferal record, *Marine Geology*, *131*(1), 89–102, doi:10.1016/0025-3227(95)00147-6.

Belt, S., P. Cabedo-Sanz, L. Smik, A. Navarro-Rodriguez, S. Berben, J. Knies, and K. Husum (2015), Identification of paleo Arctic winter sea ice limits and the marginal ice zone: Optimised biomarker-based reconstructions of late Quaternary Arctic sea ice, *Earth and Planetary Science Letters*, *431*, 127–139, doi:10.1016/j.epsl.2015.09.020.

Belt, S., L. Smik, T. Brown, J.-H. Kim, S. Rowland, C. Allen, J.-K. Gal, K.-H. Shin, J. Lee, and K. Taylor (2016), Source identification and distribution reveals the potential of the geochemical Antarctic sea ice proxy IPSO25, *Nature Communications*, *7*, 12,655, doi:10.1038/ncomms12655.

Belt, S. T. (2018), Source-specific biomarkers as proxies for Arctic and Antarctic sea ice, *Organic Geochemistry*, *125*, 277–298, doi:10.1016/j.orggeochem.2018.10.002.

Belt, S. T. (2019), What do IP25 and related biomarkers really reveal about sea ice change?, *Quaternary Science Reviews*, *204*, 216–219, doi:10.1016/j.quascirev.2018.11.025.

Belt, S. T., and J. Müller (2013), The Arctic sea ice biomarker IP25: a review of current understanding, recommendations for future research and applications in palaeo sea ice reconstructions, *Quaternary Science Reviews*, *79*, 9–25, doi:doi.org/10.1016/j.quascirev.2012.12.001.

Belt, S. T., W. G. Allard, G. Massé, J.-M. Robert, and S. J. Rowland (2000), Highly branched isoprenoids (HBIs): identification of the most common and abundant sedimentary isomers, *Geochimica et Cosmochimica Acta*, *64*(22), 3839–3851, doi:10.1016/S0016-7037(00)00464-6.

Belt, S. T., G. Massé, S. J. Rowland, M. Poulin, C. Michel, and B. LeBlanc (2007), A novel chemical fossil of palaeo sea ice: IP25, *Organic Geochemistry*, *38*(1), 16–27, doi:10.1016/j.orggeochem.2006.09.013.

Belt, S. T., T. A. Brown, A. E. Ringrose, P. Cabedo-Sanz, C. J. Mundy, M. Gosselin, and M. Poulin (2013), Quantitative measurement of the sea ice diatom biomarker IP25 and sterols in Arctic sea ice and underlying sediments: Further considerations for palaeo sea ice reconstruction, *Organic Geochemistry*, *62*, 33–45, doi:10.1016/j.orggeochem.2013.07.002.

Berger, A. (1988), Milankovitch Theory and climate, *Reviews of Geophysics*, *26*(4), 624–657, doi:10.1029/RG026i004p00624.

Beszczynska-Möller, A., E. Fahrbach, U. Schauer, and E. Hansen (2012), Variability in Atlantic water temperature and transport at the entrance to the Arctic Ocean, 1997–2010, *ICES Journal of Marine Science*, *69*(5), 852–863, doi:10.1093/icesjms/fss056.

Bianchi, C., and R. Gersonde (2002), The Southern Ocean surface between Marine Isotope Stages 6 and 5d: Shape and timing of climate changes, *Palaeogeography, Palaeoclimatology, Palaeoecology*, *187*(1), 151–177, doi:10.1016/S0031-0182(02)00516-3.

Bond, G., B. Kromer, J. Beer, R. Muscheler, M. N. Evans, W. Showers, S. Hoffmann, R. Lotti-Bond, I. Hajdas, and G. Bonani (2001), Persistent Solar Influence on North Atlantic Climate During the Holocene, *Science*, *294*(5549), 2130–2136, doi:10.1126/science.1065680.

Boon, J. J., W. I. C. Rijpstra, F. De Lange, J. W. De Leeuw, M. Yoshioka, and Y. Shimizu (1979), Black Sea sterol—a molecular fossil for dinoflagellate blooms, *Nature*, *277*(5692), 125–127, doi:10.1038/277125a0.

Born, A., and T. F. Stocker (2014), Two Stable Equilibria of the Atlantic Subpolar Gyre, *Journal of Physical Oceanography*, *44*(1), 246–264, doi:10.1175/JPO-D-13-073.1.

Born, A., K. H. Nisancioglu, and P. Braconnot (2010), Sea ice induced changes in ocean circulation during the Eemian, *Climate Dynamics*, *35*(7), 1361–1371, doi:10.1007/s00382-009-0709-2.

Bourke, R. H., A. M. Weigel, and R. G. Paquette (1988), The westward turning branch of the West Spitsbergen Current, *Journal of Geophysical Research: Oceans*, *93*(C11), 14,065–14,077, doi:10.1029/JC093iC11p14065.

Bouttes, N., D. Paillard, and D. M. Roche (2010), Impact of brine-induced stratification on the glacial carbon cycle, *Climate of the Past*, *6*(5), 575–589, doi:10.5194/cp-6-575-2010.

Broecker, W. S. (1991), THE GREAT OCEAN CONVEYOR, *Oceanography*, *4*, 79–89.

Broecker, W. S., and T.-H. Peng (1982), *Tracers in the Sea*, 690 pp., Columbia University, Palisades, New York.

Brown, T. A., S. T. Belt, A. Tatarek, and C. J. Mundy (2014), Source identification of the Arctic sea ice proxy IP 25, *Nature Communications*, *5*(1), 4197, doi:10.1038/ncomms5197.

Candy, I., D. C. Schreve, J. Sherriff, and G. J. Tye (2014), Marine Isotope Stage 11: Palaeoclimates, palaeoenvironments and its role as an analogue for the current interglacial, *Earth-Science Reviews*, *128*, 18–51, doi:10.1016/j.earscirev.2013.09.006.

cape last interglacial project members (2006), Last Interglacial Arctic warmth confirms polar amplification of climate change, *Quaternary Science Reviews*, *25*(13), 1383–1400, doi:10.1016/j.quascirev.2006.01.033.

Capron, E., A. Govin, E. J. Stone, V. Masson-Delmotte, S. Mulitza, B. Otto-Bliesner, T. L. Rasmussen, L. C. Sime, C. Waelbroeck, and E. W. Wolff (2014), Temporal and spatial structure of multi-millennial temperature changes at high latitudes during the Last Interglacial, *Quaternary Science Reviews*, *103*, 116–133, doi:10.1016/j.quascirev.2014.08.018.

Carmack, E., I. Polyakov, L. Padman, I. Fer, E. Hunke, J. Hutchings, J. Jackson, D. Kelley, R. Kwok, C. Layton, H. Melling, D. Perovich, O. Persson, B. Ruddick, M.-L. Timmermans, J. Toole, T. Ross, S. Vavrus, and P. Winsor (2015), Toward Quantifying the Increasing Role of Oceanic Heat in Sea Ice Loss in the New Arctic, *Bulletin of the American Meteorological Society*, *96*(12), 2079–2105, doi:10.1175/BAMS-D-13-00177.1.

Cavalieri, D. J., and C. L. Parkinson (2012), Arctic sea ice variability and trends, 1979-2010, *The Cryosphere*, *6*(4), 881–889, doi:10.5194/tc-6-881-2012.

Chapman, M. R., and N. J. Shackleton (1999), Global ice-volume fluctuations, North Atlantic ice-rafting events, and deep-ocean circulation changes between 130 and 70 ka, *Geology*, *27*(9), 795–798, doi:10.1130/0091-7613(1999)027⟨0795:GIVFNA⟩2.3.CO;2.

Cohen, J., J. A. Screen, J. C. Furtado, M. Barlow, D. Whittleston, D. Coumou, J. Francis, K. Dethloff, D. Entekhabi, J. Overland, and J. Jones (2014), Recent Arctic amplification and extreme mid-latitude weather, *Nature Geoscience*, *7*(9), 627–637, doi:10.1038/ngeo2234.

Coletti, A. J., R. M. DeConto, J. Brigham-Grette, and M. Melles (2015), A GCM comparison of Pleistocene super-interglacial periods in relation to Lake El'gygytgyn, NE Arctic Russia, *Climate of the Past*, *11*(7), 979–989, doi:10.5194/cp-11-979-2015.

Collins, L. G., C. S. Allen, J. Pike, D. A. Hodgson, K. Weckström, and G. Massé (2013a), Evaluating highly branched isoprenoid (HBI) biomarkers as a novel Antarctic sea-ice proxy in deep ocean glacial age sediments, *Quaternary Science Reviews*, *79*, 87–98, doi:10.1016/j.quascirev.2013.02.004.

Collins, M., R. Knutti, J. Arblaster, J.-L. Dufresne, T. Fichefet, X. Gao, W. J. G. Jr, T. Johns, G. Krinner, M. Shongwe, A. J. Weaver, M. Wehner, M. R. Allen, T. Andrews, U. Beyerle, C. M. Bitz, S. Bony, B. B. B. Booth, H. E. Brooks, V. Brovkin, O. Browne, C. Brutel-Vuilmet, M. Cane, R. Chadwick, E. Cook, K. H. Cook, M. Eby, J. Fasullo, C. E. Forest, P. Forster, P. Good, H. Goosse, J. M. Gregory, G. C. Hegerl, P. J. Hezel, K. I. Hodges, M. M. Holland, M. Huber, M. Joshi, V. Kharin, Y. Kushnir, D. M. Lawrence, R. W. Lee, S. Liddicoat, C. Lucas, W. Lucht, J. Marotzke, F. Massonnet, H. D. Matthews, M. Meinshausen, C. Morice, A. Otto, C. M. Patricola, G. Philippon, S. Rahmstorf, W. J. Riley, O. Saenko, R. Seager, J. Sedláček, L. C. Shaffrey, D. Shindell, J. Sillmann, B. Stevens, P. A. Stott, R. Webb, G. Zappa, K. Zickfeld, S. Joussaume, A. Mokssit, K. Taylor, and S. Tett (2013b), Long-term Climate Change: Projections, Commitments and Irreversibility, in *Climate Change 2013: The Physical Science Basis. Contribution of Working Group I to the Fifth Assessment Report of the Intergovernmental Panel on Climate Change[Stocker, T.F., D. Qin, G.-K. Plattner, M. Tignor, S.K. Allen, J. Boschung, A. Nauels, Y. Xia, V. Bex and P.M. Midgley (eds.)]*, Cambridge University Press, United Kingdom and New York, NY, USA.

Condron, A., and P. Winsor (2012), Meltwater routing and the Younger Dryas, *Proceedings of the National Academy of Sciences*, *109*(49), 19,928–19,933, doi:10.1073/pnas.1207381109.

Davies, S. M., P. M. Abbott, R. H. Meara, N. J. G. Pearce, W. E. N. Austin, M. R. Chapman, A. Svensson, M. Bigler, T. L. Rasmussen, S. O. Rasmussen, and E. J. Farmer (2014), A North Atlantic tephrostratigraphical framework for 130–60 ka b2k: new tephra discoveries, marine-based correlations, and future challenges, *Quaternary Science Reviews*, *106*, 101–121, doi:10.1016/j.quascirev.2014.03.024.

De Schepper, S. (2013), Combining dinoflagellate cyst studies with geochemical proxies: application to palaeoceanography, palaeoecology and biostratigraphy, pp. 31–41, doi:10.1144/TMS5.4, the Micropalaeontological Society, Special Publications. Geological Society, London.

De Schepper, S., K. M. Beck, and G. Mangerud (2017), Late Neogene dinoflagellate cyst and acritarch biostratigraphy for Ocean Drilling Program Hole 642B, Norwegian Sea, *Review of Palaeobotany and Palynology*, doi:10.1016/j.revpalbo.2016.08.005.

de Vernal, A., and C. Hillaire-Marcel (2008), Natural Variability of Greenland Climate, Vegetation, and Ice Volume During the Past Million Years, *Science*, *320*(5883), 1622–1625, doi:10.1126/science.1153929.

de Vernal, A., A. Rochon, J.-L. Turon, and J. Matthiessen (1997), Organic-walled dinoflagellate cysts: Palynological tracers of sea-surface conditions in middle to high

latitude marine environments, *Geobios*, *30*(7), 905–920, doi:10.1016/S0016-6995(97)80215-X.

de Vernal, A., R. Gersonde, H. Goosse, M.-S. Seidenkrantz, and E. W. Wolff (2013a), Sea ice in the paleoclimate system: the challenge of reconstructing sea ice from proxies - an introduction, doi:10.1016/j.quascirev.2013.08.009.

de Vernal, A., A. Rochon, B. Fréchette, M. Henry, T. Radi, and S. Solignac (2013b), Reconstructing past sea ice cover of the Northern Hemisphere from dinocyst assemblages: status of the approach, *Quaternary Science Reviews*, *79*, 122–134, doi:10.1016/j.quascirev.2013.06.022.

de Vernal, A., T. Radi, S. Zaragosi, N. Van Nieuwenhove, A. Rochon, E. Allan, S. De Schepper, F. Eynaud, M. J. Head, A. Limoges, L. Londeix, F. Marret, J. Matthiessen, A. Penaud, V. Pospelova, A. Price, and T. Richerol (2020), Distribution of common modern dinoflagellate cyst taxa in surface sediments of the Northern Hemisphere in relation to environmental parameters: The new n=1968 database, *Marine Micropaleontology*, *159*, 101,796, doi:10.1016/j.marmicro.2019.101796.

Deser, C., L. Sun, R. A. Tomas, and J. Screen (2016), Does ocean coupling matter for the northern extratropical response to projected Arctic sea ice loss?, *Geophysical Research Letters*, *43*(5), 2149–2157, doi:10.1002/2016GL067792.

Diebold, F. X., and G. D. Rudebusch (2023), Climate models underestimate the sensitivity of Arctic sea ice to carbon emissions, *Energy Economics*, *126*, 107,012, doi:10.1016/j.eneco.2023.107012.

Dieckmann, G. S., and H. H. Hellmer (2010), The Importance of Sea Ice: An Overview, in *Sea Ice*, pp. 1–22, John Wiley & Sons, Incorporated, United Kingdom.

Ding, Q., A. Schweiger, M. L'Heureux, D. S. Battisti, S. Po-Chedley, N. C. Johnson, E. Blanchard-Wrigglesworth, K. Harnos, Q. Zhang, R. Eastman, and E. J. Steig (2017), Influence of high-latitude atmospheric circulation changes on summertime Arctic sea ice, *Nature Climate Change*, *7*(4), 289–295, doi:10.1038/nclimate3241.

Dutton, A., A. E. Carlson, A. J. Long, G. A. Milne, P. U. Clark, R. DeConto, B. P. Horton, S. Rahmstorf, and M. E. Raymo (2015), Sea-level rise due to polar ice-sheet mass loss during past warm periods, *Science*, *349*(6244), aaa4019, doi:10.1126/science.aaa4019.

Evitt, W. R. (1985), *Sporopollenin dinoflagellate cysts: their morphology and interpretation*, American Association of Stratigraphic Palynologists Foundation, Dallas, TX.

Fahl, K., and R. Stein (1999), Biomarkers as organic-carbon-source and environmental indicators in the Late Quaternary Arctic Ocean: problems and perspectives, *Marine Chemistry*, *63*(3), 293–309, doi:10.1016/S0304-4203(98)00068-1.

Fahl, K., and R. Stein (2012), Modern seasonal variability and deglacial/Holocene change of central Arctic Ocean sea-ice cover: New insights from biomarker proxy records, *Earth and Planetary Science Letters*, *351-352*, 123–133, doi:10.1016/j.epsl.2012.07.009.

Flanner, M. G., K. M. Shell, M. Barlage, D. K. Perovich, and M. A. Tschudi (2011), Radiative forcing and albedo feedback from the Northern Hemisphere cryosphere between 1979 and 2008, *Nature Geoscience*, *4*(3), 151–155, doi:10.1038/ngeo1062.

Francis, J. A., and S. J. Vavrus (2012), Evidence linking Arctic amplification to extreme weather in mid-latitudes, *Geophysical Research Letters*, *39*(6), doi:10.1029/2012GL051000.

Fronval, T., and E. Jansen (1996), Rapid changes in ocean circulation and heat flux in the Nordic seas during the last interglacial period, *Nature*, *383*(6603), 806–810, doi:10.1038/383806a0.

Furevik, T. (2001), Annual and interannual variability of Atlantic Water temperatures in the Norwegian and Barents Seas: 1980–1996, *Deep Sea Research Part I: Oceanographic Research Papers*, *48*(2), 383–404, doi:10.1016/S0967-0637(00)00050-9.

Galaasen, E. V., U. S. Ninnemann, N. Irvalı, H. K. F. Kleiven, Y. Rosenthal, C. Kissel, and D. A. Hodell (2014), Rapid Reductions in North Atlantic Deep Water During the Peak of the Last Interglacial Period, *Science*, *343*(6175), 1129–1132, doi:10.1126/science.1248667.

Galaasen, E. V., U. S. Ninnemann, A. Kessler, N. Irvalı, Y. Rosenthal, J. Tjiputra, N. Bouttes, D. M. Roche, H. K. F. Kleiven, and D. A. Hodell (2020), Interglacial instability of North Atlantic Deep Water ventilation, *Science*, *367*(6485), 1485–1489, doi:10.1126/science.aay6381.

Ganachaud, A., and C. Wunsch (2003), Large-Scale Ocean Heat and Freshwater Transports during the World Ocean Circulation Experiment, *Journal of Climate*, *16*(4), 696–705, doi:10.1175/1520-0442(2003)016⟨0696:LSOHAF⟩2.0.CO;2.

Geibert, W., J. Matthiessen, I. Stimac, J. Wollenburg, and R. Stein (2021), Glacial episodes of a freshwater Arctic Ocean covered by a thick ice shelf, *Nature*, *590*(7844), 97–102, doi:10.1038/s41586-021-03186-y.

Gosselin, M., M. Levasseur, P. A. Wheeler, R. A. Horner, and B. C. Booth (1997), New measurements of phytoplankton and ice algal production in the Arctic Ocean,

Deep Sea Research Part II: Topical Studies in Oceanography, *44*(8), 1623–1644, doi: 10.1016/S0967-0645(97)00054-4.

Govin, A., P. Braconnot, E. Capron, E. Cortijo, J.-C. Duplessy, E. Jansen, L. Labeyrie, A. Landais, O. Marti, E. Michel, E. Mosquet, B. Risebrobakken, D. Swingedouw, and C. Waelbroeck (2012), Persistent influence of ice sheet melting on high northern latitude climate during the early Last Interglacial, *Climate of the Past*, *8*, doi:10.5194/cp-8-483-2012.

Govin, A., E. Capron, P. C. Tzedakis, S. Verheyden, B. Ghaleb, C. Hillaire-Marcel, G. St-Onge, J. S. Stoner, F. Bassinot, L. Bazin, T. Blunier, N. Combourieu-Nebout, A. El Ouahabi, D. Genty, R. Gersonde, P. Jimenez-Amat, A. Landais, B. Martrat, V. Masson-Delmotte, F. Parrenin, M. S. Seidenkrantz, D. Veres, C. Waelbroeck, and R. Zahn (2015), Sequence of events from the onset to the demise of the Last Interglacial: Evaluating strengths and limitations of chronologies used in climatic archives, *Quaternary Science Reviews*, *129*, 1–36, doi:10.1016/j.quascirev.2015.09.018.

Gradinger, R. (2009), Sea-ice algae: Major contributors to primary production and algal biomass in the Chukchi and Beaufort Seas during May/June 2002, *Deep Sea Research Part II: Topical Studies in Oceanography*, *56*(17), 1201–1212, doi:10.1016/j.dsr2.2008.10.016.

Gradinger, R., and J. Ikävalko (1998), Organism incorporation into newly forming Arctic sea ice in the Greenland Sea, *Journal of Plankton Research*, *20*(5), 871–886, doi: 10.1093/plankt/20.5.871.

Gray, D. D., K. A. F. Zonneveld, and G. J. M. Versteegh (2017), Species-specific sensitivity of dinoflagellate cysts to aerobic degradation: A five-year natural exposure experiment, *Review of Palaeobotany and Palynology*, *247*, 175–187, doi: 10.1016/j.revpalbo.2017.09.002.

Guarino, M.-V., L. C. Sime, D. Schröeder, I. Malmierca-Vallet, E. Rosenblum, M. Ringer, J. Ridley, D. Feltham, C. Bitz, E. J. Steig, E. Wolff, J. Stroeve, and A. Sellar (2020), Sea-ice-free Arctic during the Last Interglacial supports fast future loss, *Nature Climate Change*, *10*(10), 928–932, doi:10.1038/s41558-020-0865-2.

Haine, T. W. N., and T. Martin (2017), The Arctic-Subarctic sea ice system is entering a seasonal regime: Implications for future Arctic amplification, *Scientific Reports*, *7*(1), 4618, doi:10.1038/s41598-017-04573-0.

Haine, T. W. N., B. Curry, R. Gerdes, E. Hansen, M. Karcher, C. Lee, B. Rudels, G. Spreen, L. de Steur, K. D. Stewart, and R. Woodgate (2015), Arctic freshwater

export: Status, mechanisms, and prospects, *Global and Planetary Change*, *125*, 13–35, doi:10.1016/j.gloplacha.2014.11.013.

Hansen, B., and S. Østerhus (2000), North Atlantic–Nordic Seas exchanges, *Progress in Oceanography*, *45*(2), 109–208, doi:10.1016/S0079-6611(99)00052-X.

Harland, R., and C. J. Pudsey (1999), Dinoflagellate cysts from sediment traps deployed in the Bellingshausen, Weddell and Scotia seas, Antarctica, *Marine Micropaleontology*, *37*(2), 77–99, doi:10.1016/S0377-8398(99)00016-X.

Harting, P. (1875), *Le système Éemien*, Archives Néerlandaises Sciences Exactes et Naturelles de la Societé Hollandaise des Sciences (Harlem)10: 443-454.

Harardóttir, S., J. S. Haile, J. L. Ray, A. Limoges, N. Van Nieuwenhove, C. Lalande, P.-L. Grondin, R. Jackson, K. S. Skaar, M. Heikkilä, J. Berge, N. Lundholm, G. Massé, S. Rysgaard, M.-S. Seidenkrantz, S. De Schepper, E. D. Lorenzen, C. Lovejoy, and S. Ribeiro (2024), Millennial-scale variations in Arctic sea ice are recorded in sedimentary ancient DNA of the microalga Polarella glacialis, *Communications Earth and Environment*, *5*(1), 1–13, doi:10.1038/s43247-023-01179-5.

Hattermann, T., P. E. Isachsen, W.-J. von Appen, J. Albretsen, and A. Sundfjord (2016), Eddy-driven recirculation of Atlantic Water in Fram Strait, *Geophysical Research Letters*, *43*(7), 3406–3414, doi:10.1002/2016GL068323.

Head, M. (1996), Modern dinoflagellate cysts and their biological affnities, in *American Association of Stratigraphic Palynologists Foundation*, vol. 3, pp. 1197–1248.

Helland-Hansen, B., and F. Nansen (1909), The Norwegian Sea - Its Physical Oceanography Based Upon the Norwegian Researches 1900-1904, *422 s.*, [Fiskeridirektoratets havforskningsinstitutt].

Hillaire-Marcel, C., d. V. Anne, G. Bilodeau, and A. Weaver (2001), Absence of deep-water formation in the Labrador Sea during the Last Interglacial period, *Nature*, *410*, 1073–7, doi:10.1038/35074059.

Hirche, H. J., M. E. M. Baumann, G. Kattner, and R. Gradinger (1991), Plankton distribution and the impact of copepod grazing on primary production in Fram Strait, Greenland Sea, *Journal of Marine Systems*, *2*(3), 477–494, doi:10.1016/0924-7963(91)90048-Y.

Hoff, U., T. L. Rasmussen, R. Stein, M. M. Ezat, and K. Fahl (2016), Sea ice and millennial-scale climate variability in the Nordic seas 90 kyr ago to present, *Nature Communications*, *7*(1), 12,247, doi:10.1038/ncomms12247.

Holland, M. M., C. M. Bitz, and B. Tremblay (2006), Future abrupt reductions in the summer Arctic sea ice, *Geophysical Research Letters*, *33*(23), doi:10.1029/2006GL028024.

Häkkinen, S., and P. B. Rhines (2004), Decline of Subpolar North Atlantic Circulation During the 1990s, *Science*, *304*(5670), 555–559, doi:10.1126/science.1094917.

Hönisch, B., N. G. Hemming, D. Archer, M. Siddall, and J. F. McManus (2009), Atmospheric Carbon Dioxide Concentration Across the Mid-Pleistocene Transition, *Science*, *324*(5934), 1551–1554, doi:10.1126/science.1171477.

Ingvaldsen, R. B., K. M. Assmann, R. Primicerio, M. Fossheim, I. V. Polyakov, and A. V. Dolgov (2021), Physical manifestations and ecological implications of Arctic Atlantification, *Nature Reviews Earth & Environment*, *2*(12), 874–889, doi:10.1038/s43017-021-00228-x.

IPCC (2021), *Climate Change 2021 – The Physical Science Basis: Working Group I Contribution to the Sixth Assessment Report of the Intergovernmental Panel on Climate Change* [*Masson-Delmotte, V., P. Zhai, A. Pirani, S.L. Connors, C. Péan, S. Berger, N. Caud, Y. Chen, L. Goldfarb, M.I. Gomis, M. Huang, K. Leitzell, E. Lonnoy, J.B.R. Matthews, T.K. Maycock, T. Waterfield, O. Yelekçi, R. Yu, and B. Zhou (eds.)*], 2391 pp., Cambridge University Press, Cambridge, United Kingdom and New York, NY, USA, doi:10.1017/9781009157896.

Irvali, N., U. S. Ninnemann, E. V. Galaasen, Y. Rosenthal, D. Kroon, D. W. Oppo, H. F. Kleiven, K. F. Darling, and C. Kissel (2012), Rapid switches in subpolar North Atlantic hydrography and climate during the Last Interglacial (MIS 5e), *Paleoceanography*, *27*(2), doi:10.1029/2011PA002244.

Irvali, N., U. S. Ninnemann, H. K. F. Kleiven, E. V. Galaasen, A. Morley, and Y. Rosenthal (2016), Evidence for regional cooling, frontal advances, and East Greenland Ice Sheet changes during the demise of the last interglacial, *Quaternary Science Reviews*, *150*, 184–199, doi:10.1016/j.quascirev.2016.08.029.

Ivanov, V., A. Smirnov, V. Alexeev, N. V. Koldunov, I. Repina, and V. Semenov (2018), Contribution of Convection-Induced Heat Flux to Winter Ice Decay in the Western Nansen Basin, *Journal of Geophysical Research: Oceans*, *123*(9), 6581–6597, doi:10.1029/2018JC013995.

Ivanov, V. V., V. A. Alexeev, I. Repina, N. V. Koldunov, and A. Smirnov (2012), Tracing Atlantic Water Signature in the Arctic Sea Ice Cover East of Svalbard, *Advances in Meteorology*, *2012*, e201,818, doi:10.1155/2012/201818.

Jahn, A., J. E. Kay, M. M. Holland, and D. M. Hall (2016), How predictable is the timing of a summer ice-free Arctic?, *Geophysical Research Letters*, *43*(17), 9113–9120, doi:10.1002/2016GL070067.

Jakobsson, M., L. Mayer, B. Coakley, J. A. Dowdeswell, S. Forbes, B. Fridman, H. Hodnesdal, R. Noormets, R. Pedersen, M. Rebesco, H. W. Schenke, Y. Zarayskaya, D. Accettella, A. Armstrong, R. M. Anderson, P. Bienhoff, A. Camerlenghi, I. Church, M. Edwards, J. V. Gardner, J. K. Hall, B. Hell, O. Hestvik, Y. Kristoffersen, C. Marcussen, R. Mohammad, D. Mosher, S. V. Nghiem, M. T. Pedrosa, P. G. Travaglini, and P. Weatherall (2012), The International Bathymetric Chart of the Arctic Ocean (IBCAO) Version 3.0, *Geophysical Research Letters*, *39*(12), doi:10.1029/2012GL052219.

Jakobsson, M., J. Nilsson, L. Anderson, J. Backman, G. Björk, T. M. Cronin, N. Kirchner, A. Koshurnikov, L. Mayer, R. Noormets, M. O'Regan, C. Stranne, R. Ananiev, N. Barrientos Macho, D. Cherniykh, H. Coxall, B. Eriksson, T. Flodén, L. Gemery, Gustafsson, K. Jerram, C. Johansson, A. Khortov, R. Mohammad, and I. Semiletov (2016), Evidence for an ice shelf covering the central Arctic Ocean during the penultimate glaciation, *Nature Communications*, *7*(1), 10,365, doi:10.1038/ncomms10365.

Jansen, E., J. Overpeck, K. Briffa, J.-C. Duplessy, F. Joos, V. Masson-Delmotte, D. Olago, B. Otto-Bliesner, W. Peltier, S. Rahmstorf, R. Ramesh, D. Raynaud, D. Rind, O. Solomina, R. Villalba, and D. Zhang (2007), Palaeoclimate. In: Climate Change 2007: The Physical Science Basis. Contribution of Working Group I to the Fourth Assessment Report of the Intergovernmental Panel on Climate Change [Solomon, S., D. Qin, M. Manning, Z. Chen, M. Marquis, K.B. Averyt, M. Tignor and H.L. Miller (eds.)], *Cambridge University Press, Cambridge, United Kingdom and New York, NY, USA.*

Jeong, H. J., Y. D. Yoo, J. S. Kim, K. A. Seong, N. S. Kang, and T. H. Kim (2010), Growth, feeding and ecological roles of the mixotrophic and heterotrophic dinoflagellates in marine planktonic food webs, *Ocean Sci. J.*, *45*(2), 65–91, doi:10.1007/s12601-010-0007-2.

Johns, L., E. J. Wraige, S. T. Belt, C. A. Lewis, G. Massé, J. M. Robert, and S. J. Rowland (1999), Identification of a C25 highly branched isoprenoid (HBI) diene in Antarctic sediments, Antarctic sea-ice diatoms and cultured diatoms, *Organic Geochemistry*, *30*(11), 1471–1475, doi:10.1016/S0146-6380(99)00112-6.

Kageyama, M., L. C. Sime, M. Sicard, M.-V. Guarino, A. de Vernal, R. Stein, D. Schroeder, I. Malmierca-Vallet, A. Abe-Ouchi, C. Bitz, P. Braconnot, E. C. Brady, J. Cao, M. A. Chamberlain, D. Feltham, C. Guo, A. N. LeGrande, G. Lohmann, K. J. Meissner, L. Menviel, P. Morozova, K. H. Nisancioglu, B. L. Otto-Bliesner, R. O'ishi,

S. Ramos Buarque, D. Salas y Melia, S. Sherriff-Tadano, J. Stroeve, X. Shi, B. Sun, R. A. Tomas, E. Volodin, N. K. H. Yeung, Q. Zhang, Z. Zhang, W. Zheng, and T. Ziehn (2021), A multi-model CMIP6-PMIP4 study of Arctic sea ice at 127 ka: sea ice data compilation and model differences, *Climate of the Past*, *17*(1), 37–62, doi:10.5194/cp-17-37-2021.

Kattsov, V. M., E. Källén, H. Cattle, J. Christensen, H. Drange, I. Hanssen-Bauer, T. Jóhannesen, I. Karol, J. Räisänen, G. Svensson, and S. Vavulin (2004), Future Climate Change: Modeling and Scenarios for the Arctic, *Arctic Climate Impact Assessment*, pp. 100–144.

Kaufman, D. S., D. P. Schneider, N. P. McKay, C. M. Ammann, R. S. Bradley, K. R. Briffa, G. H. Miller, B. L. Otto-Bliesner, J. T. Overpeck, B. M. Vinther, Arctic Lakes 2k Project Members, M. Abbott, Y. Axford, B. Bird, H. J. B. Birks, A. E. Bjune, J. Briner, T. Cook, M. Chipman, P. Francus, K. Gajewski, Geirsdóttir, F. S. Hu, B. Kutchko, S. Lamoureux, M. Loso, G. MacDonald, M. Peros, D. Porinchu, C. Schiff, H. Seppä, and E. Thomas (2009), Recent Warming Reverses Long-Term Arctic Cooling, *Science*, *325*(5945), 1236–1239, doi:10.1126/science.1173983.

Kleiven, H. K. F., C. Kissel, C. Laj, U. S. Ninnemann, T. O. Richter, and E. Cortijo (2008), Reduced North Atlantic Deep Water Coeval with the Glacial Lake Agassiz Freshwater Outburst, *Science*, *319*(5859), doi:10.1126/science.1148924.

Knies, J., P. Cabedo-Sanz, S. T. Belt, S. Baranwal, S. Fietz, and A. Rosell-Melé (2014), The emergence of modern sea ice cover in the Arctic Ocean, *Nature Communications*, *5*(1), 5608, doi:10.1038/ncomms6608.

Kodrans-Nsiah, M., G. J. de Lange, and K. A. F. Zonneveld (2008), A natural exposure experiment on short-term species-selective aerobic degradation of dinoflagellate cysts, *Review of Palaeobotany and Palynology*, *152*(1), 32–39, doi:10.1016/j.revpalbo.2008.04.002.

Kolling, H. M., R. Stein, K. Fahl, H. Sadatzki, A. de Vernal, and X. Xiao (2020), Biomarker Distributions in (Sub)-Arctic Surface Sediments and Their Potential for Sea Ice Reconstructions, *Geochemistry, Geophysics, Geosystems*, *21*(10), e2019GC008,629, doi:10.1029/2019GC008629.

Kremer, A., R. Stein, K. Fahl, H. Bauch, A. Mackensen, and F. Niessen (2018a), A 190-ka biomarker record revealing interactions between sea ice, Atlantic Water inflow and ice sheet activity in eastern Fram Strait, *Arktos*, *4*(1), 22, doi:10.1007/s41063-018-0052-0.

Kremer, A., R. Stein, K. Fahl, Z. Ji, Z. Yang, S. Wiers, J. Matthiessen, M. Forwick, L. Löwemark, M. O'Regan, J. Chen, and I. Snowball (2018b), Changes in sea ice

cover and ice sheet extent at the Yermak Plateau during the last 160 ka – Reconstructions from biomarker records, *Quaternary Science Reviews*, *182*, 93–108, doi: 10.1016/j.quascirev.2017.12.016.

Käse, R. H., and W. Krauß (1996), The Gulf Stream, the North Atlantic Current, and the Origin of the Azores Current, pp. 291–337, Bornträger, Berlin, Germany.

Laskar, J., P. Robutel, F. Joutel, M. Gastineau, A. C. M. Correia, and B. Levrard (2004), A long-term numerical solution for the insolation quantities of the Earth, *Astronomy Astrophysics*, *428*(1), 261–285, doi:10.1051/0004-6361:20041335.

Lazier, J. R. N. (1973), The renewal of Labrador sea water, *Deep Sea Research and Oceanographic Abstracts*, *20*(4), 341–353, doi:10.1016/0011-7471(73)90058-2.

Lenton, T. M., H. Held, E. Kriegler, J. W. Hall, W. Lucht, S. Rahmstorf, and H. J. Schellnhuber (2008), Tipping elements in the Earth's climate system, *Proceedings of the National Academy of Sciences*, *105*(6), 1786–1793, doi:10.1073/pnas.0705414105.

Leppäranta, M. (2011), *The Drift of Sea Ice*, Springer, Berlin, Heidelberg, doi:10.1007/978-3-642-04683-4.

Levermann, A., and A. Born (2007), Bistability of the Atlantic subpolar gyre in a coarse-resolution climate model, *Geophysical Research Letters*, *34*(24), doi:10.1029/2007GL031732.

Limoges, A., S. Ribeiro, K. Weckström, M. Heikkilä, K. Zamelczyk, T. J. Andersen, P. Tallberg, G. Massé, S. Rysgaard, N. Nørgaard-Pedersen, and M.-S. Seidenkrantz (2018), Linking the Modern Distribution of Biogenic Proxies in High Arctic Greenland Shelf Sediments to Sea Ice, Primary Production, and Arctic-Atlantic Inflow, *Journal of Geophysical Research: Biogeosciences*, *123*(3), 760–786, doi:10.1002/2017JG003840.

Lisiecki, L. E., and M. E. Raymo (2005), A Pliocene-Pleistocene stack of 57 globally distributed benthic 18O records, *Paleoceanography*, *20*(1), doi:10.1029/2004PA001071.

Lofverstrom, M., D. M. Thompson, B. L. Otto-Bliesner, and E. C. Brady (2022), The importance of Canadian Arctic Archipelago gateways for glacial expansion in Scandinavia, *Nature Geoscience*, *15*(6), 482–488, doi:10.1038/s41561-022-00956-9.

Loutre, M. F., and A. Berger (2003), Marine Isotope Stage 11 as an analogue for the present interglacial, *Global and Planetary Change*, *36*(3), 209–217, doi:10.1016/S0921-8181(02)00186-8.

Lozier, M. S. (2012), Overturning in the North Atlantic, *Annual Review of Marine Science*, *4*(1), 291–315, doi:10.1146/annurev-marine-120710-100740.

Lozier, M. S., F. Li, S. Bacon, F. Bahr, A. S. Bower, S. A. Cunningham, M. F. de Jong, L. de Steur, B. deYoung, J. Fischer, S. F. Gary, B. J. W. Greenan, N. P. Holliday, A. Houk, L. Houpert, M. E. Inall, W. E. Johns, H. L. Johnson, C. Johnson, J. Karstensen, G. Koman, I. A. Le Bras, X. Lin, N. Mackay, D. P. Marshall, H. Mercier, M. Oltmanns, R. S. Pickart, A. L. Ramsey, D. Rayner, F. Straneo, V. Thierry, D. J. Torres, R. G. Williams, C. Wilson, J. Yang, I. Yashayaev, and J. Zhao (2019), A sea change in our view of overturning in the subpolar North Atlantic, *Science*, *363*(6426), 516–521, doi:10.1126/science.aau6592.

Lund, D. C., Z. Chase, K. E. Kohfeld, and E. A. Wilson (2021), Tracking Southern Ocean Sea Ice Extent With Winter Water: A New Method Based on the Oxygen Isotopic Signature of Foraminifera, *Paleoceanography and Paleoclimatology*, *36*(6), e2020PA004,095, doi:10.1029/2020PA004095.

Lüthi, D., M. Le Floch, B. Bereiter, T. Blunier, J.-M. Barnola, U. Siegenthaler, D. Raynaud, J. Jouzel, H. Fischer, K. Kawamura, and T. F. Stocker (2008), High-resolution carbon dioxide concentration record 650,000–800,000 years before present, *Nature*, *453*(7193), 379–382, doi:10.1038/nature06949.

Manley, T. O. (1995), Branching of Atlantic Water within the Greenland-Spitsbergen Passage: An estimate of recirculation, *Journal of Geophysical Research: Oceans*, *100*(C10), 20,627–20,634, doi:10.1029/95JC01251.

Marret, F., and K. A. F. Zonneveld (2003), Atlas of modern organic-walled dinoflagellate cyst distribution, *Review of Palaeobotany and Palynology*, *125*(1), 1–200, doi:10.1016/S0034-6667(02)00229-4.

Marret, F., J. Eirıksson, K. L. Knudsen, J.-L. Turon, and J. D. Scourse (2004), Distribution of dinoflagellate cyst assemblages in surface sediments from the northern and western shelf of Iceland, *Review of Palaeobotany and Palynology*, *128*(1), 35–53, doi:10.1016/S0034-6667(03)00111-8.

Marret, F., L. Bradley, A. de Vernal, W. Hardy, S.-Y. Kim, P. Mudie, A. Penaud, V. Pospelova, A. M. Price, T. Radi, and A. Rochon (2020), From bi-polar to regional distribution of modern dinoflagellate cysts, an overview of their biogeography, *Marine Micropaleontology*, *159*, 101,753, doi:10.1016/j.marmicro.2019.101753.

Martinson, D. G., N. G. Pisias, J. D. Hays, J. Imbrie, T. C. Moore, and N. J. Shackleton (1987), Age dating and the orbital theory of the ice ages: Development of a high-resolution 0 to 300,000-year chronostratigraphy, *Quaternary Research*, *27*(1), 1–29, doi:10.1016/0033-5894(87)90046-9.

Masson-Delmotte, V., M. Schulz, A. Abe-Ouchi, J. Beer, A. Ganopolski, G. Rouco, E. Jansen, K. Lambeck, J. Luterbacher, T. Naish, M. Rojas, X. Shao, T. Osborn, B. Otto-Bliesner, T. Quinn, R. Ramesh, and A. Timmermann (2013), Information from Paleoclimate Archives. In: Climate Change 2013: The Physical Science Basis. Contribution of Working Group I to the Fifth Assessment Report of the Intergovernmental Panel on Climate Change [Stocker, T.F., D. Qin, G.-K. Plattner, M. Tignor, S.K. Allen, J. Boschung, A. Nauels, Y. Xia, V. Bex and P.M. Midgley (eds.)]., *Cambridge University Press, Cambridge, United Kingdom and New York, NY, USA.*

Matthiessen, J., and J. Knies (2001), Dinoflagellate cyst evidence for warm interglacial conditions at the northern Barents Sea margin during marine oxygen isotope stage 5, *Journal of Quaternary Science*, *16*(7), 727–737, doi:10.1002/jqs.656.

Matthiessen, J., A. de Vernal, M. Head, Y. Okolodkov, K. Zonneveld, and R. Harland (2005), Modem organic-walled dinoflagellate cysts in arctic marine environments and their (paleo-) environmental significance, *Paläontologische Zeitschrift*, *79*(1), 3–51, doi:10.1007/BF03021752.

Mazaud, A., C. Laj, and M. Bender (1994), A geomagnetic chronology for antarctic ice accumulation, *Geophysical Research Letters*, *21*(5), 337–340, doi:10.1029/93GL02789.

Meier, W., S. Gerland, M. Granskog, J. Key, C. Haas, G. Hovelsrud, K. Kovacs, A. Makshtas, C. Michel, D. Perovich, J. Reist, and B. van Oort (2011), Chapter 9: Sea Ice, in *Snow, Water, Ice and Permafrost in the Arctic (SWIPA): Climate Change and the Cryosphere*, Arctic Monitoring and Assessment Programme (AMAP).

Meier, W. N., G. K. Hovelsrud, B. E. van Oort, J. R. Key, K. M. Kovacs, C. Michel, C. Haas, M. A. Granskog, S. Gerland, D. K. Perovich, A. Makshtas, and J. D. Reist (2014), Arctic sea ice in transformation: A review of recent observed changes and impacts on biology and human activity, *Reviews of Geophysics*, *52*(3), 185–217, doi:10.1002/2013RG000431.

Melles, M., J. Brigham-Grette, P. S. Minyuk, N. R. Nowaczyk, V. Wennrich, R. M. DeConto, P. M. Anderson, A. A. Andreev, A. Coletti, T. L. Cook, E. Haltia-Hovi, M. Kukkonen, A. V. Lozhkin, P. Rosén, P. Tarasov, H. Vogel, and B. Wagner (2012), 2.8 Million Years of Arctic Climate Change from Lake El'gygytgyn, NE Russia, *Science*, *337*(6092), 315–320, doi:10.1126/science.1222135.

Meredith, M., M. Sommerkorn, S. Cassotta, C. Derksen, A. Ekaykin, A. Hollowed, G. Kofinas, A. Mackintosh, J. Melbourne-Thomas, M. Muelbert, G. Ottersen, H. Pritchard, and E. Schuur (2019), Chapter 3: Polar regions — Special Report on the Ocean and Cryosphere in a Changing Climate [H.-O. Pörtner, D.C. Roberts, V. Masson-Delmotte,

P. Zhai, M. Tignor, E. Poloczanska, K. Mintenbeck, A. Alegría, M. Nicolai, A. Okem, J. Petzold, B. Rama, N.M. Weyer (eds.)]., *Cambridge University Press, Cambridge, UK and New York, NY, USA*, pp. pp. 203–320.

Mokeddem, Z., J. F. McManus, and D. W. Oppo (2014), Oceanographic dynamics and the end of the last interglacial in the subpolar North Atlantic, *Proceedings of the National Academy of Sciences*, *111*(31), 11,263–11,268, doi:10.1073/pnas.1322103111.

Montoya, M., A. Born, and A. Levermann (2011), Reversed North Atlantic gyre dynamics in present and glacial climates, *Climate Dynamics*, *36*(5), 1107–1118, doi:10.1007/s00382-009-0729-y.

Montresor, M., C. Lovejoy, L. Orsini, G. Procaccini, and S. Roy (2003), Bipolar distribution of the cyst-forming dinoflagellate Polarella glacialis, *Polar Biology*, *26*(3), 186–194, doi:10.1007/s00300-002-0473-9.

Moseley, G. E., C. Spötl, H. Cheng, R. Boch, A. Min, and R. L. Edwards (2015), Termination-II interstadial/stadial climate change recorded in two stalagmites from the north European Alps, *Quaternary Science Reviews*, *127*, 229–239, doi:10.1016/j.quascirev.2015.07.012.

Ménabréaz, L., N. Thouveny, D. L. Bourlès, and L. Vidal (2014), The geomagnetic dipole moment variation between 250 and 800 ka BP reconstructed from the authigenic 10Be/9Be signature in West Equatorial Pacific sediments, *Earth and Planetary Science Letters*, *385*, 190–205, doi:10.1016/j.epsl.2013.10.037.

Müller, J., A. Wagner, K. Fahl, R. Stein, M. Prange, and G. Lohmann (2011), Towards quantitative sea ice reconstructions in the northern North Atlantic: A combined biomarker and numerical modelling approach, *Earth and Planetary Science Letters*, *306*(3), 137–148, doi:10.1016/j.epsl.2011.04.011.

Navarro-Rodriguez, A., S. T. Belt, J. Knies, and T. A. Brown (2013), Mapping recent sea ice conditions in the Barents Sea using the proxy biomarker IP25: implications for palaeo sea ice reconstructions, *Quaternary Science Reviews*, *79*, 26–39, doi:10.1016/j.quascirev.2012.11.025.

neem community members (2013), Eemian interglacial reconstructed from a Greenland folded ice core, *Nature*, *493*(7433), 489–494, doi:10.1038/nature11789.

ngrip community members (2004), High-resolution record of Northern Hemisphere climate extending into the last interglacial period, *Nature*, *431*, 147–151.

Notz, D., and J. Stroeve (2016), Observed Arctic sea-ice loss directly follows anthropogenic CO2 emission, *Science*, *354*(6313), 747–750, doi:10.1126/science.aag2345.

Notz, D., and J. Stroeve (2018), The Trajectory Towards a Seasonally Ice-Free Arctic Ocean, *Current Climate Change Reports*, *4*(4), 407–416, doi:10.1007/s40641-018-0113-2.

nsidc accessed oct (2023), Sea Ice Index Daily and Monthly Image Viewer-https://nsidc.org/data/seaice_index, *National Snow and Ice Data Center*.

Onarheim, I. H., L. H. Smedsrud, R. B. Ingvaldsen, and F. Nilsen (2014), Loss of sea ice during winter north of Svalbard, *66*(1), 23,933, doi:10.3402/tellusa.v66.23933.

Oppo, D. W., J. F. McManus, and J. L. Cullen (2006), Evolution and demise of the Last Interglacial warmth in the subpolar North Atlantic, *Quaternary Science Reviews*, *25*(23-24), 3268–3277, doi:10.1016/j.quascirev.2006.07.006.

Palter, J. B. (2015), The Role of the Gulf Stream in European Climate, *Annual Review of Marine Science*, *7*(1), 113–137, doi:10.1146/annurev-marine-010814-015656.

Persson, A., and R. Rosenberg (2003), Impact of grazing and bioturbation of marine benthic deposit feeders on dinoflagellate cysts, *Harmful Algae*, *2*(1), 43–50, doi:10.1016/S1568-9883(03)00003-9.

Pickart, R. S., D. J. Torres, and R. A. Clarke (2002), Hydrography of the Labrador Sea during Active Convection, *Journal of Physical Oceanography*, *32*(2), 428–457, doi:10.1175/1520-0485(2002)032⟨0428:HOTLSD⟩2.0.CO;2.

Pisias, N. G., D. G. Martinson, T. C. Moore, N. J. Shackleton, W. Prell, J. Hays, and G. Boden (1984), High resolution stratigraphic correlation of benthic oxygen isotopic records spanning the last 300,000 years, *Marine Geology*, *56*(1), 119–136, doi:10.1016/0025-3227(84)90009-4.

Polyakov, I. V., G. V. Alekseev, L. A. Timokhov, U. S. Bhatt, R. L. Colony, H. L. Simmons, D. Walsh, J. E. Walsh, and V. F. Zakharov (2004), Variability of the Intermediate Atlantic Water of the Arctic Ocean over the Last 100 Years, *Journal of Climate*, *17*(23), 4485–4497, doi:10.1175/JCLI-3224.1.

Polyakov, I. V., A. V. Pnyushkov, M. B. Alkire, I. M. Ashik, T. M. Baumann, E. C. Carmack, I. Goszczko, J. Guthrie, V. V. Ivanov, T. Kanzow, R. Krishfield, R. Kwok, A. Sundfjord, J. Morison, R. Rember, and A. Yulin (2017), Greater role for Atlantic inflows on sea-ice loss in the Eurasian Basin of the Arctic Ocean, *Science*, *356*(6335), 285–291, doi:10.1126/science.aai8204.

Polyakov, I. V., T. P. Rippeth, I. Fer, T. M. Baumann, E. C. Carmack, V. V. Ivanov, M. Janout, L. Padman, A. V. Pnyushkov, and R. Rember (2020), Intensification of

Near-Surface Currents and Shear in the Eastern Arctic Ocean, *Geophysical Research Letters*, *47*(16), e2020GL089,469, doi:10.1029/2020GL089469.

Rahmstorf, S. (1994), Rapid climate transitions in a coupled ocean–atmosphere model, *Nature*, *372*(6501), 82–85, doi:10.1038/372082a0.

Rasmussen, T. L., D. W. Oppo, E. Thomsen, and S. J. Lehman (2003), Deep sea records from the southeast Labrador Sea: Ocean circulation changes and ice-rafting events during the last 160,000 years, *Paleoceanography*, *18*(1), doi:10.1029/2001PA000736.

Raynaud, D., J.-M. Barnola, R. Souchez, R. Lorrain, J.-R. Petit, P. Duval, and V. Y. Lipenkov (2005), The record for marine isotopic stage 11, *Nature*, *436*(7047), 39–40, doi:10.1038/43639b.

Regattieri, E., G. Zanchetta, R. N. Drysdale, I. Isola, J. D. Woodhead, J. C. Hellstrom, B. Giaccio, A. Greig, I. Baneschi, and E. Dotsika (2016), Environmental variability between the penultimate deglaciation and the mid Eemian: Insights from Tana che Urla (central Italy) speleothem trace element record, *Quaternary Science Reviews*, *152*, 80–92, doi:10.1016/j.quascirev.2016.09.027.

Reigstad, M., P. Wassmann, C. Wexels Riser, S. Øygarden, and F. Rey (2002), Variations in hydrography, nutrients and chlorophyll *a* in the marginal ice-zone and the central Barents Sea, *Journal of Marine Systems*, *38*(1), 9–29, doi:10.1016/S0924-7963(02)00167-7.

Rhein, M., D. Kieke, S. Hüttl-Kabus, A. Roessler, C. Mertens, R. Meissner, B. Klein, C. W. Böning, and I. Yashayaev (2011), Deep water formation, the subpolar gyre, and the meridional overturning circulation in the subpolar North Atlantic, *Deep Sea Research Part II: Topical Studies in Oceanography*, *58*(17), 1819–1832, doi:10.1016/j.dsr2.2010.10.061.

Risebrobakken, B., T. Dokken, and E. Jansen (2005), Extent and Variability of the Meridional Atlantic Circulation in the Eastern Nordic Seas During Marine Isotope Stage 5 and its Influence on the Inception of the Last Glacial, in *The Nordic Seas: An Integrated Perspective*, pp. 323–339, American Geophysical Union (AGU), doi:10.1029/158GM20.

Risebrobakken, B., E. Balbon, T. Dokken, E. Jansen, C. Kissel, L. Labeyrie, T. Richter, and L. Senneset (2006), The penultimate deglaciation: High-resolution paleoceanographic evidence from a north–south transect along the eastern Nordic Seas, *Earth and Planetary Science Letters*, *241*(3), 505–516, doi:10.1016/j.epsl.2005.11.032.

Risebrobakken, B., T. Dokken, O. H. Otterå, E. Jansen, Y. Gao, and H. Drange (2007), Inception of the Northern European ice sheet due to contrasting ocean and insolation forcing, *Quaternary Research*, *67*(1), 128–135, doi:10.1016/j.yqres.2006.07.007.

Robinson, N., G. Eglinton, S. C. Brassell, and P. A. Cranwell (1984), Dinoflagellate origin for sedimentary 4-methylsteroids and 5(H)-stanols, *Nature*, *308*(5958), 439–442, doi:10.1038/308439a0.

Rochon, A., d. V. Anne, J.-L. Turon, and M. Head (1999), Distribution of recent dinoflagellate cysts in surface sediments from the North Atlantic and adjacent seas in relation to sea-surface parameters, *American Association of Stratigraphic Palynologists Contribution Series*, *35*, 1–146.

Rohling, E. J., E. J. Rohling, A. Sluijs, H. A. Dijkstra, P. Köhler, R. S. W. van de Wal, A. S. von der Heydt, D. J. Beerling, A. Berger, P. K. Bijl, M. Crucifix, R. DeConto, S. S. Drijfhout, A. Fedorov, G. L. Foster, A. Ganopolski, J. Hansen, B. Hönisch, H. Hooghiemstra, M. Huber, P. Huybers, R. Knutti, D. W. Lea, L. J. Lourens, D. Lunt, V. Masson-Delmotte, M. Medina-Elizalde, B. Otto-Bliesner, M. Pagani, H. Pälike, H. Renssen, D. L. Royer, M. Siddall, P. Valdes, J. C. Zachos, R. E. Zeebe, and PALAEOSENS Project Members (2012), Making sense of palaeoclimate sensitivity, *Nature*, *491*(7426), 683–691, doi:10.1038/nature11574.

Rontani, J.-F., B. Charrière, R. Sempéré, D. Doxaran, F. Vaultier, J. E. Vonk, and J. K. Volkman (2014), Degradation of sterols and terrigenous organic matter in waters of the Mackenzie Shelf, Canadian Arctic, *Organic Geochemistry*, *75*, 61–73, doi:10.1016/j.orggeochem.2014.06.002.

Rosenblum, E., and I. Eisenman (2017), Sea Ice Trends in Climate Models Only Accurate in Runs with Biased Global Warming, *Journal of Climate*, *30*(16), 6265–6278, doi:10.1175/JCLI-D-16-0455.1.

Rudels, B., H. J. Friedrich, and D. Quadfasel (1999), The Arctic Circumpolar Boundary Current, *Deep Sea Research Part II: Topical Studies in Oceanography*, *46*, 1023–1062, doi:10.1016/S0967-0645(99)00015-6.

Rudels, B., E. Fahrbach, J. Meincke, G. Budéus, and P. Eriksson (2002), The East Greenland Current and its contribution to the Denmark Strait overflow, *ICES Journal of Marine Science*, *59*(6), 1133–1154, doi:10.1006/jmsc.2002.1284.

Rysgaard, S., J. Bendtsen, B. Delille, G. S. Dieckmann, R. N. Glud, H. Kennedy, J. Mortensen, S. Papadimitriou, D. N. Thomas, and J.-L. Tison (2011), Sea ice contribution to the air–sea CO2 exchange in the Arctic and Southern Oceans, *Tellus B*, *63*(5), 823–830, doi:10.1111/j.1600-0889.2011.00571.x.

Schauer, U., B. Rudels, E. P. Jones, L. G. Anderson, R. D. Muench, G. Björk, J. H. Swift, V. Ivanov, and A.-M. Larsson (2002), Confluence and redistribution of Atlantic water in the Nansen, Amundsen and Makarov basins, *Annales Geophysicae*, *20*(2), 257–273, doi:10.5194/angeo-20-257-2002.

Schauer, U., E. Fahrbach, S. Osterhus, and G. Rohardt (2004), Arctic warming through the Fram Strait: Oceanic heat transport from 3 years of measurements, *Journal of Geophysical Research: Oceans*, *109*(C6), doi:10.1029/2003JC001823.

Schlitzer, R. (2023), Ocean Data View.

Screen, J. A. (2017), Far-flung effects of Arctic warming, *Nature Geoscience*, *10*(4), 253–254, doi:10.1038/ngeo2924.

Screen, J. A., and I. Simmonds (2010), The central role of diminishing sea ice in recent Arctic temperature amplification, *Nature*, *464*(7293), 1334–1337, doi:10.1038/nature09051.

Screen, J. A., C. Deser, D. M. Smith, X. Zhang, R. Blackport, P. J. Kushner, T. Oudar, K. E. McCusker, and L. Sun (2018), Consistency and discrepancy in the atmospheric response to Arctic sea-ice loss across climate models, *Nature Geoscience*, *11*(3), 155–163, doi:10.1038/s41561-018-0059-y.

Serreze, M. C., A. P. Barrett, A. D. Crawford, and R. A. Woodgate (2019), Monthly Variability in Bering Strait Oceanic Volume and Heat Transports, Links to Atmospheric Circulation and Ocean Temperature, and Implications for Sea Ice Conditions, *Journal of Geophysical Research: Oceans*, *124*(12), 9317–9337, doi:10.1029/2019JC015422.

Shackleton, N. (1969), The last interglacial in the marine and terrestrial records, *Proceedings of the Royal Society of London. Series B. Biological Sciences*, *174*(1034), 135–154.

Shackleton, N., M. Chapman, M. Sanchez Goñi, D. Pailler, and Y. Lancelot (2002), The Classic Marine Isotope Substage 5e, *Quaternary Research*, *58*, 14–16, doi:10.1006/qres.2001.2312.

Shackleton, N. J., M. F. Sánchez-Goñi, D. Pailler, and Y. Lancelot (2003), Marine Isotope Substage 5e and the Eemian Interglacial, *Global and Planetary Change*, *36*(3), 151–155, doi:10.1016/S0921-8181(02)00181-9.

Smedsrud, L. H., M. H. Halvorsen, J. C. Stroeve, R. Zhang, and K. Kloster (2017), Fram Strait sea ice export variability and September Arctic sea ice extent over the last 80 years, *The Cryosphere*, *11*(1), 65–79, doi:10.5194/tc-11-65-2017.

Smeed, D. A., G. D. McCarthy, S. A. Cunningham, E. Frajka-Williams, D. Rayner, W. E. Johns, C. S. Meinen, M. O. Baringer, B. I. Moat, A. Duchez, and H. L. Bryden (2014), Observed decline of the Atlantic meridional overturning circulation 2004-2012, *Ocean Science*, *10*(1), 29–38, doi:10.5194/os-10-29-2014.

Spielhagen, R. F., K. Werner, S. A. Sørensen, K. Zamelczyk, E. Kandiano, G. Budeus, K. Husum, T. M. Marchitto, and M. Hald (2011), Enhanced Modern Heat Transfer to the Arctic by Warm Atlantic Water, *Science*, *331*(6016), 450–453, doi:10.1126/science.1197397.

Stein, R., and K. Fahl (2013), Biomarker proxy shows potential for studying the entire Quaternary Arctic sea ice history, *Organic Geochemistry*, *55*, 98–102, doi:10.1016/j.orggeochem.2012.11.005.

Stein, R., and R. Stax (1991), Late quaternary organic carbon cycles and paleoproductivity in the Labrador Sea, *Geo-Marine Letters*, *11*(2), 90–95, doi:10.1007/BF02431035.

Stein, R., K. Fahl, and J. Müller (2012), Proxy reconstruction of Arctic Ocean sea ice history - From IRD to IP25, *Polarforschung*, *82*, 37–71.

Stein, R., K. Fahl, M. Schreck, G. Knorr, F. Niessen, M. Forwick, C. Gebhardt, L. Jensen, M. Kaminski, A. Kopf, J. Matthiessen, W. Jokat, and G. Lohmann (2016), Evidence for ice-free summers in the late Miocene central Arctic Ocean, *Nature Communications*, *7*(1), 1–13, doi:10.1038/ncomms11148.

Stein, R., K. Fahl, P. Gierz, F. Niessen, and G. Lohmann (2017), Arctic Ocean sea ice cover during the penultimate glacial and the last interglacial, *Nature Communications*, *8*(1), 1–13, doi:10.1038/s41467-017-00552-1.

Stein, R., A. Kremer, and K. Fahl (2022), Past glacial-interglacial changes in Arctic Ocean sea-ice conditions, *PAGES Magazine*, *30*(2), 90–91, doi:10.22498/pages.30.2.90.

Stirling, C., T. Esat, K. Lambeck, and M. McCulloch (1998), Timing and duration of the Last Interglacial: Evidence for a restricted interval of widespread coral reef growth, *Earth and Planetary Science Letters*, *160*, 745–762, doi:10.1016/S0012-821X(98)00125-3.

Stocker, T., D. Qin, G.-K. Plattner, M. Tignor, S. Allen, J. Boschung, A. Nauels, Y. Xia, V. Bex, and P. Midgley (2013), *IPCC, 2013: Climate Change 2013: The Physical Science Basis. Contribution of Working Group I to the Fifth Assessment Report of the Intergovernmental Panel on Climate Change*, Cambridge University Press, Cambridge, United Kingdom and New York, NY, USA.

Stocker, T. F., and D. G. Wright (1991), Rapid transitions of the ocean's deep circulation induced by changes in surface water fluxes, *Nature*, *351*(6329), 729–732, doi:10.1038/351729a0.

Stockmarr, J. (1971), Tablets with Spores used in Absolute Pollen Analysis, *Pollen et Spores*, *13*, 615–621.

Stoner, J. S., J. E. T. Channell, C. Hillaire-Marcel, and C. Kissel (2000), Geomagnetic paleointensity and environmental record from Labrador Sea core MD95-2024: global marine sediment and ice core chronostratigraphy for the last 110 kyr, *Earth and Planetary Science Letters*, *183*(1), 161–177, doi:10.1016/S0012-821X(00)00272-7.

Stoynova, V., T. M. Shanahan, K. A. Hughen, and A. de Vernal (2013), Insights into Circum-Arctic sea ice variability from molecular geochemistry, *Quaternary Science Reviews*, *79*, 63–73, doi:10.1016/j.quascirev.2012.10.006.

Stroeve, J., M. M. Holland, W. Meier, T. Scambos, and M. Serreze (2007), Arctic sea ice decline: Faster than forecast, *Geophysical Research Letters*, *34*(9), doi:10.1029/2007GL029703.

Stroeve, J. C., M. C. Serreze, M. M. Holland, J. E. Kay, J. Malanik, and A. P. Barrett (2012), The Arctic's rapidly shrinking sea ice cover: a research synthesis, *Climatic Change*, *110*(3), 1005–1027, doi:10.1007/s10584-011-0101-1.

Svendsen, J. I., H. Alexanderson, V. I. Astakhov, I. Demidov, J. A. Dowdeswell, S. Funder, V. Gataullin, M. Henriksen, C. Hjort, M. Houmark-Nielsen, H. W. Hubberten, Ingólfsson, M. Jakobsson, K. H. Kjær, E. Larsen, H. Lokrantz, J. P. Lunkka, A. Lyså, J. Mangerud, A. Matiouchkov, A. Murray, P. Möller, F. Niessen, O. Nikolskaya, L. Polyak, M. Saarnisto, C. Siegert, M. J. Siegert, R. F. Spielhagen, and R. Stein (2004), Late Quaternary ice sheet history of northern Eurasia, *Quaternary Science Reviews*, *23*(11), 1229–1271, doi:10.1016/j.quascirev.2003.12.008.

Sánchez Goñi, M. F., P. Bakker, S. Desprat, A. E. Carlson, C. J. Van Meerbeeck, O. Peyron, F. Naughton, W. J. Fletcher, F. Eynaud, L. Rossignol, and H. Renssen (2012), European climate optimum and enhanced Greenland melt during the Last Interglacial, *Geology*, *40*(7), 627–630, doi:10.1130/G32908.1.

Thackeray, C. W., and A. Hall (2019), An emergent constraint on future Arctic sea-ice albedo feedback, *Nature Climate Change*, *9*(12), 972–978, doi:10.1038/s41558-019-0619-1.

Thomas, D. N. (2017), Overview of sea ice growth and properties, in *Sea Ice*, pp. 1–41, John Wiley & Sons, Incorporated, United Kingdom.

Tremblay, J. E., and W. O. Smith (2007), Chapter 8 Primary Production and Nutrient Dynamics in Polynyas, in *Elsevier Oceanography Series*, *Polynyas: Windows to the World*, vol. 74, edited by W. O. Smith and D. G. Barber, pp. 239–269, Elsevier, doi:10.1016/S0422-9894(06)74008-9.

Trenberth, K. E., and J. M. Caron (2001), Estimates of Meridional Atmosphere and Ocean Heat Transports, *Journal of Climate*, *14*(16), 3433–3443, doi:10.1175/1520-0442(2001)014⟨3433:EOMAAO⟩2.0.CO;2.

Tripati, A. K., C. D. Roberts, R. A. Eagle, and G. Li (2011), A 20 million year record of planktic foraminiferal B/Ca ratios: Systematics and uncertainties in pCO2 reconstructions, *Geochimica et Cosmochimica Acta*, *75*(10), 2582–2610, doi:10.1016/j.gca.2011.01.018.

Tzedakis, P. C., R. N. Drysdale, V. Margari, L. C. Skinner, L. Menviel, R. H. Rhodes, A. S. Taschetto, D. A. Hodell, S. J. Crowhurst, J. C. Hellstrom, A. E. Fallick, J. O. Grimalt, J. F. McManus, B. Martrat, Z. Mokeddem, F. Parrenin, E. Regattieri, K. Roe, and G. Zanchetta (2018), Enhanced climate instability in the North Atlantic and southern Europe during the Last Interglacial, *Nature Communications*, *9*(1), 4235, doi:10.1038/s41467-018-06683-3.

UNEP (2021), Emissions Gap Report 2021: The Heat Is On – A World of Climate Promises Not Yet Delivered, *United Nations Environment Programme*.

van der Bilt, W. G. M., J. M. Cederstrøm, E. W. N. Støren, S. M. P. Berben, and S. Rutledal (2021), Rapid Tephra Identification in Geological Archives With Computed Tomography: Experimental Results and Natural Applications, *Frontiers in Earth Science*, *8*.

Van Nieuwenhove, N., H. A. Bauch, F. Eynaud, E. Kandiano, E. Cortijo, and J.-L. Turon (2011), Evidence for delayed poleward expansion of North Atlantic surface waters during the last interglacial (MIS 5e), *Quaternary Science Reviews*, *30*(7), 934–946, doi:10.1016/j.quascirev.2011.01.013.

Vancoppenolle, M., K. M. Meiners, C. Michel, L. Bopp, F. Brabant, G. Carnat, B. Delille, D. Lannuzel, G. Madec, S. Moreau, J.-L. Tison, and P. van der Merwe (2013), Role of sea ice in global biogeochemical cycles: emerging views and challenges, *Quaternary Science Reviews*, *79*, 207–230, doi:10.1016/j.quascirev.2013.04.011.

Vavrus, S. J., M. M. Holland, A. Jahn, D. A. Bailey, and B. A. Blazey (2012), Twenty-First-Century Arctic Climate Change in CCSM4, *Journal of Climate*, *25*(8), 2696–2710, doi:10.1175/JCLI-D-11-00220.1.

Vermassen, F., M. O'Regan, A. de Boer, F. Schenk, M. Razmjooei, G. West, T. M. Cronin, M. Jakobsson, and H. K. Coxall (2023), A seasonally ice-free Arctic Ocean during the Last Interglacial, *Nature Geoscience*, *16*(8), 723–729, doi:10.1038/s41561-023-01227-x.

Vinje, T. (2001a), Anomalies and Trends of Sea-Ice Extent and Atmospheric Circulation in the Nordic Seas during the Period 1864–1998, *Journal of Climate*, *14*(3), 255–267, doi:10.1175/1520-0442(2001)014⟨0255:AATOSI⟩2.0.CO;2.

Vinje, T. (2001b), Fram Strait Ice Fluxes and Atmospheric Circulation: 1950–2000, *Journal of Climate*, *14*(16), 3508–3517, doi:10.1175/1520-0442(2001)014⟨3508:FSIFAA⟩2.0.CO;2.

Volkman, J. K. (1986), A review of sterol markers for marine and terrigenous organic matter, *Organic Geochemistry*, *9*(2), 83–99, doi:10.1016/0146-6380(86)90089-6.

Volkman, J. K., S. M. Barrett, S. I. Blackburn, M. P. Mansour, E. L. Sikes, and F. Gelin (1998), Microalgal biomarkers: A review of recent research developments, *Organic Geochemistry*, *29*(5), 1163–1179, doi:10.1016/S0146-6380(98)00062-X.

von Appen, W.-J., U. Schauer, R. Somavilla, E. Bauerfeind, and A. Beszczynska-Möller (2015), Exchange of warming deep waters across Fram Strait, *Deep Sea Research Part I: Oceanographic Research Papers*, *103*, 86–100, doi:10.1016/j.dsr.2015.06.003.

Wadhams, P. (2017), *A farewell to ice: a report from the Arctic*, Oxford University Press, New York, NY.

Wang, Q., C. Wekerle, X. Wang, S. Danilov, N. Koldunov, D. Sein, D. Sidorenko, W.-J. von Appen, and T. Jung (2020), Intensification of the Atlantic Water Supply to the Arctic Ocean Through Fram Strait Induced by Arctic Sea Ice Decline, *Geophysical Research Letters*, *47*(3), e2019GL086,682, doi:10.1029/2019GL086682.

Williams, G., R. Fensome, M. Miller, and W. Sarjeant (2000), A glossary of the terminology applied to dinoflagellates, acritarchs and prasinophytes, with emphasis on fossils: Third edition, *American Association of Stratigraphic Palynologists Contributions Series*, *no. 37*.

Williams, G. L., R. A. Fensome, and R. A. MacRae (2017), The lentin and williams index of fossil dinoflagellates 2017 edition, *American Association of Stratigraphic Palynologists Contributions Series no. 48*.

Xiao, W., L. Polyak, R. Wang, L. Löwemark, J. Mei, D. You, W. Wang, L. Wu, and X. Jin (2020), Middle to Late Pleistocene Arctic paleoceanographic changes based on

sedimentary records from Mendeleev Ridge and Makarov Basin, *Quaternary Science Reviews*, *228*, 106,105, doi:10.1016/j.quascirev.2019.106105.

Xiao, X., K. Fahl, J. Müller, and R. Stein (2015), Sea-ice distribution in the modern Arctic Ocean: Biomarker records from trans-Arctic Ocean surface sediments, *Geochimica et Cosmochimica Acta*, *155*, 16–29, doi:10.1016/j.gca.2015.01.029.

Yang, Q., T. H. Dixon, P. G. Myers, J. Bonin, D. Chambers, M. R. van den Broeke, M. H. Ribergaard, and J. Mortensen (2016), Recent increases in Arctic freshwater flux affects Labrador Sea convection and Atlantic overturning circulation, *Nature Communications*, *7*(1), 10,525, doi:10.1038/ncomms10525.

Yunker, M. B., R. W. Macdonald, D. J. Veltkamp, and W. J. Cretney (1995), Terrestrial and marine biomarkers in a seasonally ice-covered Arctic estuary — integration of multivariate and biomarker approaches, *Marine Chemistry*, *49*(1), 1–50, doi:10.1016/0304-4203(94)00057-K.

Zhuravleva, A., H. A. Bauch, and N. Van Nieuwenhove (2017a), Last Interglacial (MIS5e) hydrographic shifts linked to meltwater discharges from the East Greenland margin, *Quaternary Science Reviews*, *164*, 95–109, doi:10.1016/j.quascirev.2017.03.026.

Zhuravleva, A., H. A. Bauch, and R. F. Spielhagen (2017b), Atlantic water heat transfer through the Arctic Gateway (Fram Strait) during the Last Interglacial, *Global and Planetary Change*, *157*, 232–243, doi:10.1016/j.gloplacha.2017.09.005.

Zimmermann, H. H., K. R. Stoof-Leichsenring, V. Dinkel, L. Harms, L. Schulte, M.-T. Hütt, D. Nürnberg, R. Tiedemann, and U. Herzschuh (2023), Marine ecosystem shifts with deglacial sea-ice loss inferred from ancient DNA shotgun sequencing, *Nature Communications*, *14*(1), 1650, doi:10.1038/s41467-023-36845-x.

Zonneveld, K. A. F., and G. A. Brummer (2000), (Palaeo-)ecological significance, transport and preservation of organic-walled dinoflagellate cysts in the Somali Basin, NW Arabian Sea, *Deep Sea Research Part II: Topical Studies in Oceanography*, *47*(9), 2229–2256, doi:10.1016/S0967-0645(00)00023-0.

Zonneveld, K. A. F., G. Versteegh, and M. Kodrans-Nsiah (2008), Preservation and organic chemistry of Late Cenozoic organic-walled dinoflagellate cysts: A review, *Marine Micropaleontology*, *68*(1), 179–197, doi:10.1016/j.marmicro.2008.01.015.

Zonneveld, K. A. F., F. Marret, G. J. M. Versteegh, K. Bogus, S. Bonnet, I. Bouimetarhan, E. Crouch, A. de Vernal, R. Elshanawany, L. Edwards, O. Esper, S. Forke, K. Grøsfjeld, M. Henry, U. Holzwarth, J.-F. Kielt, S.-Y. Kim, S. Ladouceur, D. Ledu, L. Chen, A. Limoges, L. Londeix, S. H. Lu, M. S. Mahmoud, G. Marino,

K. Matsouka, J. Matthiessen, D. C. Mildenhal, P. Mudie, H. L. Neil, V. Pospelova, Y. Qi, T. Radi, T. Richerol, A. Rochon, F. Sangiorgi, S. Solignac, J.-L. Turon, T. Verleye, Y. Wang, Z. Wang, and M. Young (2013), Atlas of modern dinoflagellate cyst distribution based on 2405 data points, *Review of Palaeobotany and Palynology*, *191*, 1–197, doi:10.1016/j.revpalbo.2012.08.003.

Årthun, M., T. Eldevik, L. H. Smedsrud, Skagseth, and R. B. Ingvaldsen (2012), Quantifying the Influence of Atlantic Heat on Barents Sea Ice Variability and Retreat, *Journal of Climate*, *25*(13), 4736–4743, doi:10.1175/JCLI-D-11-00466.1.

Errata for
Sea Ice Variability in a Warmer Past:
Last Interglacial Paleoceanography of the (Sub)Arctic Oceans

Kristine Steinsland

Thesis for the degree philosophiae doctor (PhD)

at the University of Bergen

Kristine Steinsland

(19.04.2024)

Ingrid Sollhoy

(19.04.2024)

Errata

Page xi Update in the list of publications: “manuscript in review” – changed to “manuscript accepted for publication”.

Page 19 Wrong Table citation: “Table 1” – corrected to “Table 3.1”.

Page 23 Missing subscript: “$PBIP_{25}$” and “$PDIP_{25}$” – corrected to “P_BIP_{25}” and “P_DIP_{25}”.

Page 23 Wrong citation: “Belt et al. (2018)” – corrected to “Belt (2018)”.

Page 29 Misspelling: “*Impagedinium*” – corrected to “*Impagidinium*”.

Page 37 repeated word: one “periods” removed.

Page 41 Misspelling: “Quaernary” – corrected to “Quaternary”.

Page xi, 63 Misspelling: “Paleogeography, Paleoclimatology, Paleoecology” – corrected to “Palaeogeography, Palaeoclimatology, Palaeoecology”.

Page 136 repeated word: one “sea” removed.

Graphic design: Communication Division, UiB / Print: Skipnes Kommunikasjon AS

uib.no

ISBN: 9788230856802 (print)
9788230841969 (PDF)